

Materials Reliability Program:

**Technical Basis for Preemptive
Weld Overlays for Alloy 82/182 Butt
Welds in PWRs (MRP-169)**

1016602

Revision 1, April 2008

EPRI Project Manager
G. Frederick
B. Lu
C. King

DISCLAIMER OF WARRANTIES AND LIMITATION OF LIABILITIES

THIS DOCUMENT WAS PREPARED BY THE ORGANIZATION(S) NAMED BELOW AS AN ACCOUNT OF WORK SPONSORED OR COSPONSORED BY THE ELECTRIC POWER RESEARCH INSTITUTE, INC. (EPRI). NEITHER EPRI, ANY MEMBER OF EPRI, ANY COSPONSOR, THE ORGANIZATION(S) BELOW, NOR ANY PERSON ACTING ON BEHALF OF ANY OF THEM:

(A) MAKES ANY WARRANTY OR REPRESENTATION WHATSOEVER, EXPRESS OR IMPLIED, (I) WITH RESPECT TO THE USE OF ANY INFORMATION, APPARATUS, METHOD, PROCESS, OR SIMILAR ITEM DISCLOSED IN THIS DOCUMENT, INCLUDING MERCHANTABILITY AND FITNESS FOR A PARTICULAR PURPOSE, OR (II) THAT SUCH USE DOES NOT INFRINGE ON OR INTERFERE WITH PRIVATELY OWNED RIGHTS, INCLUDING ANY PARTY'S INTELLECTUAL PROPERTY, OR (III) THAT THIS DOCUMENT IS SUITABLE TO ANY PARTICULAR USER'S CIRCUMSTANCE; OR

(B) ASSUMES RESPONSIBILITY FOR ANY DAMAGES OR OTHER LIABILITY WHATSOEVER (INCLUDING ANY CONSEQUENTIAL DAMAGES, EVEN IF EPRI OR ANY EPRI REPRESENTATIVE HAS BEEN ADVISED OF THE POSSIBILITY OF SUCH DAMAGES) RESULTING FROM YOUR SELECTION OR USE OF THIS DOCUMENT OR ANY INFORMATION, APPARATUS, METHOD, PROCESS, OR SIMILAR ITEM DISCLOSED IN THIS DOCUMENT.

ORGANIZATION(S) THAT PREPARED THIS DOCUMENT

Structural Integrity Associates

ORDERING INFORMATION

Requests for copies of this report should be directed to EPRI Orders and Conferences, 1355 Willow Way, Suite 278, Concord, CA 94520. Toll-free number: 800.313.3774, press 2, or internally x5379; voice: 925.609.9169; fax: 925.609.1310.

Electric Power Research Institute and EPRI are registered service marks of the Electric Power Research Institute, Inc. EPRI. ELECTRIFY THE WORLD is a service mark of the Electric Power Research Institute, Inc.

Copyright © 2005 Electric Power Research Institute, Inc. All rights reserved.

CITATIONS

This report was prepared by

Structural Integrity Associates
6855 S. Havana St. (Suite 350)
Centennial, CO 80112

Principal Investigator
P. C. Riccardella

Other Significant Contributors:

A. F. Deardorff
A. J. Giannuzzi
M. S. Lashley
R.A. Hermann

This report describes research sponsored by EPRI.

The report is a corporate document that should be cited in the literature in the following manner:

Materials Reliability Program: Technical Basis for Preemptive Weld Overlays for Alloy 82/182 Butt Welds in PWRs (MRP-169), Rev. 1, EPRI, Palo Alto, CA, and Structural Integrity Associates, Inc., San Jose, CA: 2008. 1012843.

PRODUCT DESCRIPTION

Results & Findings

Challenges & Objectives

Applications, Values & Use

EPRI Perspective

Approach

.

Keywords

PWR Piping and Nozzles, Dissimilar Metal Welds (DMWs), Primary Water Stress Corrosion Cracking (PWSCC), Preemptive Weld Overlays (PWOLS), Mitigation

To be completed as part of EPRI Publications Process.

ABSTRACT

In recent years, the dissimilar metal, Alloy 82/182 welds (DMWs) used to connect stainless steel piping and low alloy steel or carbon steel components in nuclear reactor piping systems have experienced cracking due to primary water stress corrosion (PWSCC). Cracking and/or leakage has been observed in several operating Pressurized Water Reactors (PWRs), both in the U.S. and overseas. In several cases, the cracking was repaired using structural weld overlays, a repair technique that has been in use in the U.S. nuclear industry for over twenty years, primarily for the repair of Intergranular Stress Corrosion Cracking (IGSCC) in Boiling Water Reactors (BWRs).

The benefits of weld overlay repairs have been documented extensively in the literature, and include:

1. Structural reinforcement to meet ASME Code, Section XI margins with cracks present
2. An SCC resistant material (by appropriate weld metal selection for the overlay process)
3. Favorable residual stress reversal from tensile to compressive in the SCC susceptible inner portion of the original pipe.

Weld overlays also offer improvement in inspectability because the examination volume is moved to the outside of the pipe (the weld overlay material plus a portion of the original pipe wall), which allows easier coverage with qualified techniques. The weld overlays also minimize discontinuities between the adjoining pieces and consist of one material with uniform acoustic properties, thus making volumetric examinations easier.

Weld overlays are an acceptable ASME Code repair (Section XI Code Case N-504-2), and have been applied to hundreds of stainless steel pipe welds affected by IGSCC in BWRs. They have also been used, albeit less extensively, to repair dissimilar metal nozzle welds in BWRs and PWRs.

Although weld overlays have been used primarily as a repair for flawed piping, they can also be applied at locations that have not yet exhibited any cracking, but are considered susceptible to PWSCC. In this way, application of the overlays can be planned and scheduled in advance, and potential future cracking is mitigated by the residual stress, resistant material, and structural reinforcement benefits of the overlay. In addition, inservice inspection is facilitated because of the enhanced joint inspectability. An overlay used in this manner is termed a Preemptive Weld Overlay (PWOL). The purpose of this report is to define methodology and criteria for the use of PWOLs as a mitigation measure for PWSCC in PWR primary coolant pipe and nozzle welds. The report documents these criteria, and presents examples of their application to a set of typical PWR nozzles.

CONTENTS

1.0 INTRODUCTION	1-1
2.0 PURPOSE	2-1
3.0 OBJECTIVES	3-1
4.0 DESIGN REQUIREMENTS	4-1
4.1 Weld Overlay Sizing	4-1
4.2 Residual Stress Improvement	4-3
4.3 Inspectability Considerations	4-5
4.4 Fatigue Considerations	4-6
4.5 Leak Before Break	4-8
4.6 Evaluation of Weld Overlay Effects on Piping system	4-9
4.7 Summary	4-10
5.0 VERIFICATION OF WELD OVERLAY EFFECTIVENESS	5-1
5.1 Experimental Programs	5-1
5.2 Analytical Programs	5-5
5.3 Field Experience	5-6
6.0 MATERIALS AND WELDING CONSIDERATIONS	6-1
6.1 Background	6-1
6.2 Metallurgical Considerations on Service Performance	6-2
6.3 Welding Considerations	6-4
6.4 Summary	6-6
7.0 EXAMINATION REQUIREMENTS	7-1
7.1 Requirements for Types of Examination for Weld Overlays	7-1
7.2 Inspection Interval and Sample Size for Preemptive Weld Overlays	7-2

7.3 Dissimilar Metal Weld Examination Requirements 7-3

8.0 EXAMPLE ANALYSES..... 8-1

8.1 Weld Overlay Sizing Calculations 8-1

8.2 Residual Stress Analyses 8-2

8.3 Fatigue Crack Growth Analysis..... 8-7

8.4 Fatigue Usage Evaluation..... 8-10

9.0 CONCLUSIONS 9-1

10.0 REFERENCES 10-1

LIST OF FIGURES

Figure 4-1 – Schematic Illustration of ASME Section XI Flaw Evaluation Basic Concept	4-12
Figure 4-2 – Illustration of Full Structural and Optimized Weld Overlay Design Basis Flaw Size Assumptions	4-13
Figure 5-1 Sketch of pipe used as a container for self-contained boiling magnesium chloride residual stress test. [8].....	5-8
Figure 5-2 Sketch showing notch locations in test of Figure 5-1 [8]	5-9
Figure 5-3 Metallographic results from boiling magnesium chloride testing [8]	5-10
Figure 5-4 Liquid Penetrant test results showing cracking under welds without overlay and no cracking under overlaid welds [9].....	5-11
Figure 5-5 Liquid Penetrant test results showing cracking under welds without overlay and no cracking under overlaid welds [9].....	5-12
Figure 5-6 Liquid Penetrant test results showing cracking under welds without overlay and no cracking under overlaid welds [9].....	5-13
Figure 5-7 Illustration of Cracked Pipe and Weld Overlay Configuration Used in Battelle/USNRC Experiments [11]	5-14
Figure 5-8 Schematic illustration of test setup used in Battelle/USNRC Weld Overlay Experiments [11]	5-15
Figure 5-9 Comparison of Battelle/USNRC Degraded Piping Program Weld Overlay Tests with Full Structural Weld Overlay Design Basis Calculations [11].....	5-16
Figure 5-10 Drawing of MRP/EPRI PWOL Mockup.....	5-17
Figure 5-11 FEA Model for the PWOL Mockup	5-18
Figure 5-12 Analytical (FEA) Hoop Stress Results for the PWOL Mockup.....	5-19
Figure 5-13 Analytical (FEA) Axial Stress Results for the PWOL Mockup.....	5-20
Figure 5-14 Comparison of Analytical vs. Measured Hoop Residual Stress Results for PWOL Mockup	5-21
Figure 5-15 Comparison of Analytical vs. Measured Axial Residual Stress Results for PWOL Mockup	5-22
Figure 5-16 Effect of Wall Thickness on Maximum ID Temperature [12].....	5-23
Figure 5-17 Predicted Stresses for the 4-Inch Pipe Overlay Welded Dry [12].....	5-24
Figure 6-1 Oxide Film Developed on Alloy 600 (a) and Alloy 690 (b).....	6-8
Figure 6-2 Composition of Ni, Cr and Fe as a Function of the Distance from the Metal- Oxide Interface on Alloy 600 (a) and Alloy 690 (b) [22]	6-8
Figure 6-3 Sketch of the Oxide Film Developed on Alloy 600 and Consequences on the Underlying Metal [22]	6-9

Figure 6-4 Sketch of the Depletion in Chromium under the Oxide Scale Associated with Enrichment in Oxygen at a Triple Grain Boundary [22].....	6-9
Figure 6-5 The Effect of Cr on the Oxide Rupture Strain of Ni-9Fe-xCr Alloys in Aerated Primary Water [24]	6-10
Figure 6-6 Polarization Curves for Alloy 600 and Alloy 690 in pH 10 90 °C Water [25].....	6-11
Figure 7-1 Inspection Requirements for Weld Overlays	7-5
Figure 8-1 Pressurizer Spray Nozzle Geometry chosen for Analysis (chosen as representative of all pressurizer steam space nozzles)	8-16
Figure 8-2 Pressurizer Surge Nozzle Geometry chosen for Analysis	8-16
Figure 8-3 RPV Hot Leg Nozzle Geometry Chosen for Analysis	8-17
Figure 8-4 Illustration of Simulated In-process ID Weld Repair used as Starting Point for Residual Stress Analysis (Used for all three example nozzles.)	8-17
Figure 8-5 Finite Element Model for Pressurizer Spray Nozzle Weld Overlay Weld Residual Stress Analysis.....	8-18
Figure 8-6 Finite Element Model for Pressurizer Surge Nozzle Weld Overlay Weld Residual Stress Analysis.....	8-19
Figure 8-7 Finite Element Model for RPV Hot Leg Nozzle Weld Overlay Weld Residual Stress Analysis.....	8-20
Figure 8-8 Pressurizer Spray Nozzle Pre- and Post-WOL Residual Stress Contour Plots (Axial Stress).....	8-21
Figure 8-9 Pressurizer Spray Nozzle Pre- and Post-WOL Residual Stress Contour Plots (Hoop Stress).....	8-22
Figure 8-10 Pressurizer Spray Nozzle Inside Surface Stress Plots	8-23
Figure 8-11 Pressurizer Spray Nozzle Post-WOL Through-Wall Stress Plots.....	8-24
Figure 8-12 Pressurizer Surge Nozzle Inside Surface Stress Plots.....	8-25
Figure 8-13 Pressurizer Surge Nozzle Post-WOL Through-Wall Stress Plots.....	8-26
Figure 8-14 RPV Hot Leg Nozzle Inside Surface Stress Plots	8-27
Figure 8-15 RPV Hot Leg Nozzle Post-WOL Through-Wall Stress Plots	8-28
Figure 8-16 Spray Nozzle Post-WOL Stress Intensity Factor Plots – Normal Operating Sustained Loads plus Residual Stresses	8-29
Figure 8-17 Surge Nozzle Post-WOL Stress Intensity Factor Plots – Normal Operating Sustained Loads plus Residual Stresses	8-30
Figure 8-18 RPV Hot Leg Nozzle Post-WOL Stress Intensity Factor Plots – Normal Operating Sustained Loads plus Residual Stresses	8-31
Figure 8-19 Growth of Postulated Circumferential Crack for 500 Design Heatup/Cooldown Cycles.....	8-32
Figure 8-20 Growth of Circumferential Crack	8-32
Figure 8-21 Growth of a Postulated 0.31-inch Depth Axial Crack	8-33
Figure 8-22 Stress Intensity Factor for Axially-Oriented 2:1 Aspect Ratio Crack.....	8-33

LIST OF TABLES

Table 4-1 Summary of Weld Overlay Design Types and Associated Design and Inspection Requirements	4-11
Table 6-1 Compositions of Nickel-base Alloys and Weld Metals [21]	6-7
Table 8-1 ASME Section XI Table for Allowable Flaws in Piping (Reference 37, Appendix C)	8-12
Table 8-2 Nozzle Dimensions and Stresses (Including OBE Seismic Loads) for Example Nozzles	8-12
Table 8-3 Weld Overlay Structural Sizing Results	8-13
Table 8-4 Final Weld Overlay Design Dimensions, Reflecting Residual Stress and Inspectability Considerations	8-13
Table 8-5 Cycles Considered in Fatigue Analysis	8-14
Table 8-6 Summary of Primary-plus-Secondary Stress and Fatigue Analysis Results for Pressurizer Surge Nozzle	8-15

1.0 INTRODUCTION

Alloy 82/182 butt welds were used extensively in PWR primary coolant piping to connect dissimilar metal components, generally between stainless steel piping and low alloy steel or carbon steel components. In recent years, the dissimilar metal Alloy 82/182 bimetallic pipe-to-nozzle butt welds (DMWs) have experienced cracking due to primary water stress corrosion (PWSCC).

Volumetric examinations of large diameter butt weld locations (>4" NPS) are required by ASME Code, Section XI, generally at ten-year inspection intervals. These examinations are considered very difficult and until recently were not subject to extensive qualification procedures. After ASME Code, Section XI, 1992 edition, the examination techniques are required to be qualified by performance demonstration in accordance with Appendix VIII, which requires the procedures, equipment, and personnel to be qualified. Recent examinations with performance demonstrated techniques in accordance with Appendix VIII, as implemented through the EPRI Performance Demonstration Initiative (PDI) program, are more sensitive than previous methods, and generally reveal more cracking than has historically been observed. In addition, when one considers the possible existence of inside diameter (ID) repair welds in these joints from original construction, coupled with weld metal primary water stress corrosion cracking (PWSCC) crack growth rates (which are large), continued use of the ten-year ASME Code, Section XI inspection interval for unmitigated, PWSCC susceptible welds is not considered viable. MRP-139 [1] contains Inspection and Evaluation (I&E) Guidelines for PWSCC susceptible primary coolant system butt welds that include more frequent examinations than those required by the ASME Code.

A similar phenomenon occurred within the BWR fleet in the 1980's. Intergranular stress corrosion cracking (IGSCC) was identified to cause cracking and weld overlay repairs were used to restore structural integrity to the cracked welds. The weld overlay (WOL) repair process has been used for many years in the repair of pipe flaws associated with IGSCC in BWRs [2]. The process has been shown to offer multiple improvements to the original pipe welds, which are:

1. Structural reinforcement to meet ASME Code, Section XI margins with cracks present
2. SCC resistant material by use of appropriate weld metal during the overlay process
3. Favorable residual stress reversal from tensile to compressive in the SCC susceptible inner portion of the original pipe.

As implemented for BWRs, weld overlays also offer a significant improvement in inspectability because the examination volume is moved to the outside of the pipe (weld overlay material plus the outer 25% of the original pipe wall), which allows easier coverage with qualified techniques. The weld overlays also minimize discontinuities between the adjoining pieces and consist of one material with uniform acoustic properties, thus making volumetric examinations easier.

Weld overlay repairs have been accepted by ASME Code, Section XI (Code Cases N-504-2 and N-740-2) [3, 4] and have been applied to hundreds of stainless steel pipe welds affected by intergranular stress corrosion cracking (IGSCC) in BWRs. They have also been used, albeit less extensively, to repair dissimilar metal welds at nozzles in BWRs and PWRs. Technical justification for the weld overlay repair process is documented in References 2, 8 and 9. The weld overlay repair process was first applied to a PWR large diameter pipe weld in the Fall of 2003 [5].

Although in past applications weld overlays have been used to repair flawed piping, weld overlays can also be applied at locations that have not yet exhibited any cracking but are considered susceptible to PWSCC. In this way, a planned application of the overlay can be facilitated and any potential future cracking is mitigated because of the resulting favorable post-overlay residual stresses at the weld location. In addition, inservice inspection is facilitated because of the enhanced joint inspectability afforded by the weld overlay. An overlay used in this manner is termed a Preemptive Weld Overlay (PWOL).

2.0 **PURPOSE**

The purpose of this report is to define methodology and criteria for the use of preemptive weld overlays (PWOLs) as a mitigation measure for PWSCC in PWR primary coolant pipe and nozzle welds.

The report details design analysis, materials and examination requirements for PWOLs. It summarizes the large body of experimental and analytical evidence, as well as successful field experience that exists in support of weld overlay repairs. It includes a series of sample problems that document the application of the proposed requirements to a cross-section of PWR dissimilar metal nozzle to safe-end butt welds.

If a licensee commits to performing overlays in accordance with MRP-169, it is intended that the requirements of this document be met in their entirety. Installation of the overlays (welding, materials selection, acceptance examinations, etc.) is also subject to additional requirements of ASME Code Case N-740-2. MRP-169 contains design, analysis and inservice inspection requirements for the preemptive overlays that are in some areas more limiting than those in ASME Code Case N-740-2. If any of these requirements are not implemented, the licensee shall prepare a relief request justifying their exclusion, which is subject to NRC approval.

3.0

OBJECTIVES

Specific objectives of this report are to document and obtain NRC acceptance of a PWOL design approach that:

- Meets ASME Code, Section XI flaw evaluation margins in the presence of assumed flaws
- Mitigates against future crack initiation (or growth of existing undetected cracks) via favorable residual stresses
- Provides additional margin against leakage and pipe rupture through adding layers of structural reinforcement made from a PWSCC resistant material
- Improves examination coverage requirements (the PWOL material plus a percentage of the original pipe wall, consistent with current WOL repair requirements)
- Justifies the current Section XI inspection interval
- Reduces probability of rupture of the affected welds
- Results in weld overlay thicknesses and lengths that are economically practical to apply preemptively to susceptible dissimilar metal butt welds in a plant

4.0

DESIGN REQUIREMENTS

4.1 Weld Overlay Sizing

The fundamental assumption of structural weld overlay sizing is that a crack is present in the original pipe or nozzle weld, which must be evaluated in accordance with ASME Section XI flaw evaluation rules [36, 37]. These rules establish an end-of-evaluation-period allowable flaw size based on the maximum size flaw that can be sustained in the component without violating original design margins (typically ASME Section III for primary system components). The end-of-period allowable flaw size is illustrated by the horizontal dashed line in Figure 4-1. Section XI also includes a general restriction that in no case shall this flaw size be greater than 75% of the component nominal wall thickness.

Weld overlay sizing requirements are further defined in Code Cases N-504-2 and N-740-2 [3, 4] for Full Structural Weld Overlays (FSWOLs). Full structural weld overlays may be used for any application in which cracking has been detected in a pipe or safe-end weld. ASME Code Section XI allowable flaw size criteria (IWB-3640 and Appendix C) are used for sizing the weld overlay, based on the assumption that a circumferential crack is present completely through-wall and 360° around the original pipe or nozzle cross section. Once the FSWOL is applied, this becomes the allowable end-of-period flaw size, and any actual observed flaws must be demonstrated not to grow to this size before the next scheduled inservice inspection (generally each period, per Section XI successive inspection requirements, IWB-2420-b). Subsequent work [2] has justified extending the successive inspection interval for weld-overly repaired locations in BWR piping back to the original ten-year Section XI interval. A typical crack growth analysis justifying an inspection interval of ten years is illustrated by the solid curve in Figure 4-1.

Weld overlay sizing for FSWOLs is governed, in many cases, by the general Section XI requirement that no flaws of depth greater than 75% through-wall are acceptable. For cases in which applied piping loads are not large, the equation for full structural WOL thickness (t_{WOL}) often reduces to:

$$\text{crack depth} / (t_{\text{orig pipe}} + t_{WOL}) = 0.75$$

But, if the assumed crack depth for WOL sizing is equal to the original pipe wall thickness ($t_{\text{orig pipe}}$):

$$\begin{aligned} t_{\text{orig pipe}} / (t_{\text{orig pipe}} + t_{WOL}) &= 0.75 \\ t_{WOL} &= t_{\text{orig pipe}} / 3 \end{aligned}$$

The above equation defines a minimum WOL thickness for full structural overlays, regardless of the applied loading. Thicknesses greater than this may be required if larger applied loadings exist, but the overlay can never be thinner than this minimum thickness if it is to be classified as a “full structural” weld overlay.

For preemptive weld overlays on dissimilar metal welds, an “optimized” structural weld overlay is also defined in this document as an acceptable alternative to full structural overlays when there are no flaws present in the weld or any observed flaws are limited in size. For an optimized weld overlay, the design basis flaw assumption is still 360° around the weld, but with a depth equal to 75% of the original pipe wall. An illustration of the design basis flaw size differences for full structural and optimized overlays is provided in Figure 4-2.

The OWOL flaw size assumption is a reasonable and conservative design basis for preemptive overlays, since:

1. The pipe will have been inspected immediately prior to the overlay application, using an inspection technique qualified in accordance with ASME Section XI, Appendix VIII [27] and found to exhibit no evidence of cracking greater than 50% of the wall thickness in the original weld.
2. Post-overlay ultrasonic examinations (and future inservice inspections) will be required to verify the integrity of the applied weld overlay, and the examination volume for these inspections is increased to include the weld overlay plus the outer 50% of the original pipe wall (see Section 4.3 - Inspectability Considerations).

There are cases in which the original DMW configuration does not permit full coverage of the pre-overlay exam volume by qualified techniques (i.e. due to cast stainless steel or geometric limitations), or where flaw indications greater than 50% (but less than 75%) through-wall are detected. An OWOL may still be applied in such situations, subject to a plant-specific, nozzle-specific technical justification demonstrating that the observed or postulated worst-case flaw will not violate the OWOL design basis. Such technical justification shall be subject to NRC review and approval.

With a design basis crack depth assumption for OWOL sizing that is 75% of original wall thickness, the assumed flaw already meets the general Section XI 75% criterion without an overlay. Thus, the resulting OWOL thickness will not be controlled by this somewhat arbitrary limit, but will instead be based on the actual internal pressure and pipe loads at the location of the DMW being overlaid, and the ASME Code, Section XI IWB-3641 allowable flaw size criteria. In some cases, the minimum thickness required to provide compressive residual stresses may govern the overlay size (See Section 4.2 – Residual Stress Improvement).

In applying IWB-3641 allowable flaw size criteria to structural sizing of OWOLs, some additional considerations apply that are not applicable to FSWOLs. Specifically, since OWOLs take some credit for the underlying DMW material, the design must account for potential lower toughness of that material (particularly at the fusion line with the low alloy or carbon steel nozzle) [49]. Reference [49] defines a Z-factor approach to address this concern. Furthermore, PWSCC in the DMW may also be located near the stainless steel fusion line, and in such cases, tests and analyses have shown [50] that the limit load solution for net section collapse should use the flow stress of the lower strength stainless steel material rather than that of the Alloy 82/182 weldment. An OWOL actually represents a special case in which the piping system loads are carried by a two-layer cylinder. The above low toughness/low strength considerations are applicable to the inner layer (i.e. the outer 25% of the original DMW), but not to the outer layer

(the Alloy 52 weld overlay, which carries the majority of the load). An analysis technique for addressing this two-layer problem in weld overlay design is presented in [51]. In the design of OWOLs, either a two layer approach such as that described in [51] shall be used, or the lower strength/lower toughness properties shall be used, as applicable, to address potential cracks near the fusion lines of the DMW. More details regarding this OWOL design approach are provided in Section 8, Example Analyses.

Code Cases N-504-2 and N-740-2 [3, 4] also provide guidance for weld overlay length sizing, and these are the same for both FSWOLs and OWOLs. The underlying requirement is that sufficient weld overlay length be provided on either side of the observed crack to allow for adequate transfer of axial loads between the pipe and the weld overlay. For axisymmetric loading of a cylinder, local loading effects can be shown to attenuate to a small fraction of their peak value at an axial distance of $0.75\sqrt{Rt}$ from the point of loading [10] (where R is the outer radius and t is the nominal wall thickness of the cylinder). Thus, if the weld overlay length is set equal to $0.75\sqrt{Rt}$ on either side of the crack, resulting in a total weld overlay length of $1.5\sqrt{Rt}$, the overlay will extend beyond any locally elevated stresses due to the crack. In application of weld overlays preemptively, however, no crack will have been detected, so the above criterion is conservatively applied such that the minimum weld overlay length must be $0.75\sqrt{Rt}$ beyond either side of the susceptible material. This will result in a total weld overlay length equal to $1.5\sqrt{Rt}$ plus the length of susceptible material (Alloy 82 or 182 weld metal and buttering) on the OD surface of the original DMW. It is noted that the $0.75\sqrt{Rt}$ recommendation is only a rule of thumb, and that shorter lengths may be used if justified by stress analysis of the specific PWOL configuration, to demonstrate that adequate load transfer and stress attenuation are achieved.

Other considerations also factor into weld overlay design. These include that PWOLs be of sufficient length and thickness to achieve the desired residual stress reversal over the entire extent of susceptible material on the inside surface of the pipe or nozzle (see Section 4.2), that the length and other aspects of the weld overlay design result in an inspectable configuration (see Section 4.3), and that no unacceptable structural discontinuities are created. For PWOLs that overlay a tapered transition (or create one), the design must satisfy the ASME Code, Section III requirements of NB-4250 that allow for a maximum 30° transition angle between adjacent sections, unless detailed analyses are performed of the specific configuration to establish applicable stress indices for fatigue evaluation.

4.2 Residual Stress Improvement

A key aspect of the weld overlay design process is to demonstrate that favorable residual stress reversal occurs such that PWSCC initiation and growth is mitigated. Extensive analytical and experimental work was performed on weld-overlaid BWR pipe-to-pipe welds of various pipe sizes to demonstrate that favorable residual stresses result for full-structural weld overlays (summary provided in Section 5 below). A recent PWOL test program also demonstrated that measured residual stresses in a typical PWR mid-sized DMW weld overlay were highly favorable when applied to a weld with a severe inside surface repair (program summarized in Section 5.1 (5)). Since the geometric configuration of BWR pipe-to-pipe joints and the associated weld overlays are fairly standard, most BWR pipe weld overlays did not require weld

specific residual stress analyses. The designs relied on the large body of residual stress work that already existed.

The residual stress story for nozzle-to-pipe DMWs is not as straightforward for several reasons.

- Each nozzle / safe-end design is somewhat unique, often with significant diameter and thickness differences between the nozzle, the safe-end and the attached piping.
- Many design configurations involve two welds in relatively close proximity, which can interact with one another.
- As discussed above, an optimized structural overlay concept is being introduced for preemptive applications, and in some cases, the WOL length and thickness required to produce favorable residual stresses may govern the overlay design, rather than structural considerations.

For these reasons, a joint specific, overlay specific weld residual stress analysis is required for each unique PWOL configuration in which there is a significant geometry, material, or welding process difference from a previously analyzed overlay (beyond standard drawing/fabrication tolerances). These must be performed with analysis methods and tools that are appropriate for this type of analysis, including transient thermal analysis capability, non-linear elastic-plastic modeling capability, and temperature dependent material properties. Several such tools exist and have been demonstrated to produce residual stress results that are in agreement with (or conservatively bound) experimental measurements (see Section 5). The residual stress analysis should consider actual welding parameters to be used in applying the weld overlay, including bead sequence, welding direction, heat input, thermal boundary conditions (wet or dry) and interpass temperature limits.

Finally, the initial residual stress condition of the DMW joint has a significant bearing on its susceptibility to PWSCC, especially as influenced by in-process repairs performed during plant construction. In fact, in essentially all cases in which PWSCC has been discovered in PWR butt welds, evidence of significant in-process repairs during construction has been found. Thus to adequately demonstrate the favorable residual stress effects of a weld overlay, one must start with a highly unfavorable, pre-overlay residual stress condition such as that which would result from an ID surface weld repair during construction. If the nozzle-specific weld overlay design is shown to produce favorable residual stresses in this severe case, one can be assured that it will effectively mitigate against future PWSCC in the DMW.

Acceptable residual stresses for purposes of satisfying this requirement are those which, after application of the weld overlay, are compressive on the inside surface of the nozzle, over the entire length of PWSCC susceptible material on the inside surface, at operating temperature, but prior to applying operating pressure and loads. After application of operating pressure and loads, the resulting inside surface stresses must be less than 10 ksi tensile. As documented in References [52-54], laboratory data and field observations have shown that high stresses, on the order of the material yield strength, are necessary to initiate PWSCC. Thus limiting ID surface stresses under sustained steady state conditions to less than 10 ksi ensures a very low probability of initiating new PWSCC cracks after application of the weld overlay.

A separate PWSCC crack growth criterion must also be satisfied to demonstrate the acceptability of the post-weld overlay residual stress distribution. This criterion requires that any cracks detected in the pre- or post-overlay inspections, or that are not within the examination volumes in the PWSCC susceptible material, would not grow by PWSCC to the point that they would violate the overlay design basis (75% through-wall for OWOLs or 100% through-wall for FSWOLs). Since there is no generally accepted PWSCC crack growth threshold for Alloy 82/182 weld metals [45], satisfying this criterion generally requires that the cracktip stress intensity factor due to residual stresses, operating pressure and sustained, steady-state loads, be compressive up to the greater of the maximum flaw size detected (either pre- or post-overlay) or the maximum flaw size in PWSCC susceptible material that could be missed by the applicable inspections.

The above combination of ID surface stress and crack growth criteria, in conjunction with required post-overlay inspections, provides protection against initiating new PWSCC cracks after application of the weld overlay and/or propagation of pre-existing cracks that would violate the overlay design basis.

4.3 Inspectability Considerations

One additional aspect of WOL design is that it must be inspectable. As discussed previously, post overlay examination requirements include the weld overlay itself, plus the outer 25% of the original pipe wall thickness. This examination requirement applies to FSWOLs, which use as their design basis a crack completely through the original pipe wall thickness. The 25% of original pipe wall thickness examination requirement is seen as providing added margin by verifying the arrest of an existing flaw and advanced warning in the unlikely case that the crack is not arrested before propagating into the WOL. In the case of optimized weld overlays, a flaw would violate the design basis if it extended into the outer 25% of the pipe wall. Thus the examination must provide additional coverage to preserve a similar “advanced warning” examination volume. Thus, since the OWOL design basis flaw is 75% of the original pipe wall, then the post WOL examination (and subsequent inservice inspections) must cover the WOL material plus the outer 50% of the original wall thickness in the PWSCC susceptible material.

A summary of the required examination volumes for post overlay inspections is provided in Figure 7-1. Two separate exam volumes are illustrated, one for the overlay acceptance examination (Figure 7-1(a)), and a second for the overlay pre- and inservice inspections (Figure 7-1(b)).

ASME Code, Section XI, 1995 Edition and later includes NRC accepted rules for inspection of welds in piping that require the procedures, equipment, and personnel to be qualified by a performance demonstration in accordance with Appendix VIII, Supplement 11. The utilities sponsored a performance demonstration initiative (PDI), implemented at the EPRI NDE Center, which satisfies these requirements, as amended for weld overlay repairs, and a number of organizations have successfully qualified personnel and techniques to inspect weld overlays under that program. Therefore, as has been the case for weld overlay repairs, ASME Section XI, Appendix VIII, Supplement 11 shall be implemented for PWOLs. The PWOL design, including

surface preparation specifications, should be reviewed to confirm that a PDI qualified examination can be performed.

4.4 Fatigue Considerations

There are two issues that must be addressed from a fatigue viewpoint relative to installation of a weld overlay on an existing weld. The first involves evaluation of potential growth of cracks due to cyclic loadings at the overlay location. The second involves assuring that additional stresses are not created by the application of the overlay that would contribute to an unacceptable end-of-life fatigue usage factor in the region where the overlay is being applied.

The sensitivity to fatigue effects depends upon whether or not there are significant cyclic loadings at the overlay location and if there are structural discontinuities in addition to the overlay that result in stress concentrations. The most severe cyclic loading effects are generally due to thermal transients. The effects of pressure cycles are generally not significant since the applied stresses must meet primary stress limits in the design process. Piping thermal expansion moments are generally not significant, unless there are a significant number of thermal transients or if there are stratification effects in the associated piping. By performing fatigue evaluations for the overlaid locations, the potential for adverse fatigue effects is evaluated and an appropriate inspection interval determined.

Fatigue Crack Growth

The potential for growing a flaw from an initial flaw size to the allowable size for the overlay is evaluated by performing a crack growth analysis. The following steps are included:

- Determine the loading conditions that must be considered. The loadings considered in the original plant design, including any later changes, must be determined. For purposes of crack growth analysis, the number of cycles per heatup/cool-down cycle is established.
- Determine the applied stresses, including through-wall and circumferential distribution, at the weld overlay location for each loading condition. Stresses in both the hoop and axial direction must be quantified. This may include loads due to:
 - Pressure
 - Bending moments due to dead weight, piping thermal expansion, nozzle anchor movement effects, seismic OBE, and stratification, as applicable
 - Local thermal stratification, if applicable
 - Thermal transient through-wall stresses
 - Residual stresses
- Characterize the initial flaw depth and aspect ratio. If the location is inspected and no flaws are detected prior to application of the weld overlay, an initial circumferential flaw depth greater than or equal to 10% of the nominal pipe or nozzle thickness shall be assumed, with a length equal to the wall thickness ($a/l = 0.1$ aspect ratio flaw). An

initial axial flaw greater than or equal to 10 percent of the pipe wall thickness with an aspect ratio (l/a) equal to the length of the Alloy 600 weld at the outside surface divided by the pipe wall thickness shall also be assumed.

- If PDI qualified examination of the PWOL location is not performed prior to application of the PWOL, then a larger initial flaw size shall be assumed, consistent with the post-PWOL examination requirement (50% or 75% of the original wall thickness).
- The fatigue crack growth law will be based on that for Alloy 600 in the PWR environment, as reported in [6 and 47]. Reference 47 indicates that the fatigue crack growth rate (FCGR) of Alloy 182 in the PWR environment is a factor ~ 5 higher than that of Alloy 600 in air under the same loading conditions. The FCGR for Alloy 600 in air obtained from Reference 6 is given by:

$$(da/dN)_{air} = C_{A600} (1-0.82R)^{-2.2} (\Delta K)^{4.1}, \text{ units of m/cycle} \quad (2)$$

where:

$$C_{A600} = 4.835 \times 10^{-14} + 1.622 \times 10^{-16} T - 1.49 \times 10^{-18} T^2 + 4.355 \times 10^{-21} T^3$$

T = temperature inside pipe, °C (taken as the maximum during the

transient)

R = R-ratio = (K_{min}/K_{max})

ΔK = $K_{max} - K_{min}$ = range of stress intensity factor, $Mpa\cdot m^{0.5}$

Note that a factor of 5 should be applied to Equation (2) to account for the PWR environment [47]. Also, note that Equation (2) in accordance with Reference 47 is independent of rise time of the transient. Alternate crack growth laws may be used if justified on a case-by-case basis (e.g. as further data become available).

- Crack growth analysis is then conducted on a cycle-by-cycle basis for a period equal to standard ASME Section XI inspection interval (ten years) or to end of life, including license renewal period where applicable.
- If a flaw is detected in either pre- or post-overlay inspections that is greater than the flaw sizes specified above for fatigue crack growth calculations, then the calculations must address that larger flaw.

The allowable end-of-evaluation period flaw size is that considered in the design basis for structural sizing of the weld overlay (i.e. 75% or 100% of the original wall thickness, as applicable). If the crack growth analysis shows that fatigue crack growth will not grow a flaw to the design basis depth for the normal ASME Code, Section XI inspection interval or greater, then the Section XI ten-year interval is justified for subsequent inservice inspections (after any intermediate inspections imposed by MRP-139, as discussed in Section 7). If the crack growth analysis shows that the crack will grow to the allowable flaw size, then the inspection interval must be based on the time to reach that size, except that the inspection interval cannot be greater

than the ASME Section XI ten-year interval. For example, referring to the illustration in Figure 4-1, the crack growth curve reaches the allowable flaw size at exactly ten years, which justifies a ten year inspection cycle exactly. If the intersection of the two curves occurred to the left, at say six years, then the inspection interval would have to be reduced to six years. If, however, the intersection moved to the right, then the inspection interval would still be truncated at ten years.

Fatigue Usage Evaluation

The fatigue usage at a PWOL location may be increased due to addition of the weld overlay since the through-wall thermal stresses may be increased (greater thickness) and there will be structural discontinuities at the weld overlay to piping and nozzle transitions. To assess this potential, the usage factor at the location without the weld overlay is an indicator of the severity of loads at the location. If the usage factor at the weld location, or adjacent locations, is less than 0.2 and the location is not subject to thermal transients more severe than that associated with normal and upset reactor coolant hot leg/cold leg transients, then no further consideration need be given to fatigue due to application of the weld overlay.

Locations that experience cycling due to more severe thermal transients (e.g., associated with charging nozzles, pressurizer spray nozzles, or surge lines with stratification) may be adversely affected from the standpoint of fatigue. For these locations, a fatigue re-evaluation shall be conducted at the transitions between the weld overlay and the adjacent pipe or nozzle locations. The fatigue evaluation shall consider the plant design transients, or an alternate less severe set of transients (as allowed by ASME Code, Section XI, Appendix L). Consideration may be given to the effect of the actual plant operating transients at the PWOL locations if such data are available.

The fatigue analysis shall be conducted using the applicable rules of ASME Code, Section III for Class 1 components (NB-3600 for piping and NB-3200 for vessel nozzles). Code Editions and Addenda later than the original construction Code may be used, as allowed by ASME Code, Section XI, Appendix L.

4.5 Leak Before Break

The original plant design basis included the postulation of high energy line breaks to ensure the dynamic effects of such an event could be mitigated, the plant could be safely shut down, and the health and safety of the public would be protected. In many instances this led to engineered solutions to prevent or diminish the effects of the postulated ruptures. However, over time NRC research showed that the probability of failure of some piping systems was low enough in certain specific circumstances that such measures taken to protect against failure did not contribute significantly to overall plant safety and 10CFR50, Appendix A, General Design Criterion (GDC) 4 was revised to include the following statement:

“However, dynamic effects associated with postulated pipe ruptures in nuclear power units may be excluded from the design basis when analyses reviewed and approved by the Commission demonstrate that the probability of fluid system piping rupture is extremely low under conditions consistent with the design basis for the piping.”

Under this revised rule, larger diameter RCS piping in many plants has been evaluated following regulatory guidance in U.S. NRC Standard Review Plan 3.6.3, “Leak-Before-Break Evaluation Procedures,” to justify that the dynamic effects associated with pipe rupture can be excluded from the design bases. These evaluations have been reviewed and, in general, approved by the NRC staff. As a result utilities have been allowed to remove pipe whip restraints and other protective barriers that would otherwise be required to protect against the local effects of high-energy line break. Leak-before-break (LBB) has also been used to eliminate the dynamic effects of pipe break for other situations (e.g., reduction of reactor internals loadings as a result of pipe break).

However, the current technical basis for regulatory approval of LBB applications does not provide for evaluation of active degradation mechanisms other than fatigue and thus is at odds with recent operating experience with PWSCC and the actions being taken to mitigate and manage its effects. Consequently, efforts are underway within the NRC and EPRI to develop a more robust technical basis for determining that “. . . *the probability of fluid system piping rupture is extremely low under conditions consistent with the design basis for the piping.*”

Until this effort is complete, plants applying structural weld overlays (FSWOL or OWOL) to current LBB locations should update the original LBB calculations with an evaluation demonstrating that due to the efficacy of the overlay for PWSCC mitigation, concerns for original weld susceptibility to cracking have been resolved. Once additional regulatory guidance is provided, the licensee should review this evaluation to determine if additional analysis is needed.

4.6 Evaluation of Weld Overlay Effects on Piping system

Stresses may develop in other locations of a piping system due to the weld shrinkage at the overlays. These stresses are system wide, and similar in nature to restrained free end thermal expansion or contraction stresses. The level of stresses resulting from weld overlay shrinkage depends upon the amount of shrinkage that occurs and the piping system geometry (i.e. its stiffness). Overlay weld shrinkage may also produce displacements at locations in the system such as pipe hangers and pipe whip restraints that need to be checked against design tolerances. Finally, the added mass and stiffness produced by the weld overlay may have an effect on the dynamic response characteristics of the system

To address these effects, the following actions are recommended following application of a weld overlay:

1. Measurement of Weld Overlay Shrinkage - Common practice is to apply punch marks at several azimuthal locations on the piping and/or nozzles, beyond the ends of the overlays, and to measure the distance between those punch marks before and after application of the overlays.
2. Evaluation of Shrinkage Stresses - The stresses due to the measured shrinkage are then evaluated via a piping model, or other evaluation means. Although there are no directly applicable ASME Section III stress limits that apply to such sustained secondary stresses, a guideline is to compare them to the primary plus secondary stress limit (3 Sm). Such

stresses may also affect PWSCC crack growth evaluations of other susceptible welds in the system (with or without weld overlays).

3. System Walk Downs - Due to displacements produced by weld overlay shrinkage in the piping system, it is also required that, after application of the overlay, a walk-down be performed to check hanger set points and clearances at any pipe whip restraints to ensure that they are within tolerance.
4. Evaluation of Mass and Stiffness Effects - The mass added to the piping systems by the weld overlay and the effect of the overlay on piping system stiffness should also be evaluated, based on as-built dimensions, to determine if they have any significant effects on dynamic analyses of the system.

4.7 Summary

In summary, weld overlays can be applied either preemptively or as repairs to observed PWSCC indications, and overlays performing either function may be either full structural (FSWOLs) or optimized (OWOLs), subject to specific design, analysis and inspection requirements defined in this section. Table 4-1 provides a summary of the applicable design and inspection requirements (pre- and post-overlay) for all categories of weld overlays, including FSWOLs and OWOLs applied either preemptively or as repairs. It also cross references requirements from other applicable documents (i.e. MRP-139 and ASME Code Cases).

Table 4-1 Summary of Weld Overlay Design Types and Associated Design and Inspection Requirements

Weld Overlay Type	Pre-WOL Inspection Completed?	Design Basis Flaw for WOL	Crack Growth Design Basis	Post-WOL Exam Volume (PSI and ISI)	Post-WOL Inservice Inspection Schedule (MRP-139/169 vs. ASME Code Cases)
Repair – Full Structural	Yes	100% thru-wall, full circ.	Actual observed flaw shall not exceed design basis flaw size in next inspection interval	WOL + outer 25% of DMW (Fig. 7-1)	<u>MRP-139/169</u> : (Cat. F) Once in the next 5 years, and then if no growth 100% in subsequent 10 year interval <u>CC N-740-1</u> : Once in the next two RFOs, and then if no growth, a 25% sample population on a 10 year basis
Repair – Full Structural	No	100% thru-wall, full circ.	Assumed 75% flaw shall not exceed design basis flaw size in next inspection interval	WOL + outer 25% of DMW (Fig. 7-1)	<u>MRP-139/169</u> : (Cat. F) Once in the next 5 years, and then if no growth 100% in subsequent 10 year interval <u>CC N-740-1</u> : Once in the next two RFOs, and then if no growth, a 25% sample population on a 10 year basis
Preemptive – Full Structural	Yes	100% thru-wall, full circ.	Assumed 10% flaw shall not exceed design basis flaw size in next inspection interval	WOL + outer 25% of DMW (Fig. 7-1)	<u>MRP-139/169</u> : (Cat. B) 100% every interval (10 years) <u>CC N-740-1</u> : A 25% sample population on a 10 year basis
Repair – Optimized	Yes	75% thru-wall, full circ.	Actual observed flaw shall not exceed design basis flaw size in next inspection interval	WOL + outer 50% of DMW (Fig. 7-1)	<u>*MRP-139/169</u> : (Cat. F) Once in the next 5 years, and then if no growth 100% in subsequent 10 year interval <u>CC N-754</u> : Once in the next two RFOs, and then if no growth, a 25% sample population on a 10 year basis (outer 50%)
Preemptive – Optimized	Yes	75% thru-wall, full circ.	Assumed 10% flaw shall not exceed design basis flaw size in next inspection interval	WOL + outer 50% of DMW (Fig. 7-1)	<u>*MRP-139/169</u> : (Cat. B) 100% every interval (10 years) <u>CC N-754</u> : A 25% sample population on a 10 year basis

* - MRP-139, Rev. 0 states that a weld overlay must be full structural to qualify as Category B or F, however a Technical Justification and Interim Guidance has been prepared justifying these categories for OWOLs subject to them meeting the specific requirements of this section. MRP-139 Rev. 1 will incorporate these changes.

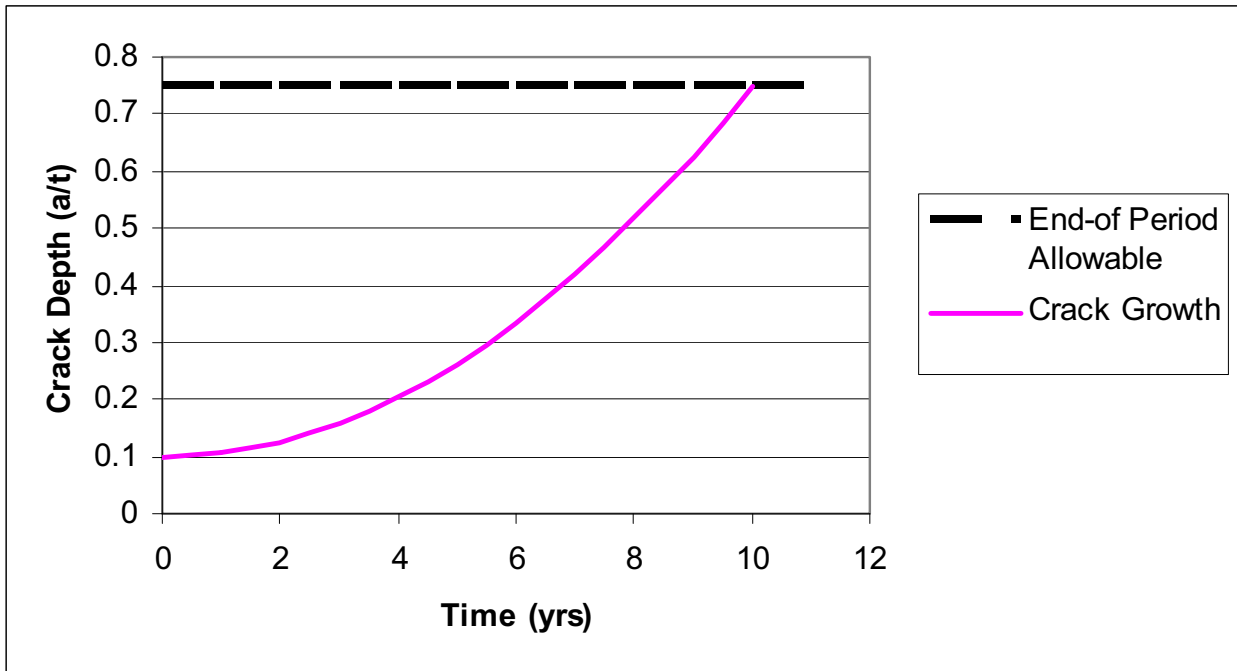
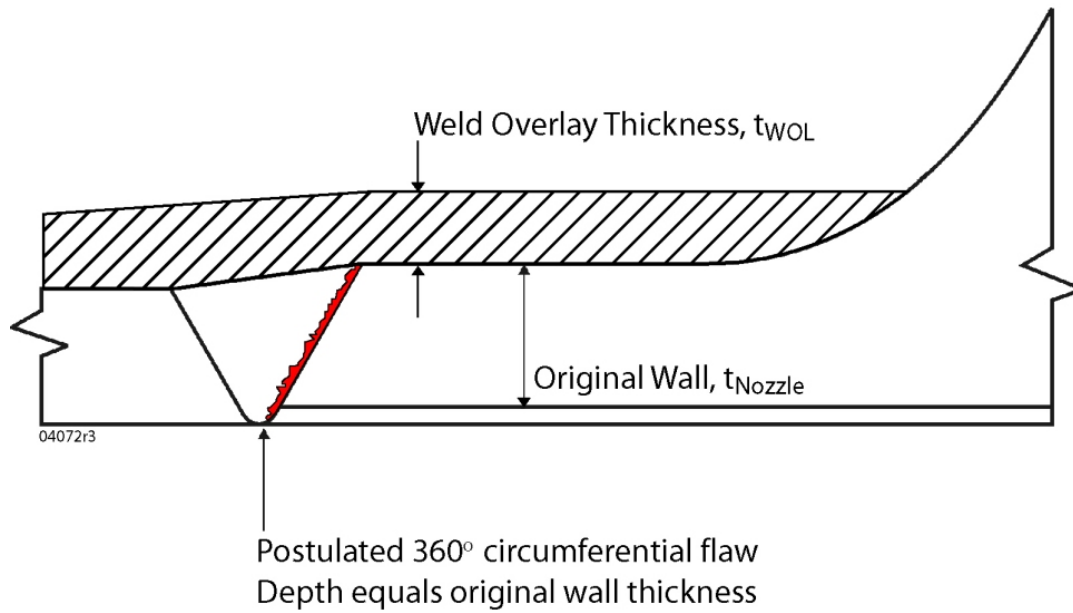
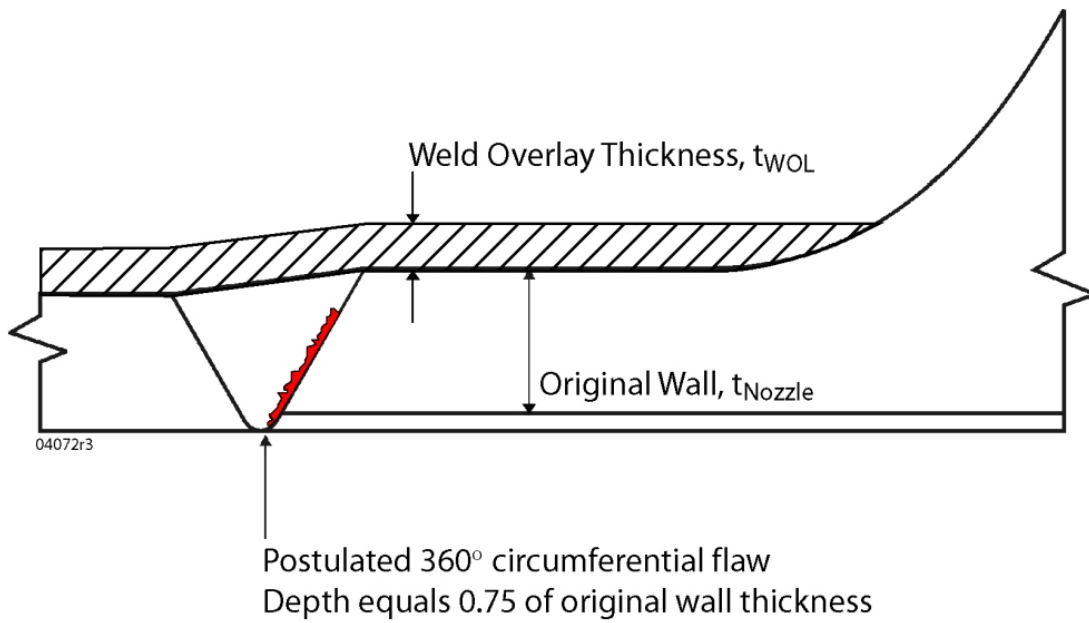


Figure 4-1 – Schematic Illustration of ASME Section XI Flaw Evaluation Basic Concept



a) Full Structural Weld Overlay (FSWOL)



b) Optimized WOL (OWOL)

Figure 4-2 – Illustration of Full Structural and Optimized Weld Overlay Design Basis Flaw Size Assumptions

5.0 VERIFICATION OF WELD OVERLAY EFFECTIVENESS

5.1 Experimental Programs

Since the initial use on BWR piping, weld overlays have been demonstrated analytically to produce beneficial residual stresses in a variety of pipe sizes and joint configurations. In addition to the analytical work, a number of laboratory programs have been undertaken to verify experimentally the effectiveness of the weld overlays in arresting the growth of pre-existing cracks under BWR conditions. The following paragraphs summarize some of the experimental studies performed to demonstrate the residual stress crack arrest and structural capabilities of the weld overlay repair.

(1) 28-Inch Notched Pipe Test [8]

A 28-inch diameter schedule 80 Type 316 stainless steel pipe that contained a distribution of machined notches on the pipe ID in the vicinity of the girth weld was weld overlay repaired and tested in an aggressive chemical solution (boiling magnesium chloride) to demonstrate the effectiveness of the overlay in producing a compressive residual stress field at the tip of the crack. The test introduced crack-like defects into a welded pipe, tested part of the pipe in an environment that would produce cracks at locations where tensile stresses are present (boiling magnesium chloride for stainless steel components), then weld overlaid the pipe and repeated the test of the entire pipe in the aggressive magnesium chloride solution.

The test configuration included a number of notched defects of axial and circumferential orientation, in order to examine the post overlay residual stress state at the extremities of the pre-existing flaws.

Two sections of a 28-inch diameter, 1.5-inch thick Type 316 stainless steel pipe were welded together using a joint configuration and weld parameters typical of those used in the original recirculation system piping fabricated for the Hatch Unit 1 plant. Following the butt weld, a bottom stainless steel plate was welded to the pipe, so that the pipe could be used as a container for a self-contained boiling magnesium chloride residual stress test Figure 5-1 [8]. A stainless steel baffle plate was fillet welded to the bottom plate and to the inside surface of the test pipe, to divide the pipe into two equal chambers. Axial and circumferential notches of varying depth were ground into the ID of the pipe at various locations near the girth weld. The notches were introduced symmetrically in both halves of the pipe Figure 5-2 [8].

One half of the pipe was exposed to the boiling magnesium chloride solution following the introduction of the notches. A standard weld overlay was then deposited over the outside surface of the entire girth weld and the entire pipe was re-exposed to the magnesium chloride solution. The pipe was liquid penetrant inspected and sections were removed for metallurgical analysis following the liquid penetrant examination.

Typical results of this testing are presented in Figure 5-3. Figure 5-3(a) presents a metallographic section of the tip of a moderate depth circumferential notch that was exposed to the chloride solution prior to the weld overlay application. The extensive cracking at the tip of the notch indicates the presence of tensile residual stress in the vicinity of the crack tip. Figure 5-3 (b) presents a similar metallographic section of the corresponding notch in the section of the pipe following the weld overlay application. No evidence of magnesium chloride cracking is observed indicating that the weld overlay process produced a zero or compressive residual stress state. Similar results were obtained at the tips of the notches. The tests thus confirmed the effectiveness of weld overlay repairs in producing compressive ID surface residual stresses at simulated cracks that extended well into the component thickness.

(2) EPRI/GE Degraded Pipe Program [9]

Major analytical and experimental studies were performed in an EPRI program evaluating remedies for IGSCC cracked austenitic stainless steel pipe. Weld overlay, induction heating stress improvement, and last pass heat sink welding processes were evaluated. The results of the studies are presented in Reference [9] and the experimental results are highlighted here for the weld overlay repair.

Pipe test experiments were performed on 4-inch and 12-inch schedule 80 Type 304 stainless steel specimens that had been IGSCC pre-cracked in the General Electric Pipe Test Laboratory in a simulated BWR environment, to produce inter-granular cracks.

The 4-inch pipe tests included testing four pre-cracked pipe specimens in boiling magnesium chloride to determine the ID stress state following the weld overlay application. These pipes had been IGSCC pre-cracked by exposure to 550°F, 200 ppb dissolved oxygen simulated BWR water. The cracks varied in depth with the deepest determined to be approximately 60% of wall thickness. Following the weld overlay application, the four specimens were exposed to boiling magnesium chloride, and the pipe sections were split and the ID examined by liquid penetrant Figures 5-4, 5-5, and 5-6 [9]. In all of the photomicrographs, no penetrant indications are seen in any instance under the weld overlay. This is a clear indication that high tensile residual stress, which would have caused transgranular chloride stress corrosion cracks, was not present on the ID surfaces under the weld overlays. One can observe the extensive cracking of the non-overlay repaired welds adjacent to the weld overlay repair in Figures 5-5 and 5-6, respectively [9]. It is particularly noteworthy that none of the IGSCC pre-cracks under the weld overlays were detected by the penetrant, although all of these circumferential cracks were detected on the heat affected zones that were not overlay repaired. This indicates that high compressive residual stresses existed under the weld overlays that tightly closed up the cracks and prevented penetration by the dye.

Weld overlay repairs were also applied to 12-inch diameter pipes that had previously been IGSCC pre-cracked part through the pipe wall in the GE laboratories as discussed above. The weld overlays consisted predominantly of standard, full structural weld overlays but one leakage barrier overlay was applied over one joint.

The results of this IGSCC test program demonstrated that even under “worst case” design and welding conditions encountered during field application, protection from IGSCC crack growth was provided at applied stresses up to the AMSE Section III allowable stress, S_m , except for one case of a through-wall crack that had subsequently been weld overlay repaired without cooling water flow. Even in that case, the measured crack growth rate was an order of magnitude lower than for the same pipe condition without the weld overlay. “Worst Case” conditions included through-wall cracks requiring special weld procedures for repair, high weld heat input, no cooling water flow, furnace sensitized piping, high reactor water conductivity, and severe loading conditions up to S_m . For the longer exposure tests, minimum factors-of-improvement of 13 and higher were calculated, indicating protection from crack growth equivalent to a 40-year plant life.

(3) EPRI Weld Overlay Large Diameter Pipe Test Program [8]

The BWR Owners Group and EPRI sponsored an IGSCC pipe test program to evaluate the effectiveness of residual stress remedies in retarding or arresting IGSCC growth in large diameter Type 304 stainless steel pipe welds. Two 24-inch diameter 1.2-inch wall thickness Type 304 stainless steel pipes, each containing two test welds, were tested. Each of the pipes was IGSCC cracked in a simulated BWR environment by loading to an axial load of approximately 18 ksi in 550°F high purity water containing 6 ppm dissolved oxygen.

Following the IGSCC pre-crack exposure or approximately 4000 hours, and crack depth determination, one pipe was returned to test and crack growth occurred in both test joints over approximately an additional 6000 hours on test. The pipe was removed from test, the crack locations were inspected by UT and PT, and a full structural weld overlay was applied to one of the joints. The weld overlay was designed to be approximately 0.29-inches thick.

The weld overlay repaired joint was on test for more than 10,000 additional hours. No additional IGSCC initiation was observed in this weld since the application of the overlay, as measured by UT and by PT. Furthermore, no apparent change in crack depth occurred in the existing IGSCC after the weld overlay was applied.

The companion as-welded reference joint accumulated approximately 19,000 hours on test since the IGSCC was first observed. During that period of time, the deepest cracks have grown to approximately 300 to 350 mils in depth. The crack growth rate was observed to be lowering measurably as determined by UT and acoustic emission and the deepest cracks appeared to be arresting. Additional ID crack initiation and lengthening of previously initiated cracks in this reference weld were also observed by UT and PT.

(4) Battelle/NRC Degraded Pipe Tests [11]

An experimental program to confirm the structural integrity of weld overlay repairs was conducted by Battelle Columbus Laboratories on behalf of the U.S. Nuclear Regulatory Commission [11]. The purpose of the program was to evaluate the margins of the Section XI net section collapse methodology which has been used as the basis for weld overlay design in the U.S. and elsewhere. In this program, weld overlays were applied to pipes containing deep flaws,

the pipes were loaded to failure, and the actual failure stresses were compared to the predicted values. An assessment of the actual margins of safety from the test results was performed for comparison to the Section XI predicted margins.

Four experiments were performed, three on 6-inch diameter pipe, and a fourth on 16-inch diameter pipe (Schedule 120 Type 304 stainless steel). Each pipe had a flaw introduced which was through the original pipe wall and which extended circumferentially approximately 50% of the circumference in the 6-inch pipe and 38% of circumference in the 16-inch pipe (Figure 5-7). The flaws were produced by first introducing notches ~50% of wall depth, extending ~17% of circumference by electric discharge machining. These notched specimens were then cycled in three-point bending to grow fatigue cracks through-wall and to the desired extent of circumference (50% or 38%). The flawed pipes were then weld overlay-repaired using techniques typical of field practice. The weld overlays were an average of 0.31 inches thick on the 6-inch pipes and 0.53 inches thick on the 16-inch pipe. Each pipe was pressurized at a temperature of 550°F to different levels of internal pressure. With the internal pressure maintained, the samples were then loaded in bending under displacement control to failure (Figure 5-8).

As illustrated in Figure 5-9, the experimental failure data are in good agreement with the theoretical net section collapse criteria (NSCC) failure predictions that serve as the basis for weld overlay design. The lines plotted in the figure represent the analytical method used (Section XI IWB-3640 source equation or Table IWB-3641-1) with safety factors of 1 and 2.77 as indicated. The points represent failure data from the test program. The test data fall above the two “no-safety factor” theoretical curves, indicating that the theoretical basis for sizing the weld overlays is conservative. Sample 3 was tested twice, first at relatively low internal pressure, in which failure was not achieved (data point 3a) and subsequently at higher pressure to failure (data point 3b). The lower lines in the diagram illustrate the theoretical design basis including the full Section XI design margin (2.77), demonstrating that this design margin was achieved or exceeded by the weld overlays in the tests.

(5) MRP/EPRI PWOL Development Program for Alloy 600 PWSCC Mitigation [48]

A PWOL development program was sponsored by the MRP/EPRI to validate analytical finite element residual stress analysis (FEA) techniques with experimental residual stress, microstructures, hardness and chemistry measurements. A detailed description of the program and results is contained in MRP-208 [48] and a brief summary is provided below.

Structural Integrity Associates (SI) with the aid of Welding Services Inc. (WSI) designed and fabricated a mockup representing a steel pressurizer nozzle welded to a stainless steel pipe with Alloy 82/182 filler material containing a significant weld repair on the ID (Figure 5-10). SI performed finite element analyses to determine residual stress distribution in the mockup, pre- and post-overlay (Figures 5-11 – 5-13). The mockup was examined by surface and UT examinations and residual stresses in the mockup were characterized non-destructively by the x-ray diffraction method prior to application of the weld overlay. Subsequently a weld overlay was applied and the overlaid mockup was again examined by surface and UT methods and residual stresses measured by x-ray diffraction on the OD and ID surfaces. Post overlay residual stress

measurements were also taken at one ID location using the hole-drilling method. The mockup was then cut up and examined metallographically.

Figures 5-14 and 5-15 present a comparison of measured versus analytical residual stresses on the ID surface of the nozzle, both pre- and post-overlay. It can be seen from these figures that the analytical predictions are in reasonable agreement with the measurements as are the results from the two different measurement techniques (XRD and hole drilling). Both analyses and measurements show that application of the overlay changed the ID surface stresses from very highly tensile at some locations, in both the hoop and axial directions, to uniformly high compression. The results of this program:

1. Add confidence in the analytical procedures used to predict weld overlay residual stresses (per Section 4.2), and
2. Demonstrate the residual stress benefits of a PWOL on a prototypical PWR nozzle safe-end geometry with a severe ID surface repair.

5.2 Analytical Programs

Many analytical studies have been performed using finite element analyses to demonstrate the effectiveness of the weld overlay repair to produce favorable residual stresses on the ID and into the wall thickness of small and large diameter pipes. The projects have examined standard and design overlays as well as the limited service “leakage barrier overlays” as residual stress mitigation measures. This section describes special evaluation activities that were performed on the weld overlay repair.

(1) Evaluation of Weld Overlay Repair Without Water Backing [12]

In this program, an analytical study was performed to determine the effect of water backing on weld overlay repair residual stress effectiveness. A three-phase approach was used to determine the effect of a heat sink on the residual stress distribution beneath a weld overlay repair. In the first phase, a heat transfer analysis was used to determine the through wall temperature distributions of an overlay repaired pipe welded with complete water backing and no water backing. A qualitative assessment concluded that acceptable residual stresses could be achieved in either case for relatively thick pipes based on similarity of temperature distributions during the welding process. In phase two, thermo-plastic residual stress analysis was performed to determine the post-weld overlay residual stresses for smaller pipe sizes. Again, it was shown that residual stresses would be acceptable. In the third phase, the effects of no water backing on the sensitization of the underlying stainless steel material was considered.

The results of this investigation are presented in Figures 5-14 and 5-15 [12]. One observes from Figure 5-14 that for pipe thicknesses greater than about 0.7 inches, the maximum ID temperature is affected very little by producing the weld overlay while the pipe is dry. For thicknesses, less than 0.7 inches, nucleate boiling becomes significant and the effect on temperature changes due to the presence of the water becomes much more pronounced.

In Figure 5-15, one observes that favorable axial and hoop weld residual stresses are produced even in a four-inch diameter pipe using standard weld overlay parameters for the welding. The sensitization study revealed that for thicknesses of pipe greater than 0.5 inches, the weld overlay would not produce ID sensitization beneath the weld overlay.

The study concluded that weld overlays could be performed without water backing for pipes with thicknesses 0.5 inches or greater.

5.3 Field Experience

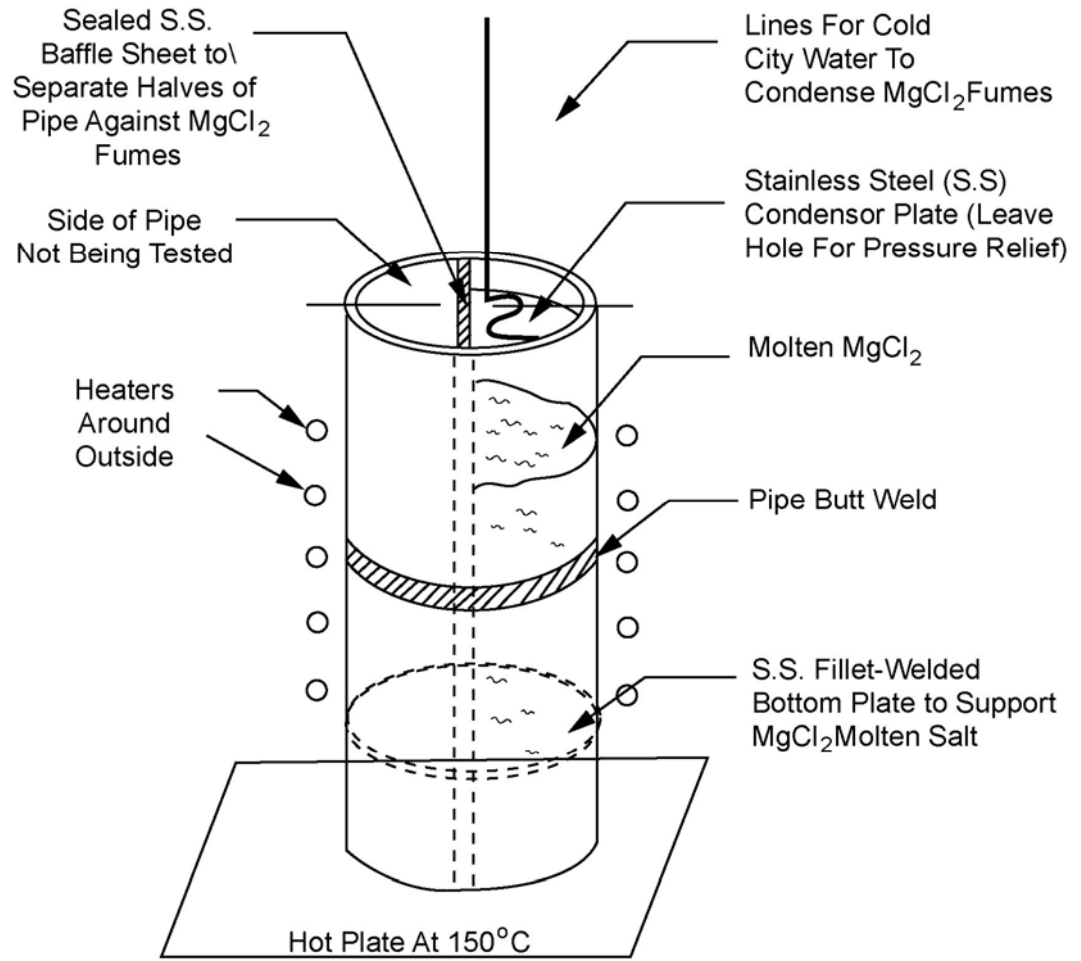
The analytical and experimental verification of the effectiveness of weld overlays to produce beneficial residual stresses in a variety of pipe sizes and joint configurations and to arrest the growth of pre-existing cracks under BWR conditions is validated by a wealth of documented field experience. BWR Vessel and Internals Project (BWRVIP-75) Technical Basis for Revisions to Generic Letter 88-01 Inspection Schedules [2] summarizes the basis for extending the interval between inservice inspections for welds that have had weld overlay repairs with low carbon/high ferrite material or an IGSCC resistant nickel-based alloy, such as Inconel 82 or 52. Table 3-2 of Reference [2] lists 262 weld overlays that had been applied through early 1999 in BWR plants based on survey responses from 33 of the 34 then operating BWRs. Based on the history of these weld overlays, Reference 2 reported that there are 15 years of data that indicates these welds are performing well, no overlay has developed flaws in the overlay and none have leaked in service. Reference 2 further states that the compressive stresses on the ID as a result of the application process have reduced the probability of IGSCC growing through-wall. Recent field experience with weld overlay repairs since the publication of Reference [2] in 1999 is consistent with the experience prior to that time.

The Reference [2] summary is based on a detailed technical justification document [13] that provides an extensive discussion of the weld overlay history, their excellent performance and their technical attributes. Reference [2] quotes an excerpt from the conclusions of Reference [8] as follows: “The conclusion of this discussion is that there is no active mechanism present that is likely to lead to degradation of the weld repair overlay structural margin in the future. Therefore, consideration of these repairs as permanent mitigation of the original mechanism (IGSCC) at the repair locations is justified. Such credit is similar to that afforded to nuclear grade replacement materials. Weld overlays fabricated from Type 308L and 309L stainless steel weld metal or Alloys 82 and 52 are at least as IGSCC resistant as nuclear grade materials in the BWR environment.”

The initial weld overlay repair to a dissimilar metal weld involving a low alloy steel component welded with nickel base filler metal was performed at Vermont Yankee during the 1985-1986 refueling outage (Reference 13). The development work to qualify this temperbead weld overlay repair had been part of a joint EPRI/Georgia Power project with Structural Integrity Associates acting as one of the technical advisors [14]. The project activity consisted of specimen testing to

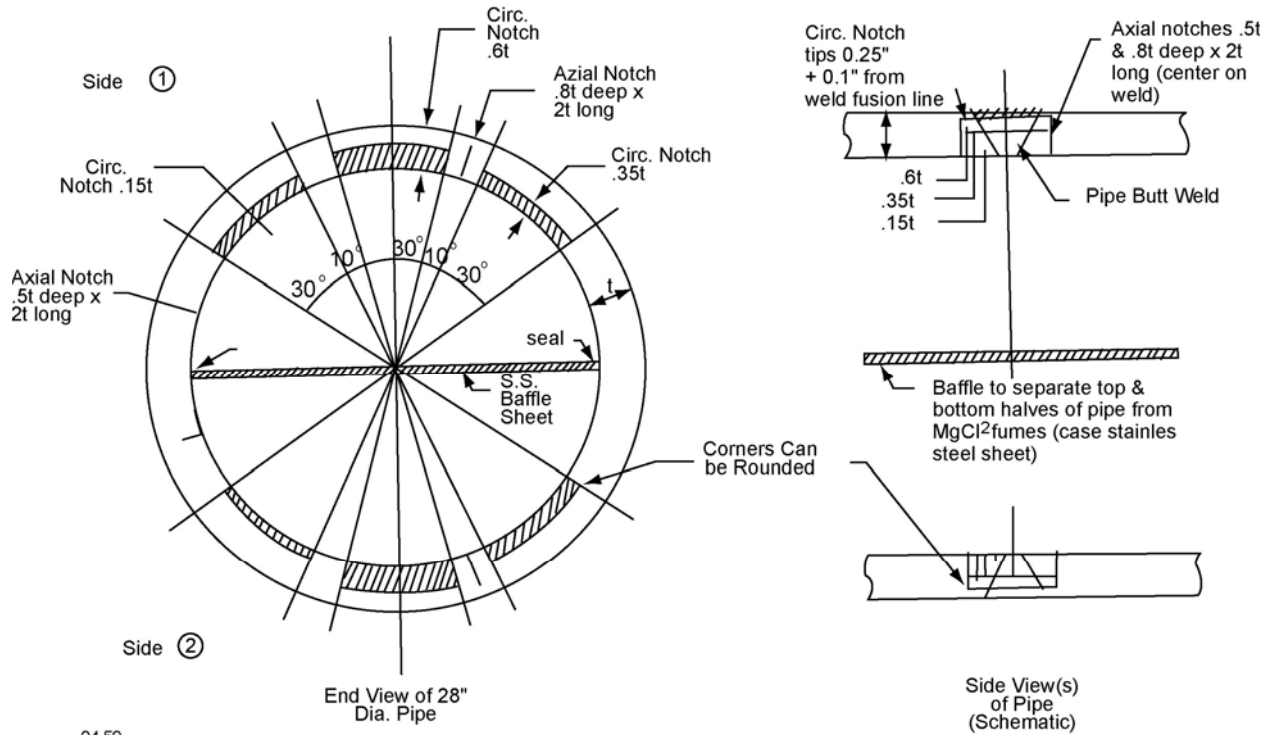
develop the parameters for the temperbead repair, full scale testing and evaluation on a mockup nozzle to safe end joint, and a procedure demonstration of the parameters [14]. The results of these activities were presented to the NRC and relief was given for use of this technology for BWR dissimilar metal welds. To date, tens of joints have been weld overlay repaired using the temperbead welding technology, with many of the recent dissimilar metal weld overlay repairs being performed at ambient temperature, with water backing. The Vermont Yankee weld overlay repair continues successfully in service to this date.

With regard to overlays in the PWR environment, the same improvements to mitigation of PWSCC are realized by changing the stresses to compressive on the ID of the original nozzle weld as for BWR repairs and WOL PWSCC resistance is achieved and the use of a weld filler material high in Cr (Alloy 52). To date numerous overlays of dissimilar metal welds joining nozzles to piping in PWRs have been implemented since November of 2003. The first of these repairs was the overlay of a surge line to reactor coolant pipe nozzle at Three Mile Island Unit 1 [5]. Subsequent PWR overlays were applied as mitigation or repairs to a over 200 pressurizer nozzles during 2006, 2007 and 2008 outages. Relief requests for these Full Structural Weld Overlays (FSWOLs) were submitted to and accepted by the NRC.



04.58

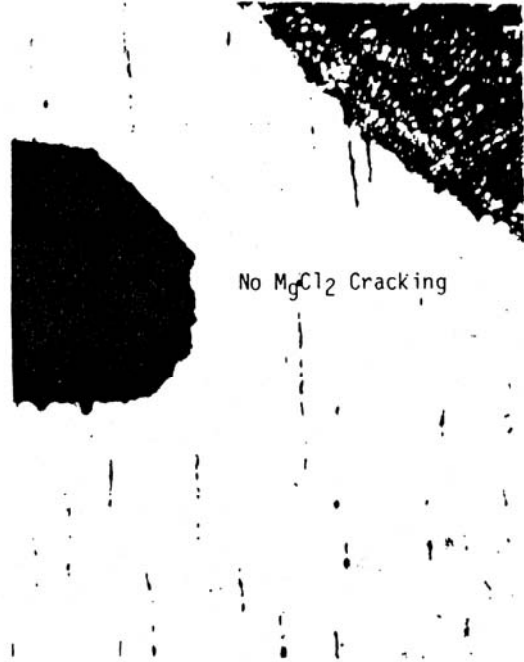
Figure 5-1
Sketch of pipe used as a container for self-contained boiling magnesium chloride residual stress test. [8]



04.59
Figure 5-2
 Sketch showing notch locations in test of Figure 5-1 [8]

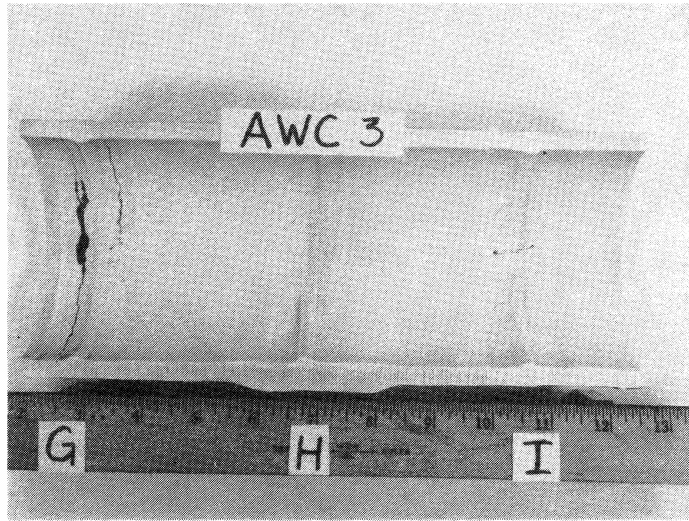


a) Notch Tested Before Weld Overlay

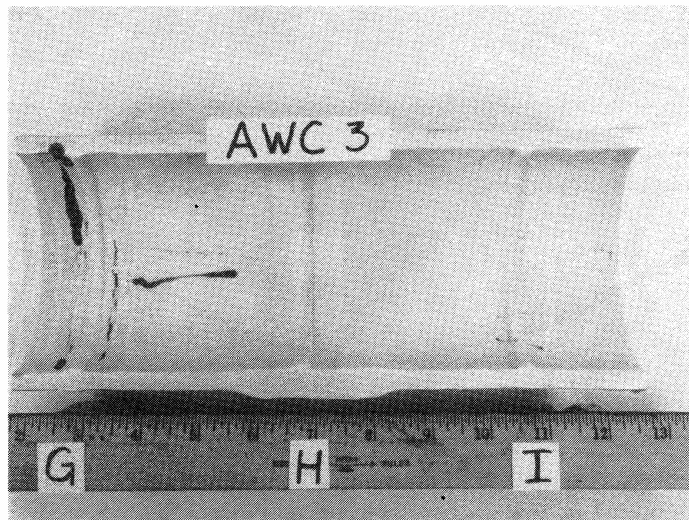


b) Notch Tested After Weld Overlay

Figure 5-3
Metallographic results from boiling magnesium chloride testing [8]

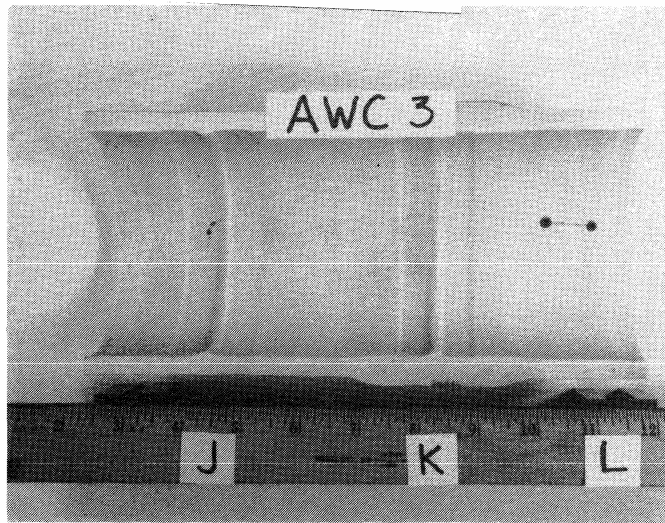


0° TO 180°

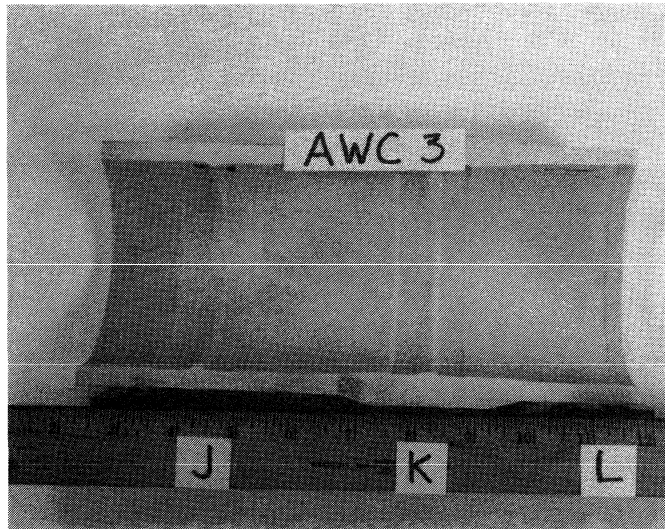


180° TO 360°

Figure 5-4
Liquid Penetrant test results showing cracking under welds without overlay and no cracking under overlaid welds [9]



0° TO 180°



180° TO 360°

Figure 5-5
Liquid Penetrant test results showing cracking under welds without overlay and no cracking under overlaid welds [9]

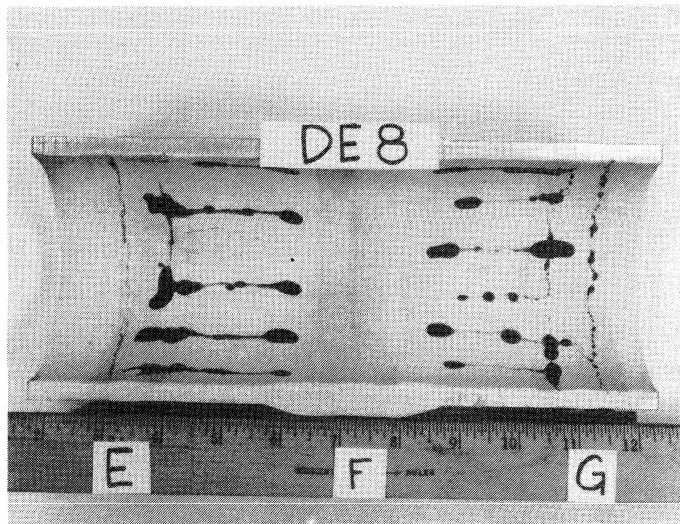
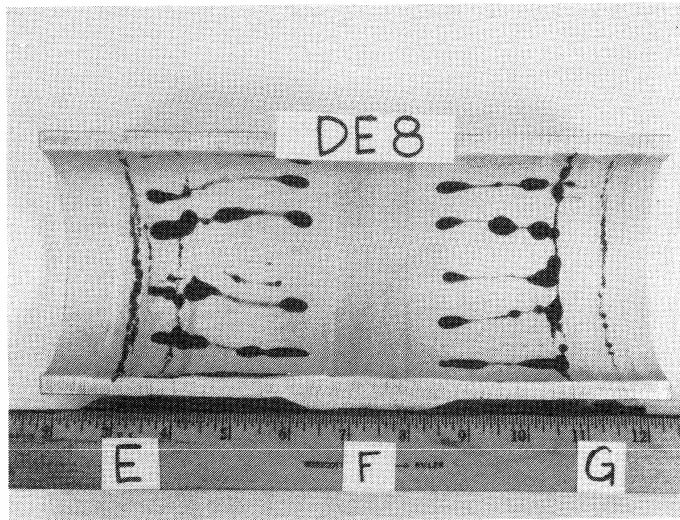


Figure 5-6
Liquid Penetrant test results showing cracking under welds without overlay and no cracking under overlaid welds [9]

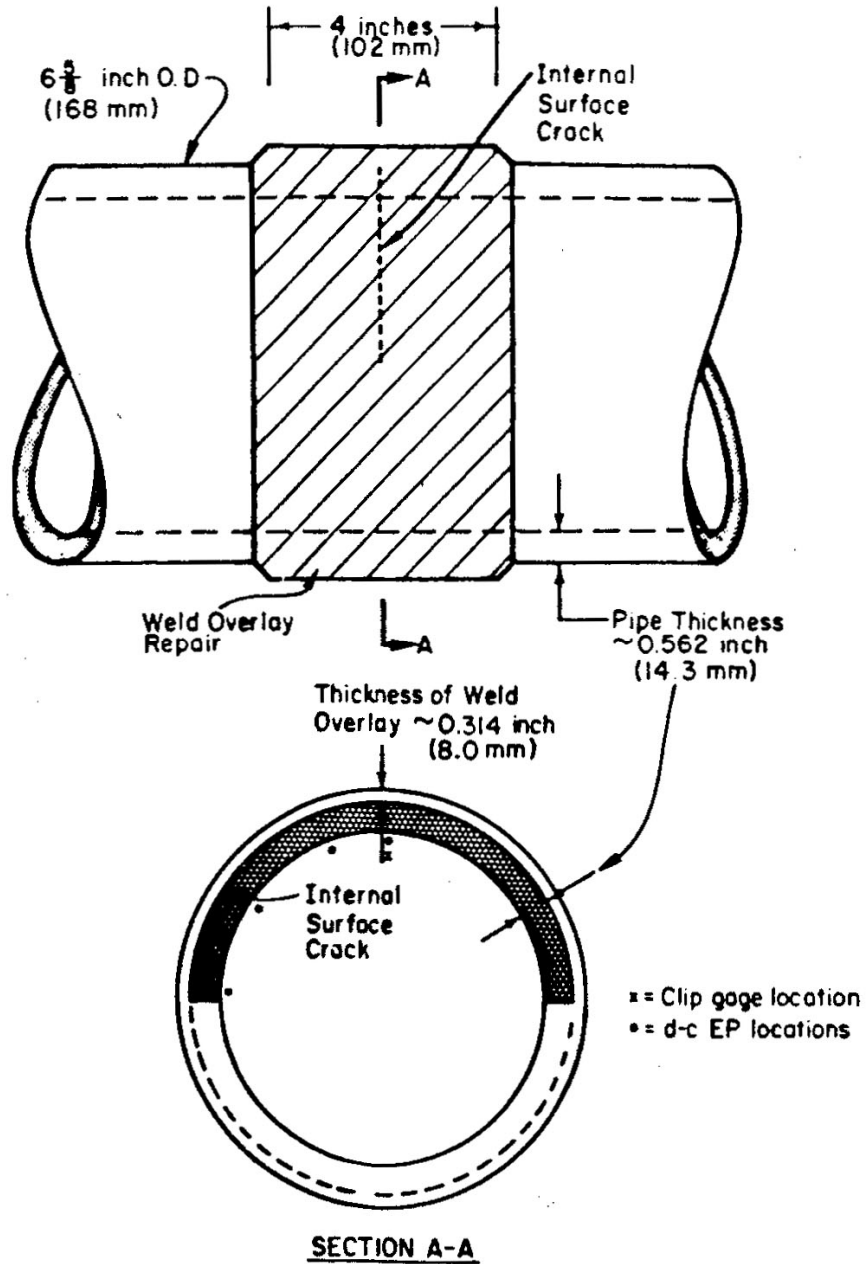


Figure 5-7
Illustration of Cracked Pipe and Weld Overlay Configuration Used in Battelle/USNRC Experiments [11]

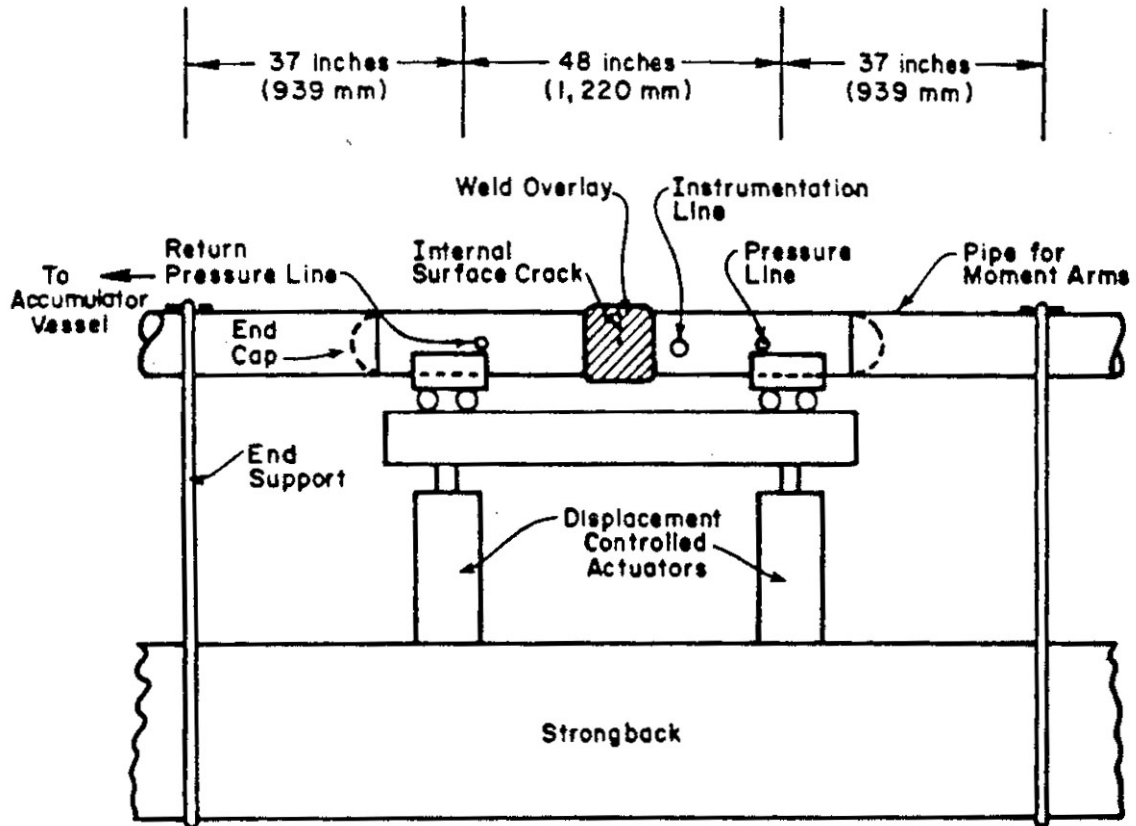


Figure 5-8
Schematic illustration of test setup used in Battelle/USNRC Weld Overlay Experiments [11]

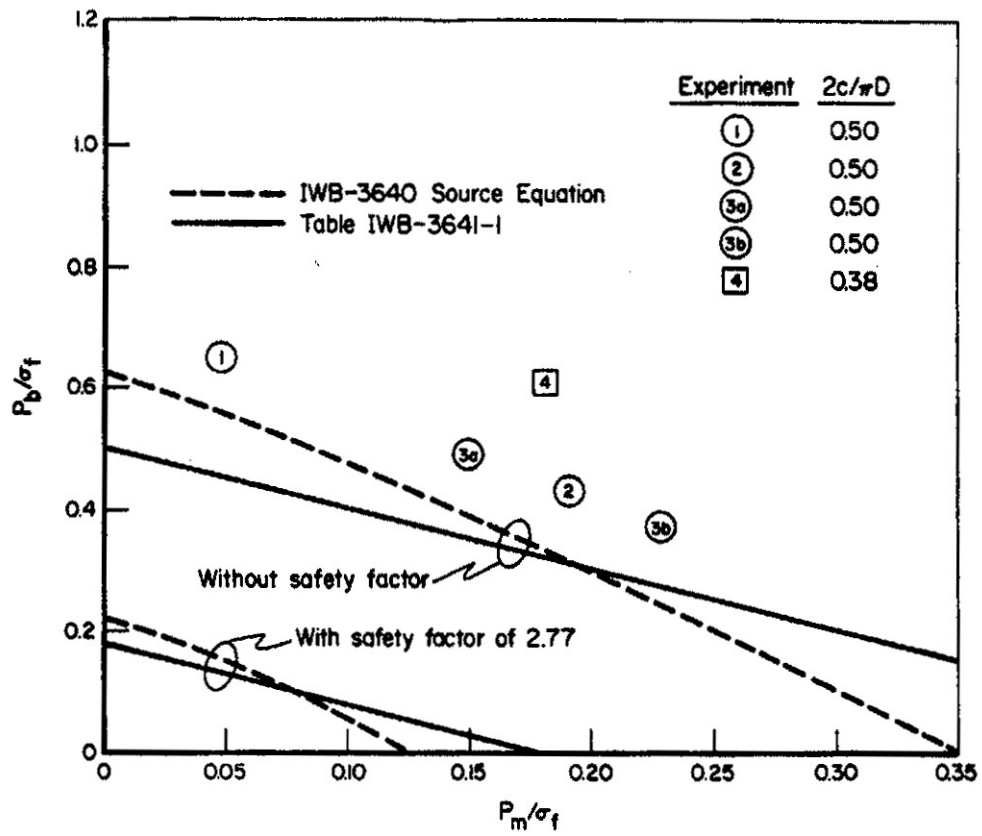


Figure 5-9
 Comparison of Battelle/USNRC Degraded Piping Program Weld Overlay Tests with Full Structural Weld Overlay Design Basis Calculations [11]

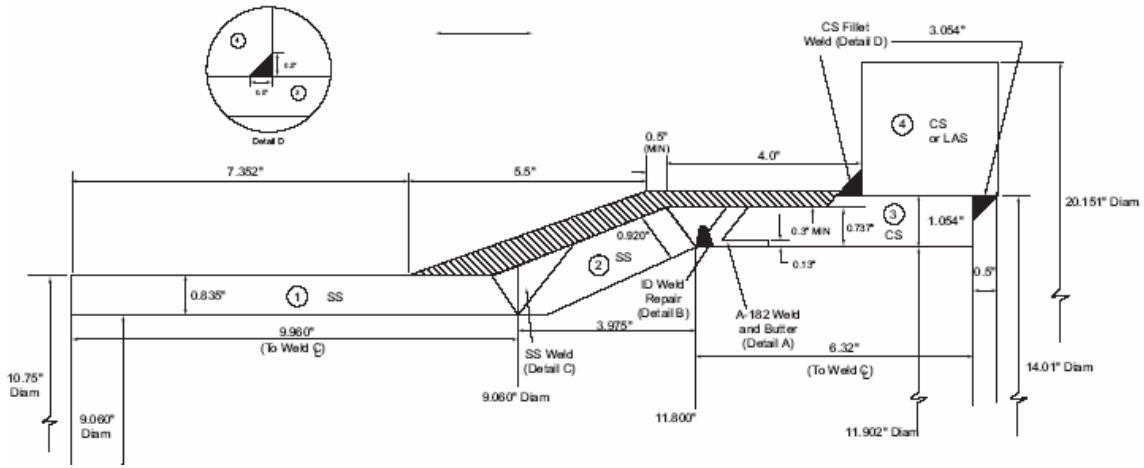


Figure 5-10
Drawing of MRP/EPRI PWOL Mockup

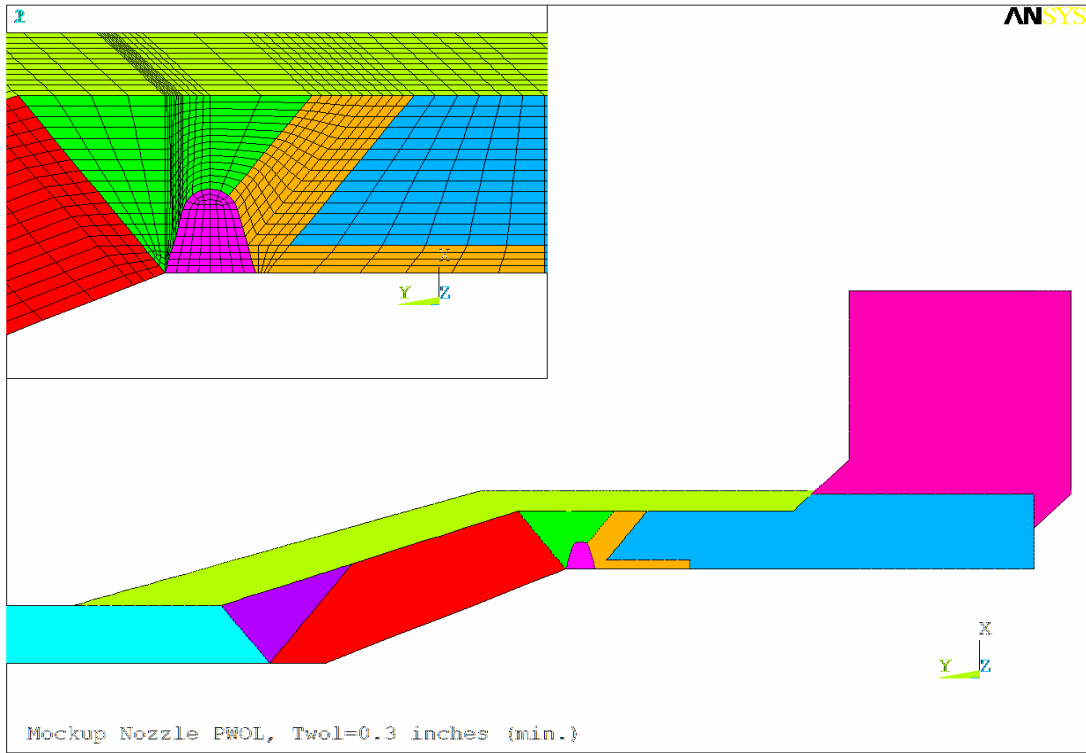
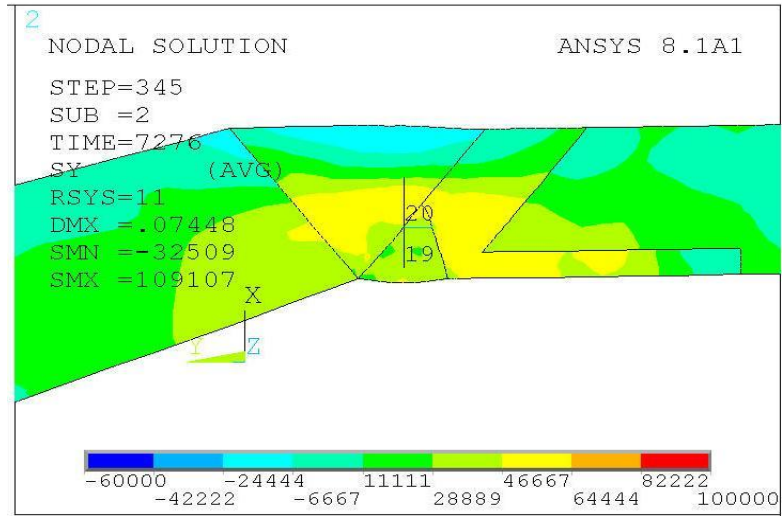
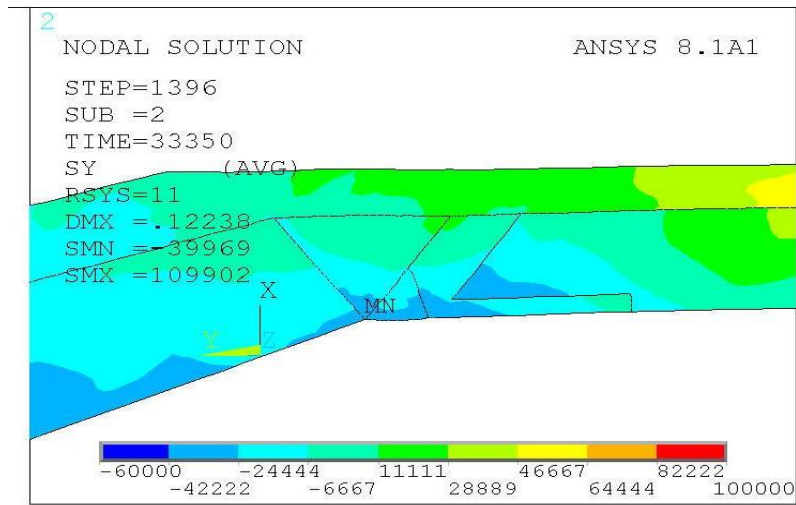


Figure 5-11
FEA Model for the PWOL Mockup

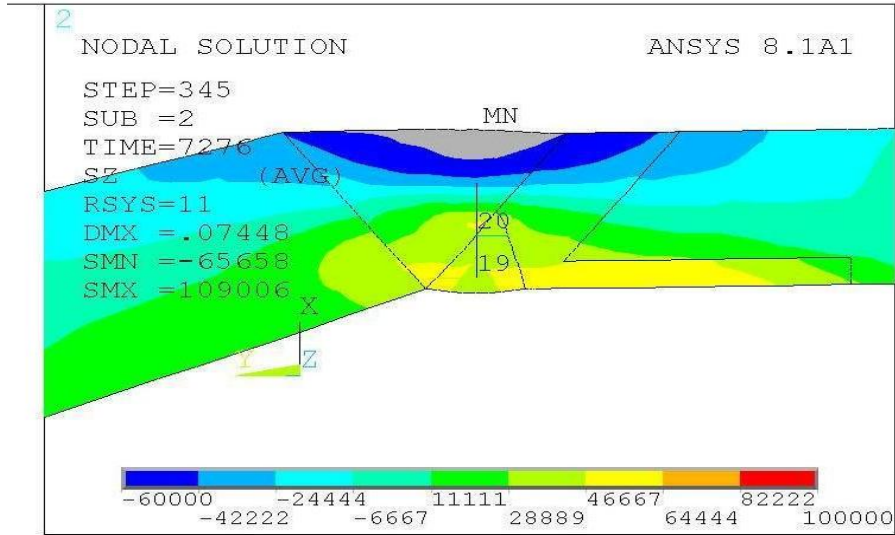


Pre-overlay

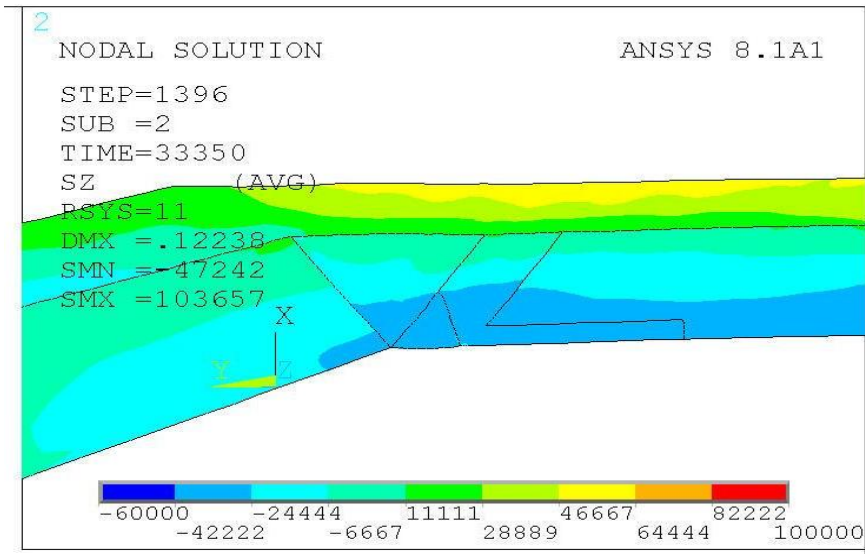


Post-overlay

Figure 5-12
Analytical (FEA) Hoop Stress Results for the PWOL Mockup



Pre-overlay



Post-overlay

Figure 5-13
Analytical (FEA) Axial Stress Results for the PWOL Mockup

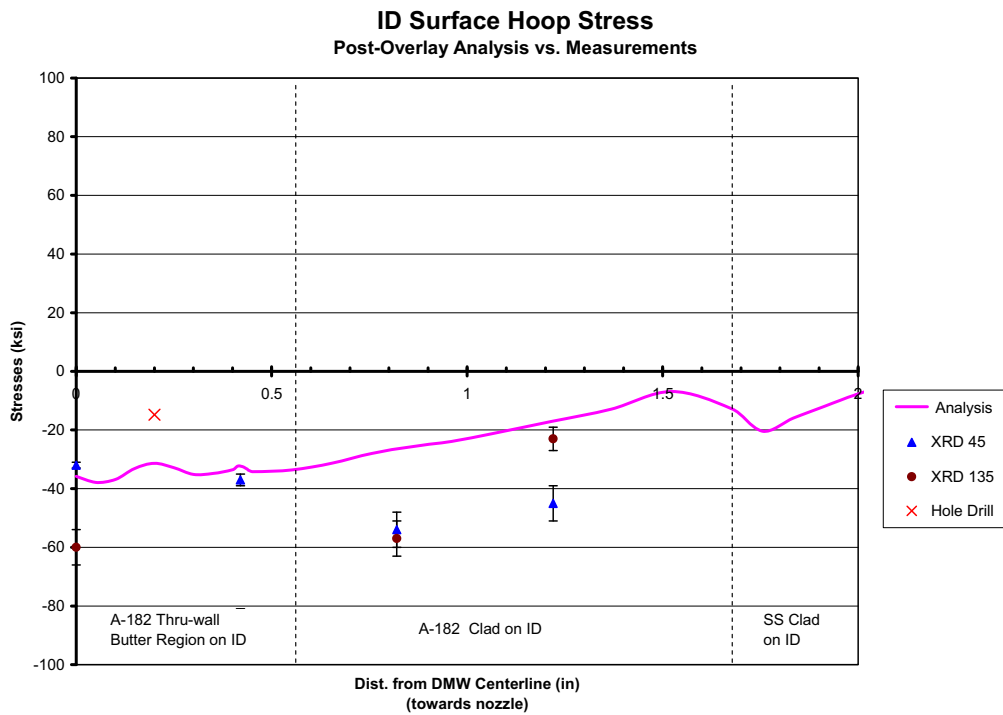
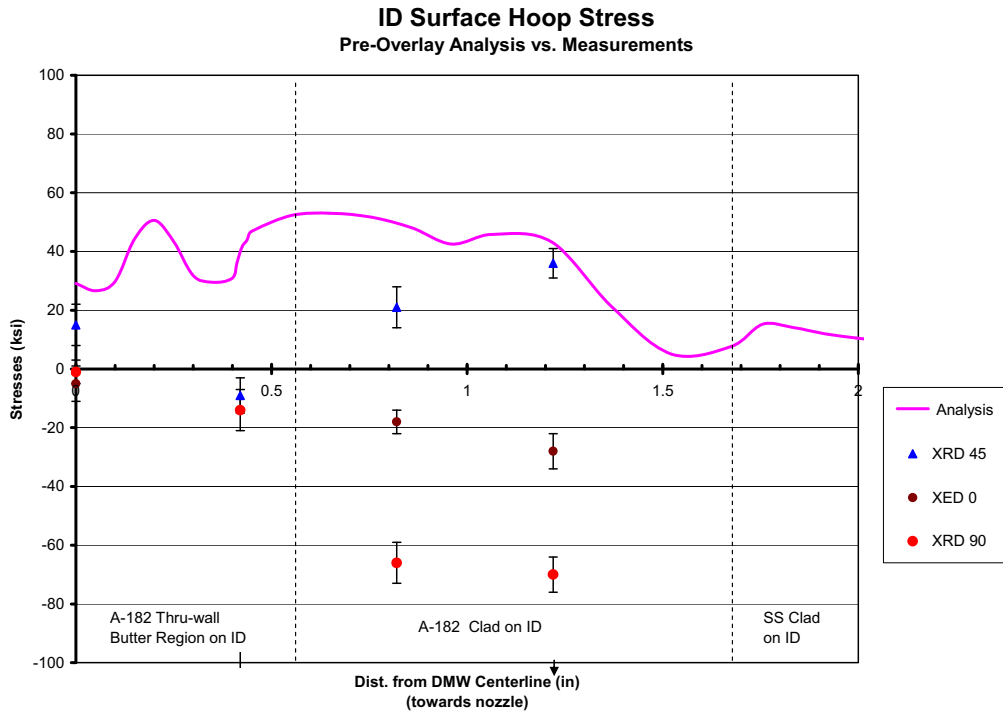


Figure 5-14
Comparison of Analytical vs. Measured Hoop Residual Stress Results for PWOL Mockup

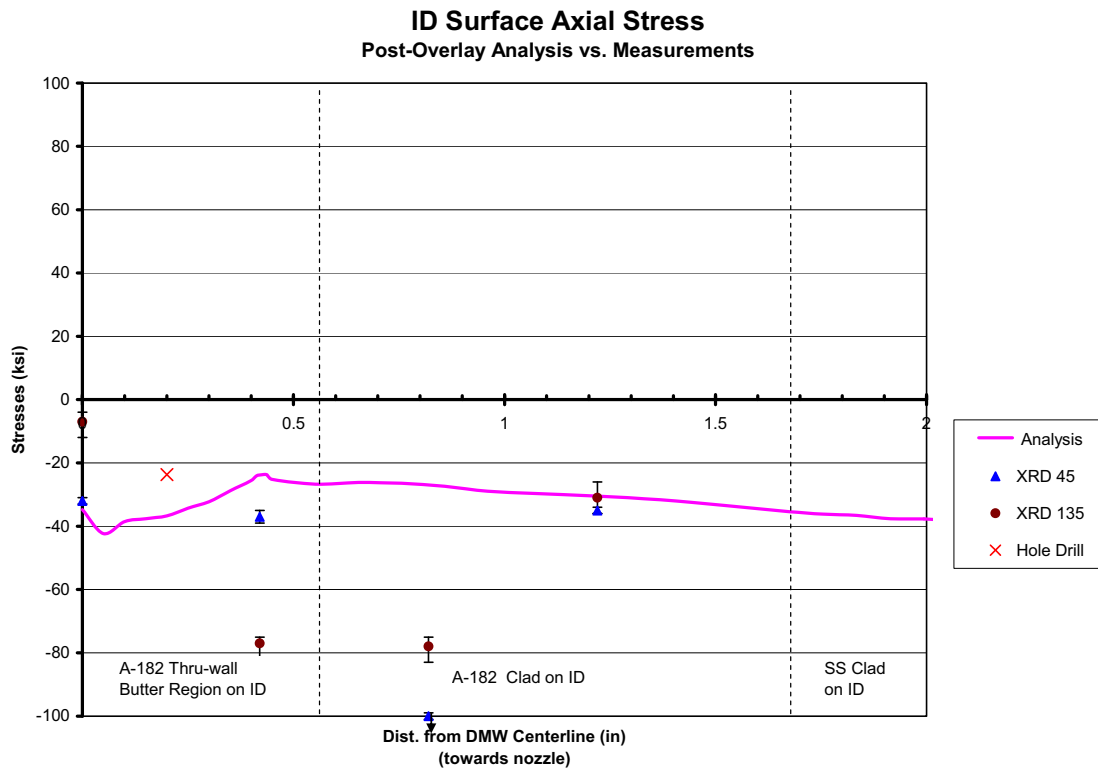
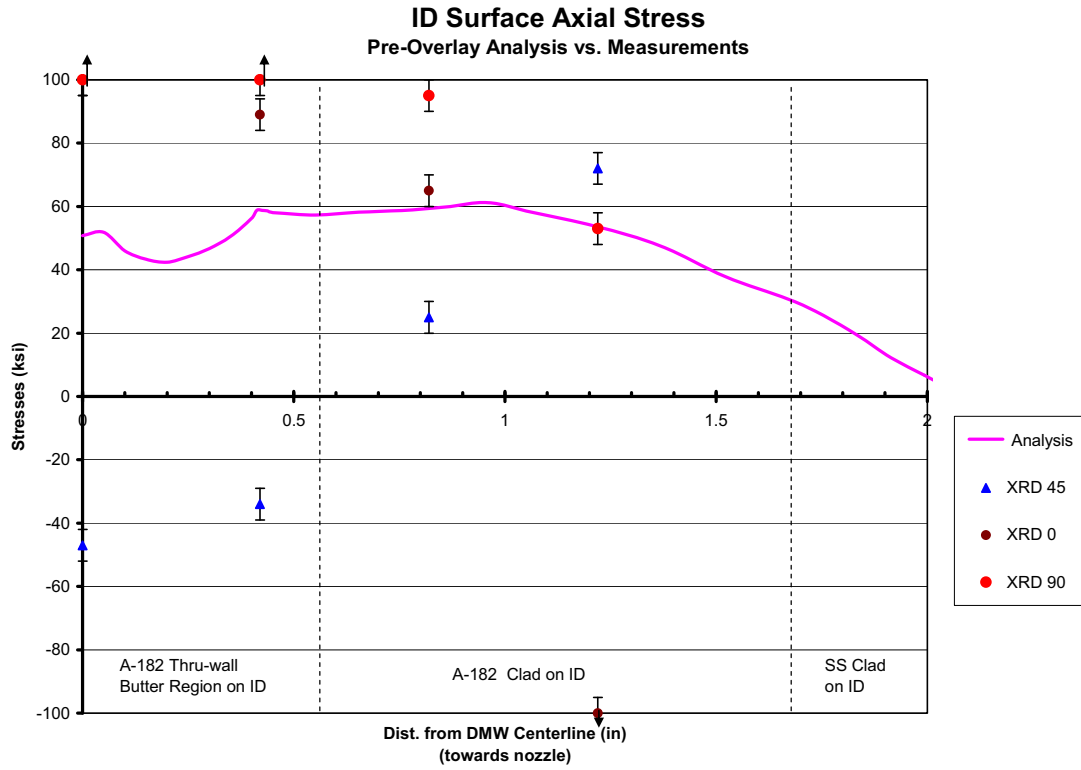


Figure 5-15
Comparison of Analytical vs. Measured Axial Residual Stress Results for PWOL Mockup

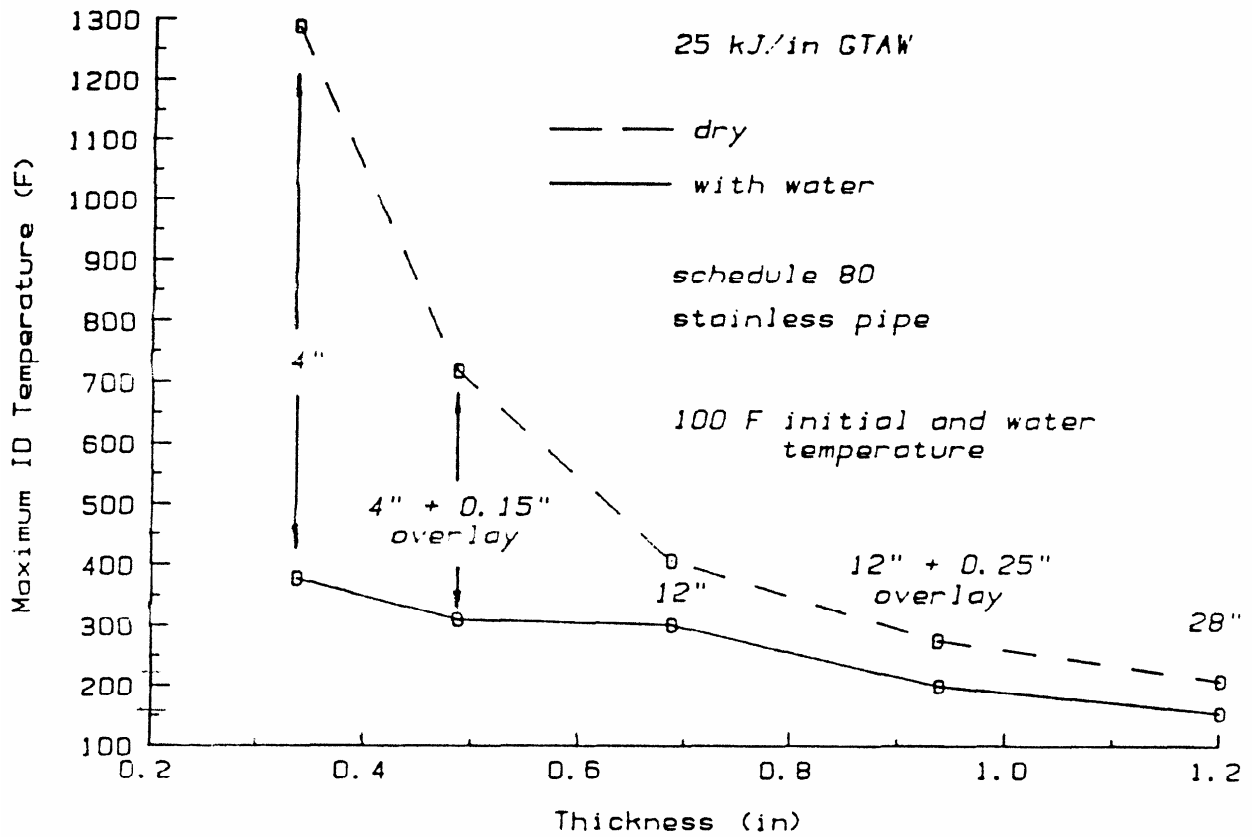


Figure 5-16
Effect of Wall Thickness on Maximum ID Temperature [12]

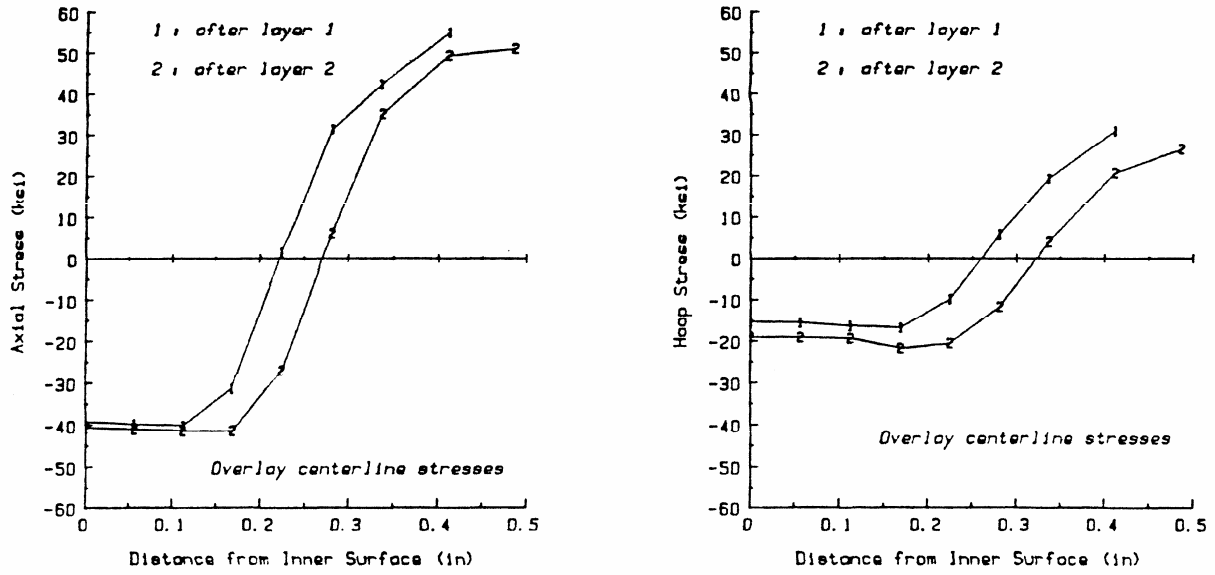


Figure 5-17
 Predicted Stresses for the 4-Inch Pipe Overlay Welded Dry [12]

6.0 MATERIALS AND WELDING CONSIDERATIONS

6.1 Background

Coriou first reported cracking of high nickel alloys in pure water in 1959. In 1986, a leak occurred from a pressurizer instrument nozzle welded into the pressure vessel by a J-groove weld at San Onofre Unit 3. Leaking of pressurizer heater sleeves was first reported in 1987 at Arkansas Nuclear One (ANO) Unit 2 and in 1989 in 20 pressurizer heater sleeves at Calvert Cliffs Unit 2. The pressurizer heater sleeves at Calvert Cliffs were reamed on the inside surface to facilitate installation of the heaters. Several other failures in pressurizer instrument nozzles, steam generator drain nozzles, steam generator plugs and tubes occurred in the late 1980's.

The first leak in a control rod drive mechanism (CRDM) nozzle occurred in Bugey 3 in 1991. Additional cracking was identified in an EDF "cold head" (554°F) plant in 1992. In addition to axial cracking above the J-groove weld, circumferential cracking and cracking in the J-groove weld were identified on the OD surface of the nozzle removed from Bugey 3. Further, a small crack was found from the results of NDE examinations of CRDM nozzle at D C Cook 2 in 1994. Several other leaks occurred at other nozzles and safe ends in the 1990s.

In 2000 and 2001, cracks were found in Reactor Coolant System piping butt welds at Ringhals and V C Summer plants. In addition cracks and or leaks were found at some of the CRDMs at all units of the Oconee plant, at both of the North Anna plants in some CRDMs, at Arkansas Nuclear One Unit 1 in one CRDM, at some of TMI CRDMs, at some of the Surry Unit 1 CRDMs and at one CRDM at Crystal River Unit 3.

In 2002 and 2003 cracking and associated severe wastage around the CRDMs were found at Davis Besse Plant. In addition, more cracking/leakage of CRDMs/CEDMs and thermocouple penetrations in the reactor vessel head were found at Milestone Unit 2, North Anna Unit 2, ANO 1, Oconee 1 and 2, and St. Lucie Unit 2. In addition, cracking of the bottom head instrument nozzles was found at South Texas Project Unit 1. Further additional cracking was found in pressurizer instrument, heater sleeve and safety relief nozzles at four additional plants.

The common thread to all of these failures was primary water stress corrosion cracking (PWSCC) of Alloy 600 nozzles and associated Alloy 182 weldments in Reactor Vessel Heads and Pressurizers. The causes of the failures were high residual stresses from the weld and operating stresses and susceptible materials in the nozzles and welds and the aggressive PWR water environment. In some cases the cracking was exacerbated by cold working of the surface exposed to reactor coolant. The PWSCC also demonstrates temperature sensitivity; both in the laboratory and in the field with higher temperature locations such as RCS hot leg and pressurizer attachments exhibiting far more cracking than colder locations. The cracking in the South Texas Project Bottom Head Instrument nozzles, however, demonstrates that even components operating at essentially RCS cold leg temperatures are not completely immune to PWSCC.

As a result of the cracking incidents in Alloy 600 and its associated weld metals in the PWR environment, the PWR industry has undertaken a major initiative to understand the mechanism responsible for the PWSCC, and to identify and develop new nickel base wrought and weld metals that are highly resistant to PWSCC. These alloys currently include Alloy 690 and its weld metals, Alloy 52 and 152, Alloy 52M and Alloy 52 MS.

6.2 Metallurgical Considerations on Service Performance

This section includes technical discussion on the metallurgical and chemical characteristics that have been studied to help understand why Alloy 690 and its weld filler materials are more resistant to SCC in a PWR primary system aqueous environment than Alloy 600 and its filler metals. Operating experience with these higher chromium, Alloy 690 materials in such applications as steam generator tubes, CRDM and CEDM nozzles, pressurizer heater sleeves, and instrument nozzle replacements have provided proof of the efficacy of the laboratory and research test results.

Microstructural Morphological Characteristics That Maximize PWSCC Resistance in Alloy 690

There has been a significant body of work (spanning 30+ years) attempting to determine and define the metallurgical mechanism (or mechanisms) that initiate and grow PWSCC cracks in Alloy 600, however none has been proven and universally accepted.

Since Alloy 600 and 690 vary only in their chromium to nickel ratios, Alloy 600 has nominally 15.5 w% chromium and 72 w% nickel, whereas alloy 690 nominally has 30 w% chromium and 60 w% nickel; the same unknown mechanism that afflicts Alloy 600 is commonly assumed to affect Alloy 690 as well. Therefore, the same micro-structural morphological characteristics that improve Alloy 600's PWSCC resistance are assumed to improve Alloy 690's as well.

Although the exact mechanism for PWSCC has not been identified, extensive laboratory research and empirical field evidence has determined the optimal micro-structural features that maximize Alloy 600's and Alloy 690's resistance to PWSCC [15-18], which include:

- A nearly continuous network of chromium carbides that have heterogeneously precipitated on the grain boundaries increases the PWSCC resistance of Alloy 600 and general SCC resistance of Alloy 690. There does not seem to be any difference in effectiveness of varying thermal treatment as long as the grain boundary carbide network is created [19]. In contrast, a homogeneously nucleated intra-granular dispersion of fine carbides has been shown to decrease resistance to PWSCC (relative to a grain boundary network).
- In addition to having carbon segregated as second phase carbides on grain boundaries, investigators [21] have indicated that having carbon in solution also helps prevent PWSCC.
- A finer grain size is more susceptible to PWSCC than a larger one [21].

- A cold worked microstructure is more susceptible to PWSCC [22]. If the cold worked microstructure is completely compressive then cracking will not occur, but if the applied stress exceeds the new yield strength of the cold worked material, cracking susceptibility is increased by the dislocation structure.

Compositional Chemistry Effects and Differences between Alloy 690 and Alloy 600

The nominal chemical compositions of the reference Alloy 600, candidate Alloy 690 and their weld metals (Alloys 52 and 152 for Alloy 690, and Alloys 82 and 182 for Alloy 600), are presented in Table 6-1 [20]. The most obvious difference among the alloys listed in the table is the dramatically higher chromium content and lower carbon content for Alloys 690, 52, 152 and 72. These compositional limits were initially specifically designed to minimize chromium carbide precipitation at the grain boundaries and increase intergranular stress corrosion cracking (IGSCC) resistance in high temperature oxygenated environments that exist in BWRs. The higher chromium in the Alloy 690 and its weld metals, combined with the presence of a nearly continuous network of carbides at the grain boundaries also convey the PWSCC resistance to this family of alloys.

Surface Oxide Differences between Alloy 690 and Alloy 600

Alloys 600 and 690 were tested in simulated PWR primary water (1200 ppm B and 2 ppm Li) at 680°F (360°C) under electrochemical conditions corresponding to Ni/NiO equilibrium potential that corresponds to the maximum sensitivity of Alloy 600 to the initiation of PWSCC [22]. The resulting oxidized structures (corrosion scale and underlying metal) were examined by transmission electron microscopy (TEM) using cross section specimens, Figure 6-1, and by energy dispersive X-ray spectroscopy (EDX) analysis, Figure 6-2. In both the Alloy 690 and Alloy 600 cases a non-compact external oxide scale was evidenced while an inner thin continuous layer rich in chromium was observed. Consequently, a chromium depleted zone just in the underlying alloy was observed, Figure 6-3. For Alloy 600, the particular importance of the depletion was found to be also associated with the presence of oxygen. Chromium oxide was even found in a triple grain boundary as far as 3 μm from the metal-oxide interface as sketched in Figure 6-4.

These test results tend to support the crack initiation mechanism induced by intergranular oxidation of the chromium-depleted zones [23]. Assuming that this mechanism is operative in these exposure conditions, it is then possible to explain, at least in terms of local reactivity, the effect of the carbide precipitation sites (transgranular- intergranular) on the crack initiation resistance of Alloy 600 exposed to PWR experimental conditions. The chromium depletion of Alloy 600 from only 16% to 5% is below the 10% Cr “threshold” where internal oxidation occurs. Most importantly, when considering Alloy 690, despite its chromium depletion from 29% to 17% in the underlying alloy, chromium content of Alloy 690 remains so high (17%) that the proposed mechanism becomes inoperative and the immunity of Alloy 690 to crack initiation can be explained.

Oxide rupture strain measurements were conducted at 550°F (288°C) on N-9Fe-xCr specimens with chromium levels from 4.6 to 39% wires in aerated (2-3 ppm dissolved oxygen) primary-

type water using the constant extension rate test (CERT) technique [24]. The oxide rupture strain, ϵ_T , was approximately 0.0010 from 4.6 to 23% Cr, but dramatically increased to 0.0020 to 0.0025 for 23 to 39% Cr, Figure 6-5. This result demonstrates that the oxide film on Alloy 690 is indeed more protective due to the higher chromium content and requires a higher strain to rupture the protective film.

Corrosion Potential Differences Between Alloy 600 and Alloy 690

Although little corrosion propensity data can be gleaned from the corrosion potential, per se, it is anticipated that due to Alloy 690's significantly higher chromium content, Alloy 690's passivation region will be larger than Alloy 600's region of passivation. This hypothesis is verified in Figure 6-6 where the anodic polarization curves for Alloy 600 and Alloy 690 exposed to identical pH 10 NaOH environments at 90°C indicate that the passivation range is indeed greater for Alloy 690 [25].

6.3 Welding Considerations

Technology

Considerable experience has been gained in welding Alloy 690 components in repair and replacement activities over the past few years. The alloy and filler materials used have been incorporated in the ASME Boiler and Pressure Vessel Code and may be used without dialog with the regulatory authority. The filler materials are designated SFA 5.14, ER NiCrFe-7 (Alloy 52) filler wire and E NiCrFe-7 (Alloy 152) covered electrode. In the case of these filler materials for Alloy 690, the compositions of the wire and electrode, including the Cr content, are similar to the base material, unlike the Alloy 182 covered electrode used to weld Alloy 600 base material. Most welding activities to date have used the Alloy 52 wire applied with the automated GTAW process. There has been some use of manual GTAW where access or geometry limits the use of automated equipment. SMAW using Alloy 152 has been used for buttering of dissimilar materials, often prior to a post weld heat treatment. All three of these materials are nickel based having the same high chromium composition (28% to 30% Cr). The main difference in composition between the coated electrode and the solid wire is in the niobium (columbium) and tantalum content introduced for carbide control. The proper balance of these stabilization elements is required to eliminate hot cracking. GTAW, nonetheless, may be preferable for buttering since the process generally reduces the inclusion content in the weld metal.

Both Alloy 82 and Alloy 52 are fairly difficult to weld [26]. In the early 1990s micro fissuring was identified in Alloy 82 welds. The concern was that the micro-fissures could be exposed to the reactor operating environment and serve as initiation sites for IGSCC. In particular three types of problems are associated with welding with Alloy 52. The first problem associated with welding with this material is the formation of oxides from the Al and Ti deoxidizers and small amounts of tramp Mg in the alloy. These oxides manifest themselves as floaters that give problems in the downward progression when welding. Filler material suppliers are studying modifications to chemistry of the filler material by reducing the amount of deoxidizers to mitigate this problem. The second problem with the both Alloy 82 and 52 filler material is solidification

(hot) cracking. Alloy 52 is believed to be somewhat more resistant to hot tearing than Alloy 82. The third problem associated with Alloy 52 and some heats of Alloy 82 is ductility dip cracking. Ductility dip cracking (DDC) is an elevated temperature solid-state cracking phenomenon that occurs in normally ductile materials. DDC occurs inter-granularly during the cooling cycle due to a sharp dip or loss of ductility at or slightly below the recrystallization temperature. DDC is typically defined as occurring above $\frac{1}{2} T_L$ (liquidus temperature) at grain boundaries free of liquid films. Cracking occurs when weld shrinkage strains or fabrication strains intercept this dip in ductility. Testing has shown that the filler materials, Alloy 52 and 82, are susceptible to DDC in the temperature range of 650°C (1202°F) to 1200°C (2192°F). A comprehensive discussion of this problem and the supporting test data can be found in [26]. When welding with Alloy 52, restraint should be reduced in the weldment design, welding should be uphill only and heat input should be well controlled within the parameters qualified.

More recently slight modifications in the chemical composition have been made to Alloy 52(UNS N06052) filler materials by increasing the Mn in the typical composition to 0.80, increasing the Nb(Cb) in the specification 0.50-1.0 with the typical composition to 0.80 and reducing the Al typical composition to 0.15 and the Ti typical composition to 0.30 to a filler material designated 52M(UNS N06054). In addition the filler material has received special processing to reduce impurities. With the changes in chemistry and improvements in welding technique, most of the problems discussed above have been eliminated.

Implementation

Welding with Alloy 52 and 52M filler materials requires care because of the concerns identified above. Weld overlays have been used in both BWR and PWR applications using these materials. In most BWR and PWR applications, a dissimilar metal weldment (Alloy 182 filler) between a low alloy steel nozzle (i.e. SA 508) and an austenitic stainless steel piping component/safe-end or an Alloy 600 safe-end is the location requiring repair or mitigation. Provisions in ASME Code Case N-504-2 have been utilized for the design, fabrication, and examination of these weld overlays. A Code Case providing specific requirements for weld overlays of dissimilar weldments (N-740) is currently under development by ASME, Section XI Code Committees. The requirements of ASME Code Case N-638 for ambient temperature temper bead welding have been used to provide adequate tempering of the low alloy steel nozzle material to assure that sufficient fracture toughness and ductility are maintained. Work is under way at ASME to expand or eliminate the 100 square inch surface area limitation for temperbead welding on low alloy steels from the Code Case. Alloy 52 filler material with a Cr content of 28 to 30% has been used exclusively in past overlay applications. This provides an overlay that is highly resistant to PWSCC crack initiation. In past Alloy 52 welding applications, restraint has been reduced in the weldment design welding with GTAW process. It can be beneficial to weld uphill to control floaters. A controlled heat input, within the parameters qualified, can also improve the ability to obtain a sound weld meeting the required acceptance standards. Considerable progress has been made using strict control of power ratio to increase deposition rates and limit dilution especially of the first layer. In a white paper supporting Code Case N-740, 20% Cr was found acceptable for the first layer for BWR applications and 24% Cr was found acceptable for PWR applications, if the composition of the layer is confirmed by chemical analysis of the layer in the field or on a mockup. In cases in which of a layer on a mockup is used to qualify first layer

chromium content, the welding parameters used to deposit the layer on the mock up would have to be used for the field weld. Code Case N-740 and the supporting white paper are posted on the ASME Code website.

Industry design and welding resources are well aware of the potential problems associated with welding these high nickel alloys and have utilized the uphill welding progression (for orbital welding), and the heat input controls necessary to control the welding problems. This care in welding has resulted in successful application of Alloy 52 or 52M to many dissimilar metal welding applications in both BWRs and PWRs.

6.4 Summary

This section of the report described the materials and welding issues associated with the use of Alloy 690 and its weld metals Alloy 52 and 152 for PWR primary water application. The following observations were presented:

- The microstructure of the wrought Alloy 690 can be controlled such that resistance to PWSCC can be optimized.
- Controls are specified to reduce the likelihood of hot cracking, oxide formation, and ductility dip cracking when welding using the Alloy 690 weld metals. Even with these controls, these weld metals remain difficult to weld and when welding with Alloy 52 restraint should be reduced in the weldment design, welding should be uphill only during orbital welding and heat input should be well controlled within the parameters qualified.
- Alloy 52M and 52 MS along with care and attention to power ratio and other welding parameters have improved the ability of vendors to deposit sound overlays.

In summary, the combination of the high chromium in the Alloy 690 family of nickel based alloys combined with materials and fabrication controls as described above, produce materials highly resistant to PWSCC initiation and growth in the PWR environment. Care must be taken in welding these alloys as noted in this section and in supporting reference materials. Implementation of the welding technology has been included in the ASME Code and been demonstrated by successful past field projects.

Table 6-1
Compositions of Nickel-base Alloys and Weld Metals [21]

Alloying Element	Alloy 690 (Nuclear)	Alloy 52 Filler metal (R-127)	Alloy 152 Electrode (R-135)	Alloy 72 Filler metal (nominal)	Alloy 600	Alloy 82 Filler metal	Alloy 182 electrode
Ni + Co	58.0 min.	Balance	Balance	55	72.0 min.	67.0 min.	59.0 min.
C	0.04 max.	0.04 max.	0.05 max.	0.05	0.15 max.	0.10 max.	0.10 max.
Mn	0.5 max.	1.0 max.	5.0 max.	0.1	1.0 max.	2.5-3.5	5.0-9.5
Fe	7.0-11.0	7.0-11.0	7.0-12.0	0.2	6.0-11.0	3.0 max.	10.0 max.
S	0.015 max.	0.015 max.	0.015 max.	0.008	0.015 max.	0.015 max.	0.015 max.
Si	0.50 max.	0.50 max.	0.75 max.	0.1	0.50 max.	0.50 max.	1.0 max.
Mo		0.50 max.	0.50 max.				
Cu	0.50 max.	0.30 max.	0.50 max.	0.20	0.50 max.	0.50 max.	0.50 max.
Cr	28.0-31.0	28.0-31.5	28.0-31.5	44.0	14.0-17.0	18.0-22.0	13.0-17.0
Ti		1.0 max.	0.50 max.	0.6		0.75 max.	1.0 max.
Al		1.10 max.	0.50 max.				
P		0.020 max.	0.030 max.			0.030 max.	0.030 max.
Nb + Ta		0.10 max.	1.0-2.5			2.0-3.0	1.0-2.5
Al + Ti		1.5 max.					
Others		0.50 max.	0.50 max.			0.50 max.	0.50 max.
N bar (>12)	0	6.82	9.1	3.12	0	5.85	5.85
SCRI (>34)	26.34	37.34	43.18	44.18	-0.48	32.85	22.85

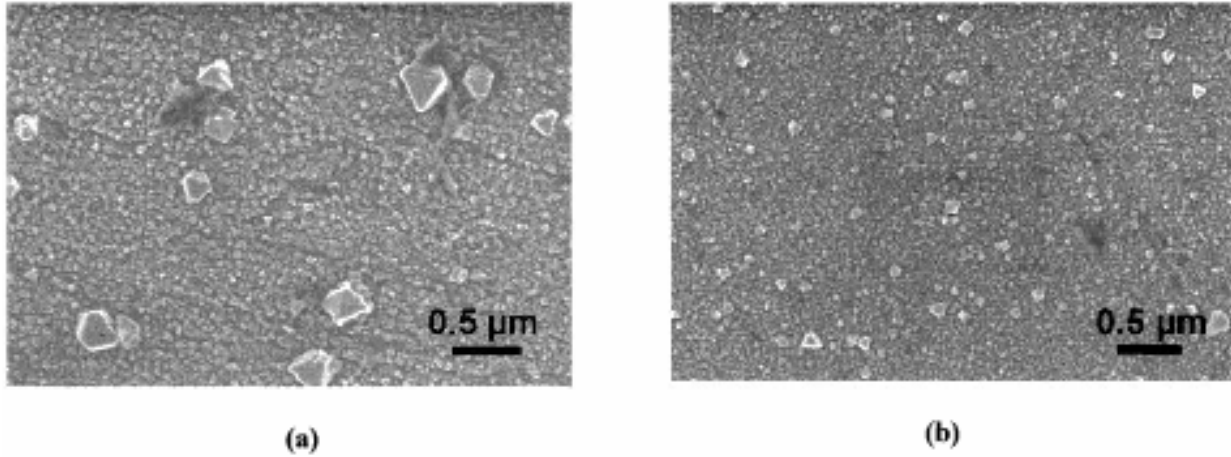


Figure 6-1
Oxide Film Developed on Alloy 600 (a) and Alloy 690 (b)

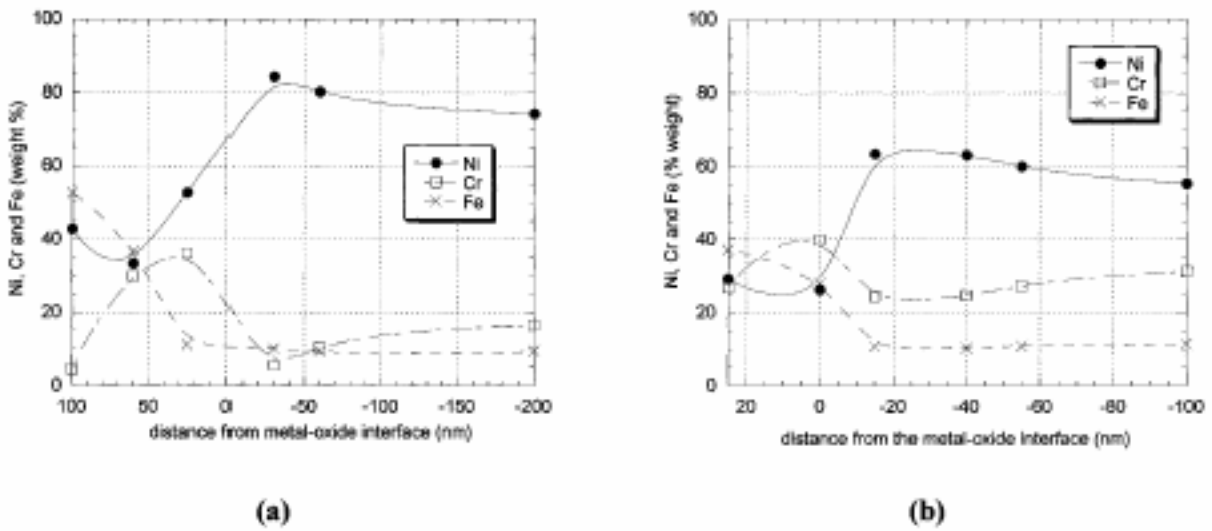


Figure 6-2
Composition of Ni, Cr and Fe as a Function of the Distance from the Metal-Oxide Interface on Alloy 600 (a) and Alloy 690 (b) [22]

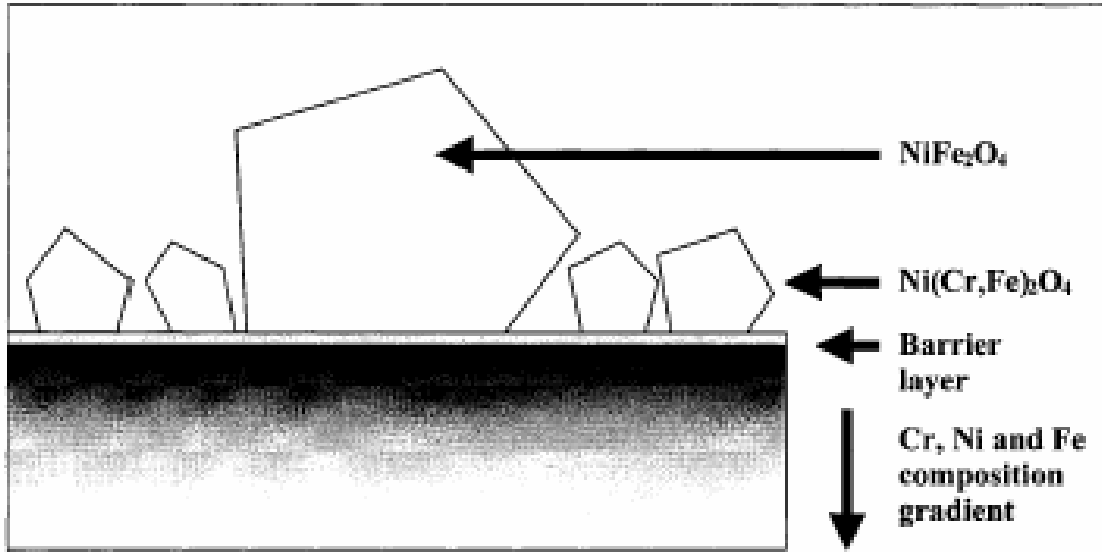


Figure 6-3
Sketch of the Oxide Film Developed on Alloy 600 and Consequences on the Underlying Metal [22]

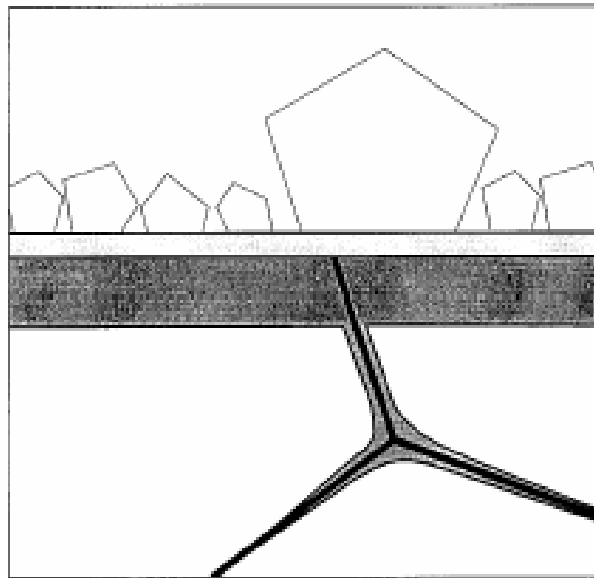


Figure 6-4
Sketch of the Depletion in Chromium under the Oxide Scale Associated with Enrichment in Oxygen at a Triple Grain Boundary [22]

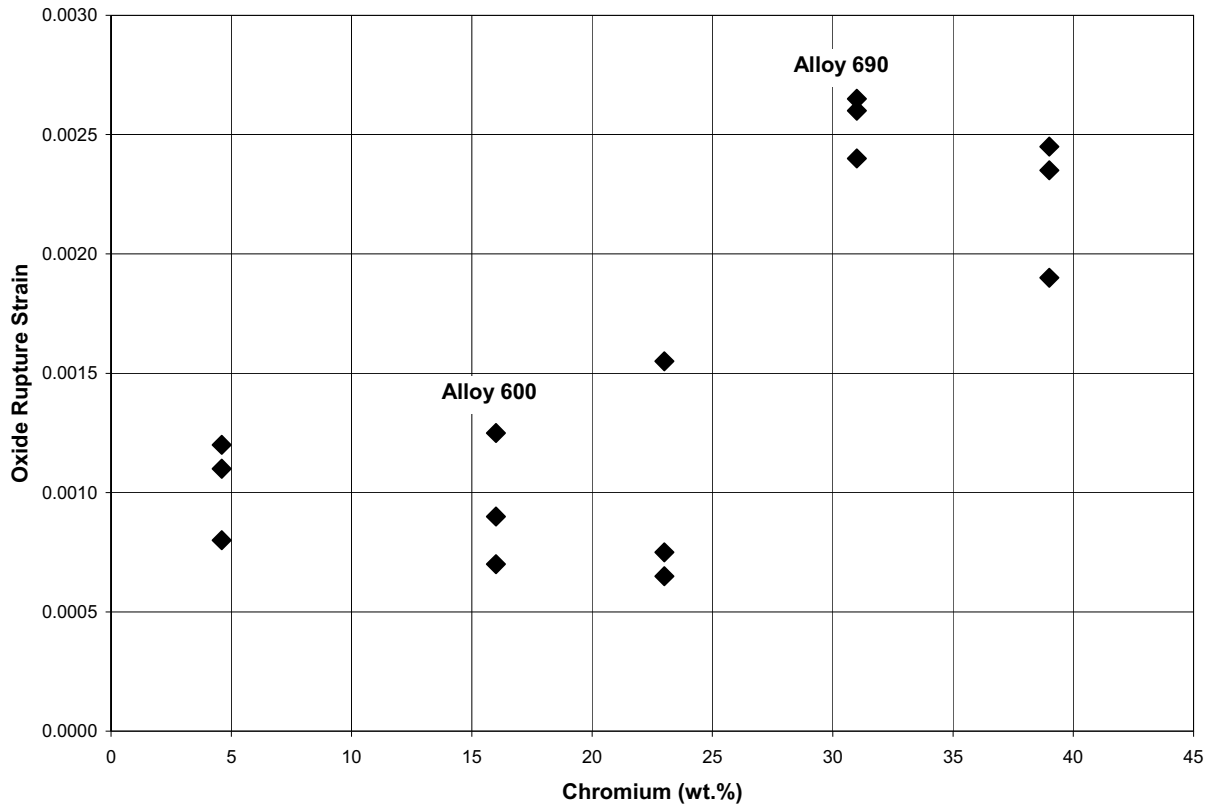


Figure 6-5
The Effect of Cr on the Oxide Rupture Strain of Ni-9Fe-xCr Alloys in Aerated Primary Water
[24]

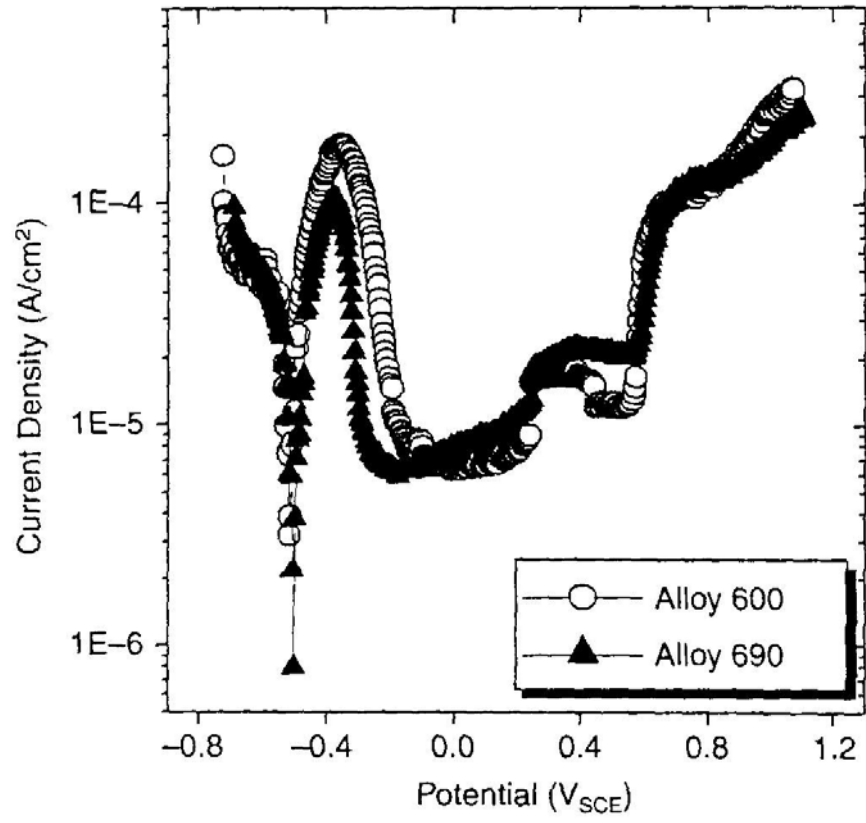


Figure 6-6
Polarization Curves for Alloy 600 and Alloy 690 in pH 10 90 °C Water [25]

7.0 EXAMINATION REQUIREMENTS

Examination requirements for weld overlays of PWR system butt welds involve two aspects. One is the type of examination and the other is the required interval. Both of these aspects of examination requirements are well defined for BWR system weld overlays due to significant experimental, analytical and field experience, such that a reasonable adaptation can be developed for preemptive weld overlays of PWR system butt welds.

7.1 Requirements for Types of Examination for Weld Overlays

The requirements for the type of examinations and associated examination volumes for full structural weld overlays are defined in Section XI Appendix Q and ASME Code Cases N-504-2 and N-740-2.

These requirements are consistent with current PDI techniques and were originally developed for weld overlay repairs of IGSCC in BWR stainless steel welds, where the initiating flaws are fully characterized with respect to length and depth. Since the full structural weld overlay designs for these repairs assumed that the original flaw is completely through the original pipe wall, inspection of the outer 25% of the original pipe wall along with the weld overlay is specified for pre-service and subsequent inservice examinations, such that it provides some advance warning if flaw were to unexpectedly propagate into that region, before they violate the overlay design basis. Also, the ultrasonic examination technology available at the time Code Case N-504-2 was issued could reliably support examinations of the outer 25% of the original pipe wall.

For optimized overlays (OWOLs), where the weld overlay design assumes the existence of a flaw 75% through the original wall thickness, it is desired to provide a similar “advance warning” examination volume for the unlikely event that a flaw would initiate and begin propagating after application of the PWOL. For this design assumption, examination coverage for weld overlay preservice inspections and subsequent inservice inspections is increased to include the thickness of the weld overlay plus the outer 50% of the original pipe wall thickness. This will provide additional margin to account for the uncertainty regarding the pre-weld overlay status of the original weld and is well within current ultrasonic examination capabilities. For full structural preemptive weld overlays, where the weld overlay design assumes the existence of a flaw 100% through the original pipe wall, inspection of the outer 25% of the original pipe wall along with the weld overlay will continue to be the requirement. Details of the examination requirements and exam volumes for both FSWOLs and OWOLs are provided in Figure 7-1. These are consistent with the current requirements for FSWOLs (Section XI Appendix Q and ASME Code Cases, N-504-2 and N-740-2) and the expanded exam volume requirement for OWOLs described above).

The following coverage requirements apply to the exam volumes specified in Figure 7-1. For the overlay acceptance examination, 100% of the required UT and PT exam volumes in Figure 7-1 a) shall be examined. For post-overlay pre- and inservice inspections, essentially 100% (>90%)

of the required exam volume in Figure 7-1 b) shall be examined, but shall include no less than 100% of any PWSCC susceptible material within the exam volume.

As discussed in Section 4, weld overlays must conform to the rules in the ASME Code, Section XI for welds in piping that require the procedures, equipment, and personnel to be qualified by a performance demonstration in accordance with Appendix VIII, as amended in 10CFR50.55a. Currently, the utilities use the PDI qualification process to satisfy these requirements. Procedures, equipment, and personnel used for examination of preemptive weld overlays shall be qualified in accordance with these rules [27, 42].

As an alternative to the above requirements, for cases in which current inservice inspection requirements are satisfied by inspecting the inner 1/3 of the original DMW from the inside surface of the nozzle, the utility may continue to perform such examinations, in lieu of the outside surface WOL examinations specified above. In such cases, the acceptance examination of the WOL plus the underlying HAZ (Figure 7-1(a)) is still required from the outside surface. Existing inside surface examination procedures may continue to be adequate for such inspections, but will require additional demonstration or qualification on weld overlay mockups to demonstrate that ID connected flaws are still detectable after application of the overlay and the associated compressive stresses.

7.2 Inspection Interval and Sample Size for Preemptive Weld Overlays

The inspection interval and sample size for IGSCC mitigating weld overlays in BWR weldments are defined in NUREG-0313. NUREG-0313 defines examination requirements in terms of the category of IGSCC susceptible weldment. The categories of weldments are based on 1) the IGSCC resistance of the materials in the original weldment, 2) whether or not stress improvement (or overlay) has been performed on the original weldment, 3) whether or not a post stress improvement UT examination has been performed, 4) the existence (or not) of cracking in the original weldment, and 5) the likelihood of undetected cracking in the original weldment prior to the application of the overlay. The categories range from A through G, with the higher letter categories requiring augmented inspection intervals and/or sample size. Category A is the lowest category, consisting of piping that has been replaced (or originally fabricated) with IGSCC resistant material.

The MRP Primary System Piping Butt Welds Inspection and Evaluation Guidelines (MRP-139) utilize a similar classification scheme [1]. Specifically, in accordance with MRP-139, PWSCC susceptible weldments with no known cracks (based on examination) that have been reinforced by a full structural weld overlay made of PWSCC resistant material are designated Category B. PWSCC susceptible weldments that contain known cracks that have been repaired by a full structural weld overlay are designated Category F.

For PWOL applications in which a pre-overlay examination is performed and no PWSCC-like indications are detected, the absence of cracking in the original weldment, the structural reinforcement and resistant material supplied by the overlay, the residual stress improvement provided by the PWOL, and the requirement to do a PDI qualified examination immediately following application of the PWOL are deemed to be consistent with MRP-139 Category B for

either full structural or optimized structural overlays. Therefore the following requirements for subsequent inservice inspections shall be satisfied:

1. For PWSCC susceptible weldments for which an inservice inspection is performed in accordance with ASME Code, Section XI, Appendix VIII, Supplement 2, 3 or 10 [27] immediately prior to application of the PWOL, and such inservice inspection demonstrates the weld to be absent of any flaws or crack-like indications, future ISI of the welds shall be performed in accordance with current ASME Section XI Code requirements. This requirement is consistent with MRP-139 Category B, except that it is independent of whether the PWOL is a full structural or optimized structural overlay.
2. For PWSCC susceptible weldments for which an inservice inspection in accordance with ASME Code, Section XI, Appendix VIII, Supplement 2, 3, or 10 [27] is not performed immediately prior to application of the PWOL, or in which flaws or crack-like indications are detected, the weldment must be assumed to be cracked. In such cases, future inservice inspections shall be performed consistent with requirements for cracked, WOL-repaired weldments (MRP-139 Category F). After the weld overlay and initial post-overlay examination, such weldments shall be inspected once in the next 5 years. If no new indications are seen or if no growth of existing indications is observed in the examination volume, the inspection interval shall revert to the existing ASME Code program.
3. In any case, if a post-overlay inservice inspection detects a planar flaw in the weld overlay PSI/ISI examination volume (Figure 7.1(b)), it shall be addressed in the crack growth analyses described in Sections 4.2 and 4.4. If the flaw is found acceptable, the weld overlay examination volume shall be reexamined during the first or second refueling outage following discovery of the flaw.

7.3 Dissimilar Metal Weld Examination Requirements

The current requirements for inservice inspection of dissimilar metal welds (> 4 Inch NPS) are defined in ASME Code, Section XI and summarized as follows:

Initial Preservice and Subsequent Inservice Inspections:

Surface: Liquid penetrant examination of weld and heat affected zone surfaces

Volumetric: Ultrasonic examination of inner 33% of original weld and heat affected zone

Requirements for the inspection interval and sample size for dissimilar metal welds are defined in ASME Code, Section XI as 100% of welds inspected every 10 years (Category B-F).

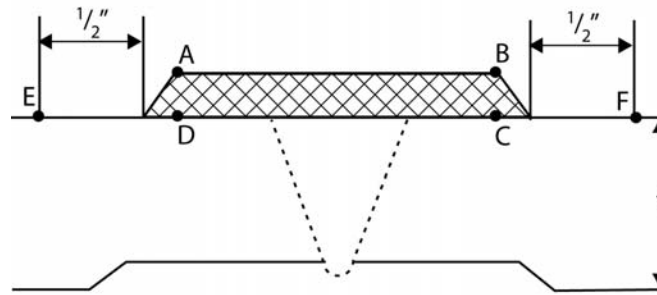
As noted above, the Materials Reliability Program (MRP), sponsored by EPRI, has issued MRP-139 containing guidelines requiring augmented examinations for PWSCC susceptible butt welds [1] that are similar in concept to the NUREG-0313 requirements for BWR IGSCC susceptible welds. These guidelines are not repeated here, but involve inspections as often as once every inspection period (3 1/3 years) for unmitigated welds in higher temperature locations of the reactor coolant system (e.g. pressurizer and hot leg nozzles).

In recent years, building on industry experience, many utilities have implemented risk-informed inspection approaches, consistent with ASME Code, Section XI Code Cases 560-2, 577-1 and 578-1. Some of these applications have resulted in elimination or reduction of examination of Alloy 82/182 locations. However, risk-informed ISI programs are required to be living programs. As such, recent industry experience with Alloy 82/182 cracking, including MRP-139 inspection guidance, must be incorporated as these programs are updated. For weld overlays performed on PWSCC-susceptible locations, either preemptively or as repairs, RI-ISI programs should be modified to include inspections consistent with the requirements of this document and Ref. [1]. However, it is anticipated that, at some future time, after inservice inspections have demonstrated successful operating experience with PWR overlays, additional inspection relief may be provided, as was done for BWR overlays in BWRVIP-75 [2]. Technical justification for such relief will be submitted for NRC review and approval.

a) Initial Acceptance Examination

Surface: Liquid penetrant examination of overlay material surface + ½ inch of base metal on either side of overlay (E-A-B-F)

Volumetric: Ultrasonic examination of overlay material (A-B-C-D) plus underlying HAZ (C-D) for fabrication welding defects

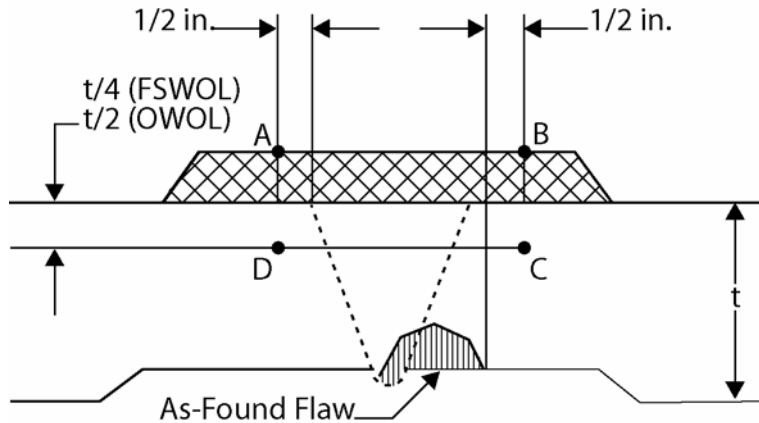


WOL Acceptance Examination Volume A-B-C-D

b) Preservice and Subsequent Inservice Inspections

Surface: Liquid penetrant examination of overlay material surface

Volumetric: Overlay directly over original PWSCC susceptible weldment (including nozzle, buttering, DMW and PWSCC susceptible safe-end if present) plus ½ inch to either side, to a depth of the outer 25% (FSWOL) or 50% (OWOL) of underlying material . (A-B-C-D)



Preservice and Inservice Examination Volume A-B-C-D

**Figure 7-1
Inspection Requirements for Weld Overlays**

8.0

EXAMPLE ANALYSES

Analyses are presented in this section demonstrating the design analysis requirements defined in Section 4 above for three example nozzles in high temperature regions of a typical PWR. The nozzles chosen for the example analyses are:

- Pressurizer upper head spray nozzle (Figure 8-1, chosen as representative of all pressurizer steam space nozzles),
- Pressurizer lower head surge nozzle (Figure 8-2), and
- Reactor Pressure Vessel hot leg nozzle (Figure 8-3).

The analyses performed and documented in this section include weld overlay sizing calculations based on typical nozzle loadings for both optimized structural and full structural overlays (Section 8.1); residual stress analyses to demonstrate the effectiveness of the weld overlays in mitigating future PWSCC (Section 8.2); PWSCC and fatigue crack growth analyses to demonstrate that cracks potentially missed by the applicable examinations will not grow unacceptably during the next inspection interval (Sections 8.3 and 8.4); and fatigue usage analysis to show acceptable fatigue life for the transition ends of a weld overlay (Sections 8.5). The sizing, residual stress and PWSCC crack growth analyses were performed for all three sample nozzles. The fatigue crack growth and fatigue analyses were performed only for the surge nozzle, since this nozzle is subject to significant flow stratification cyclic loadings, and therefore expected to be most limiting from a fatigue standpoint.

The analyses presented herein are examples only, based on industry-typical nozzle designs and loads. They are presented to illustrate the analytical methods and typical results. Implementation of a preemptive weld overlay on a particular plant or nozzle will require such analyses to be completed using plant-specific nozzle designs and loads, as well as the specific overlay designs to be implemented, to demonstrate that the design requirements of Section 4 are satisfied.

8.1 Weld Overlay Sizing Calculations

Structural sizing of weld overlay thickness is performed in accordance with ASME Code, Section XI rules for allowable flaw sizes in austenitic piping (IWB-3640 and Appendix C) [37]. Table 8-1 presents a copy of the controlling allowable flaw size table from Appendix C for Service Level B (upset) loading conditions. (Service Level B loading generally controls WOL sizing, since it includes OBE seismic loads.) Allowable flaw depths are presented in this table for flaw lengths ranging from 0 to 50% of the circumference or greater, as a function of primary membrane plus bending stress ratio, defined in Note 2 to the table. The allowable depths are presented in terms of fractions of the pipe wall thickness. As discussed in Section 4 above, for preemptive weld overlays, two types of design basis flaw assumptions will be considered – a crack depth equal to 100% of the original nozzle wall thickness (full structural overlays), and a depth equal to 75% of the original wall thickness (optimized structural overlays). In both cases,

the flaw length will be assumed to be 360° around the nozzle circumference (i.e. the last column in Table 8-1).

The weld overlay sizing algorithm is an iterative process, in which the overlay is applied, the stress ratio adjusted based on the new overlaid nozzle wall thickness, and the allowable flaw size determined for the new stresses and wall thickness. If the design basis flaw assumption is still larger (or smaller) than the new allowable, the weld overlay thickness is increased (or decreased), and the process is repeated until it converges to an overlay thickness and allowable flaw size that exactly equal the design basis flaw assumption. The iteration can be performed either using the tabulated allowables, as illustrated in Table 8-1, or alternatively using the “Analytical Solution” documented in Section XI, Appendix C. Since the weld overlay is being applied with Alloy 52 GTAW weld metal, the flow stress for the overlay material is approximated as $3 \times S_m$, where $S_m = 23.3$ ksi for Alloy 600 and 690 piping material at 650°F. For OWOLs, the flow stress for the lower strength stainless steel safe-end material (typically SA-376 Grade TP304 or TP316) must also be considered, based on $S_m = 16.1$ ksi for at 650°F.

Table 8-2 presents nozzle dimensions and Service Level B primary stresses (including normal operating and OBE seismic loads) for the three example nozzles. These loads are typical, but are by no means considered generic or bounding. These data were used in conjunction with the two-layer analytical process described in [51], to determine minimum required overlay thicknesses for the three nozzles for both the 100% thru-wall (FSWOL) and 75% thru-wall (OWOL) design basis flaw assumptions. In the case of OWOLs, the analyses also utilized Z-Factors from Ref. [49] to account for potentially lower toughness of the portion of the underlying DMW fusion line that is credited in OWOL design. The results are presented in Table 8-3. The resulting, optimized structural WOL thicknesses for the Spray and Surge nozzles were very small (< 0.1 ”). However, since the requirements of Code Case N-740-2 for temper bead welding require a minimum of three layers, the minimum weld overlay thicknesses have been set at 0.21” to accommodate three weld layers, assumed to be 0.07” each.

Minimum required weld overlay lengths were also calculated for the three example nozzles. In accordance with the length sizing criteria in Section 4.2, the minimum weld overlay length was set at $0.75\sqrt{Rt}$ beyond either end of the susceptible material on the nozzle outside surfaces. Based upon the lengths of PWSCC susceptible material (Alloy 82 /182 weld and buttering), and other dimensions shown in Figures 8-1 through 8-3, the resulting minimum weld overlay lengths have been computed, and are tabulated in the last column of Table 8-3.

The structural sizing results reported in Table 8-3 are minimum thicknesses and lengths. As discussed in Section 4.1, additional considerations of residual stress and inspectability must also be addressed, which may result in increased WOL thicknesses and lengths above these minimums.

8.2 Residual Stress Analyses

The primary purpose of preemptive weld overlays is to modify the as-welded residual stresses (caused by the butt weld, butter and possible in-process weld repairs during plant construction) to mitigate the concerns for PWSCC in these welds. The desired result is that post-WOL

residual stress on the inside surface of the nozzle, over the entire region of PWSCC susceptible material, in both the axial and circumferential directions, be sufficiently compressive, such that the total stress, when sustained operating loads are added, remain less than 10 ksi tension. This result will inhibit PWSCC crack initiation in any orientation. A further goal is that the residual plus operating stresses remain compressive for at least some portion of the nozzle wall thickness away from the inside surface, such that any PWSCC cracks which might already exist at the time of WOL application will be arrested and no longer a concern to cause leakage or loss of structural integrity.

As discussed in Section 5, extensive prior analysis and experimental verification have been performed for weld overlays in BWR piping and nozzles. Most of this work was performed for full structural overlays, but some analyses were performed that showed the benefits of designed weld overlays as well. To date, hundreds of weld overlays have been applied to welds in BWRs and there have been no reports of crack extension after application of the weld overlay. Thus, the compressive stresses caused by the weld overlay have been effective in mitigating crack growth in BWRs.

To obtain a bounding assessment of the impact of preemptive weld overlays on the PWSCC susceptible location, the residual stress assessment must consider residual stresses that exist prior to application of the overlay. Thus, the weld overlay analyses include residual stresses assumed to be present due to the as-welded condition plus any machining or weld repairs that may have previously occurred. Due to uncertainty in the initial weld condition, a severe as-welded stress distribution (significant tensile stress) that would promote PWSCC is assumed. ID weld repairs are known to develop severe residual stress fields and can also provide for flaw initiation sites due to grinding and weld defects. Thus, a fully circumferential, 50% of wall ID repair (Illustrated in Figure 8-4) was simulated in the three example nozzles, and the resulting stress fields are used as the initial stress states for the weld overlay residual stress analyses.

Original ID Weld Repair Weld Parameters

For the ID weld repair, the number of layers depends on the wall thickness and bead layer thickness. Typical heat inputs and torch velocities were assumed for the weld repair. A preheat temperature of 200°F was assumed before the weld root repair, with a maximum interpass temperature of 350°F.

Preemptive Weld Overlay Weld Parameters

For the weld overlays, actual weld parameters for a typical weld overlay were used in the analysis [29], including bead sequence and direction of welding. For the weld overlay, the weld torch travel speed was three inches/min. The bead width was assumed to be 0.25" and bead thicknesses were assumed to be 0.07" to 0.1". These assumptions were used to calculate the equivalent number of bead passes in the lumped weld pass approach used in the finite element analyses. Three to five lumped bead passes were used in each of the weld overlay layers depending on the length of the overlay. The number of equivalent bead passes was estimated from the lump pass areas in the model divided by the area of each bead pass.

A maximum interpass temperature of 350°F was used for the weld overlay. The progression of the overlay welding was from the safe end side to the nozzle side of the weld for the surge and hot leg nozzles or from the nozzle side to the safe end side for nozzles at the top of the pressurizer. A thermal efficiency of 75% was assumed for the welding process in the analyses.

Finite Element Models

The analyses were performed using ANSYS [30]. The finite element models for the residual stress evaluations of the three example nozzles are presented in Figures 8-5 through 8-7. These figures also illustrate the various materials in the models (via color coding). For inspectability reasons, the weld overlays on the spray and surge nozzles were assumed to cover both the stainless steel and Alloy 82/182 welds, which makes them longer than the minimum lengths listed in Table 8-3. Thicknesses were applied in incremental layers of 0.070" to 0.100" thicknesses, up to and beyond the minimum thicknesses in Table 8-3. Resulting stresses were checked at the end of each layer, and additional layers were applied until the residual stresses at the inside surface were deemed sufficiently compressive so as to meet the residual stress goals defined above.

Axisymmetric models were used for both the thermal and stress passes of the analyses. The lumped weld bead deposits were simulated by element "birth and death" capabilities in ANSYS. A roller boundary condition was applied at the thick nozzle end of the model in the stress pass instead of modeling the entire vessel. Temperature-dependent, non-linear material properties were used in the analysis as well as an appropriate strain-hardening model.

The analysis consists of a thermal pass to determine the temperature response of the model to each individual lumped pass as it is added in sequence, followed by an elastic-plastic stress pass to calculate the residual stress due to the temperature cycling from the application of each lumped weld pass. Since residual stresses are a function of the welding history, the stress passes for each lumped pass were applied sequentially, on top of the residual stress fields from the ID repair and all previously applied weld passes.

For the thermal analyses, heat convective boundary conditions were assumed consistent with the anticipated weld process for each nozzle. Pressurizer steam space nozzles were assumed to be welded dry, with a convection/radiation heat transfer coefficient of 5 Btu/hr-ft²-°F, consistent with air on the pipe ID. Pressurizer surge and RPV hot leg nozzles were assumed to be welded with water inside the pipe and vessel, assuming a convection heat transfer coefficient of 100 Btu/hr-ft²-°F to simulate water backing. These were shown to be conservative for the actual temperature and convective conditions that exist during welding, and thus this analysis is expected to under-predict the benefit from the weld overlay process. In the actual process, local boiling would provide a significant benefit in keeping the ID surface cold.

After the weld overlay simulations were completed, the models were allowed to cool to a uniform 70°F, cycled through a simulated pressure test and then heated up to a uniform 650°F in order to obtain the residual stresses at the maximum operating/upset temperature of the nozzles. Finally, applied operating pressure and sustained operating loads were applied.

It is recognized that there are many analytical assumptions in this modeling process. However, efforts were made in each case to make conservative assumptions, and the analytical process is similar to that used in analyses weld overlay mockups, for which stresses have been measured experimentally, and the process demonstrated to conservatively predict overlay residual stress benefits. The analytical process is being further validated via additional mockups and measurements.

Residual Stress Results

Pressurizer Spray Nozzle

Residual stress results for the pressurizer spray nozzle are presented in Figures 8-8 to 8-11. Figures 8-8 and 8-9 present contour plots of axial and hoop residual stresses before and after application of the PWOL. These are typical of the results for all nozzles, indicating high tensile residual stresses on the inside surface prior to the WOL application (red and orange contours in the upper plots of Figures 8-8 and 8-9) with a complete reversal to compressive stresses after PWOL application (blue, light blue, and light green contours in the lower plots of Figures 8-8 and 8-9). Figures 8-10 and 8-11 further illustrate and quantify these results. Figure 8-10 presents spray nozzle stress results along the inside surface of the nozzle, for three conditions, pre-WOL at 650°F and post-WOL at 650°F, with and without sustained operating loads. It is seen that the inside surface residual stresses are compressive in the post-WOL cases over the inside surface of the entire PWSCC-susceptible region of the nozzle to safe-end weld. Figure 8-11 presents through-wall stress plots, from inside to outside, over three paths in the PWSCC susceptible region. Path 1 is near the stainless steel safe end side of the original butt weld, Path 3 is near the LAS nozzle side, and Path 2 is in the middle, near the center of the assumed original construction repair weld. This figure illustrates that the axial stresses remain compressive on all three paths up to a depth of approximately 0.7", and the hoop stresses remain compressive or near zero up to a depth of approximately 0.45". The final spray nozzle overlay dimensions that produced these results are a WOL thickness of 0.3" and a WOL length of ~7.2", making this effectively a full structural overlay as defined in Table 8.3, but with the length increased for inspectability.

Pressurizer Surge Nozzle

Residual stresses for the surge nozzle are presented in Figures 8-12 and 8-13, in the form of pre- and post-WOL inside surface and through-wall residual stress plots. (Note that contour plots are not repeated for the other surge and hot leg example nozzles, since they all exhibit the same basic characteristics as shown in Figures 8-8 and 8-9, and the main results demonstrating the effectiveness of the PWOL process are more effectively illustrated and quantified via the surface and through-wall stress plots). Figure 8-12 illustrates the surge nozzle stress results along the inside surface of the nozzle, for three conditions, pre-WOL at 650°F and post-WOL at 650°F, with and without sustained operating loads. It is seen that the inside surface residual stresses are compressive in the post-WOL case over the inside surface of the entire PWSCC-susceptible region of the nozzle to safe-end weld, and after applying operating pressure and loads, remain compressive or very small (< 3,000 psi). Figure 8-13 presents through-wall stress plots, from inside to outside, over the six paths illustrated in Figure 8-6. Paths 1 and 2b are in the non-PWSCC susceptible stainless steel material and are included for information only. The other

four paths are at various locations in the PWSCC-susceptible region (Alloy 82 or 182 weld or buttering). This figure illustrates that the post-WOL axial stresses remain compressive on all paths up to a depth of approximately 0.8", and the hoop stresses remain compressive or near zero up to a depth of approximately 0.25". The final surge nozzle overlay dimensions that produced these results are a WOL thickness of 0.44" and a WOL length of ~9.8", making this effectively a full structural overlay as defined in Table 8.3, but with the length increased for inspectability.

Reactor Pressure Vessel Hot Leg Nozzle

Residual stresses for the RPV hot leg nozzle are presented in Figures 8-14 and 8-15, in the form of pre- and post-WOL inside surface and through-wall residual stress plots. Figure 8-14 illustrates the hot leg nozzle stress results along the inside surface of the nozzle, for three conditions, pre-WOL at 650°F and post-WOL at 650°F, with and without sustained operating loads. It is seen that the inside surface residual stresses are compressive in the post-WOL case over the inside surface of the entire PWSCC-susceptible region of the nozzle to safe-end weld, and after applying operating pressure and loads, remain compressive or very small (< 3,000 psi). Figure 8-15 presents through-wall stress plots, from inside to outside, over three paths in the PWSCC susceptible region. Path 1 is near the LAS nozzle side of the original butt weld, Path 3 is near the stainless steel safe end side, and Path 2 is in the middle, near the center of the original butt weld. This figure illustrates that the post WOL axial stresses remain compressive on all three paths up to a depth of approximately 1.25", and the hoop stresses remain compressive or near zero up to a depth of approximately 0.6". The final hot leg nozzle overlay dimensions that produced these results are a WOL thickness of 0.5" and a WOL length of ~11.6", making this an optimized structural overlay as defined in Table 8.3.

8.3 PWSCC Crack Growth Analysis

In accordance with the requirements of Section 4.2, the thru-wall stress distributions for the bounding paths in Figures 8-11, 8-13 and 8-15 were input to fracture mechanics models using the pc-CRACK computer program [28] to determine stress intensity factor versus assumed crack size under normal, sustained operating conditions. The results are illustrated in Figures 8-16, 8-17 and 8-18. The axial stress distributions were used in conjunction with a 360° circumferential flaw model in a cylinder of appropriate thickness to radius ratio. The hoop stress distributions were used in conjunction with an axial flaw model with an assumed aspect ratio (flaw depth over length) of 0.2. The vertical black lines in these figures represent the inner boundaries of the post overlay ISI examination volumes (75% through the original DMW for the FSWOLs on the spray and surge nozzles and 50% through the original DMW for the OWOL on the RPV hot leg nozzle). The results indicate that the resulting WOL residual stress distributions are very effective in arresting any circumferential cracks that might be present, since the stress intensity factors are highly compressive up to and beyond the post-WOL exam volumes. However, the stress intensity factors for axial cracks, although compressive for some depth, turn tensile at depths below the post overlay exam volumes. This result indicates that these overlay designs, and associated residual stress results, could not be used without a pre-overlay inspection. Such an inspection would have to confirm no axial cracking of depths greater than the points at which the stress intensity factors transition from compression to tension (0.52" for the spray nozzle,

0.3” for the surge nozzle, and 1.0” for the RPV hot leg nozzle). If cracking of greater depths than these were observed, larger, repair overlays would be required.

8.4 Fatigue Crack Growth Analysis

In this section a sample fatigue crack growth analysis is presented for a typical surge nozzle, including flow stratification loads.

Plant Transient Evaluation

For the fatigue crack growth evaluation, two major types of events were considered. First, the plant transients defined in a typical plant design specification were considered and included 500 heatup/cooldown events plus a range of additional transients associated with normal, upset and emergency plant operation. Secondly, surge line stratification transients evaluated as a result of NRC Bulletin 88-11 evaluations were included.

Detailed transient thermal analysis was conducted to evaluate the through wall thermal stress distribution for all thermal transients. For each thermal transient or other event, including stratification, two or more bounding stress states were defined. For each state, the pressurizer pressure, surge line mean temperature, reactor coolant hot leg temperature and maximum potential surge line stratification ΔT were defined, along with cubic polynomial stress coefficients to define the through wall distribution of stresses.

Thermal Stratification Stresses

The stresses due to thermal stratification at the pressurizer surge nozzle location are due to global thermal stratification moments and forces. There is no local stress distribution resulting from stratification because the nozzle is vertical. The stratification stresses were determined in accordance with same methodology that was used in the CE Owner’s Group report [31] that demonstrated that surge line fatigue usage was acceptable for a 40-year life.

Weld Residual Stresses

The weld residual stresses determined from the analysis presented in Section 8.2 were used. Residual stress results were determined at both room temperature and 650°F. For analysis of transients at intermediate temperatures, the residual stresses were linearly interpolated.

Pressure Stresses

The pressure stress distribution was determined from the finite element analysis described in the previous section.

Loading Combinations

For each event state, specific thermal conditions were evaluated. The “unit load” stresses were then scaled and combined to derive a total stress condition for each stress state. This resulted in

a set of four stress coefficients describing a cubic polynomial stress distribution for each stress state. The scaling was accomplished as follows:

- Dead weight stress was held constant
- Residual stresses were determined based on the surge line temperature at the weld overlay location. For outsurge transient with surge line stratification, the pressurizer temperature was used. For insurge transient with no stratification, the hot leg temperature was used.
- Bending stresses due to thermal stratification were scaled proportionally to the event ΔT between the pressurizer and hot leg..
- Surge line thermal expansion stresses were scaled proportionally to the surge line mean temperature.
- Hot leg thermal anchor movement stresses were scaled proportionally to the hot leg temperature.
- Pressure stresses were based on the pressurizer pressure.
- For the moment-related stresses, the stress distribution around the circumference of the piping was considered in developing the local stresses through the wall at different locations around the pipe circumference.

Fracture Mechanics Model

Fracture mechanics flaw growth evaluations were conducted to evaluate the growth of both hypothetical circumferentially-oriented cracks and axially-oriented cracks.

The fracture mechanics analysis for circumferentially-oriented cracks was based on a hypothetical initial 10-to-1 (l/a) aspect ratio inside surface circumferential flaw with depth equal to 10 percent of the initial pipe wall thickness. The fracture mechanics model was that developed by Chapuliot, et. al for a semi-elliptical flaw [32] and was used to calculate the crack growth at the deepest point and the surface point separately. The input to the fracture mechanics model was the cubic polynomial stress coefficients previously described.

The fracture mechanics analysis for the axially-oriented crack was based on a hypothetical initial 2-to-1 (l/a) aspect ratio inside surface semi-elliptical axial flaw with depth equal to 10 percent of the initial pipe wall thickness. The fracture mechanics model was that described in the EPRI Fracture Mechanics Handbook [33] and calculated the crack growth at the deepest point. The flaw aspect ratio was held constant. This is conservative since the crack would actually have to grow into the adjacent low alloy steel or stainless steel materials in the axial direction. The input to the fracture mechanics model was the cubic polynomial stress coefficients previously described. The stress cycling was that due to hoop pressure stresses, change of hoop residual stresses due to temperature, and thermal transient stresses.

Crack Growth Laws

The crack growth law was that described in Section 4.4 (Equation 2).

Growth of Postulated Circumferential Cracks

Figure 8-19 shows the maximum growth of a hypothetical 10:1 (l/a) 0.1515-inch initial depth crack after 500 heatup/cooldown cycles. As shown, the resulting crack depth and length are a function of position around the circumference since the sign and magnitude of moment stresses change with position around the pipe. After 500 cycles, the crack aspect ratio has not changed significantly, since essentially all of the crack growth occurred due to the plant loading and plant unloading events, which have relatively large surface stresses. The axial residual stresses were compressive enough that there was essentially no crack growth due to stratification moment cycling.

Figure 8-20 shows the growth in both the depth and length for the circumferential crack for 1000 heatup/cooldown cycles, or twice that projected for the plant design life. Even at this large number of cycles, the initially assumed crack is not predicted to propagate to the PWOL design basis (100% through the original wall thickness, since this is a full structural overlay). This 'stable' predicted growth for the circumferential crack clearly justifies a 10-year inspection interval for the PWOL.

Growth of Postulated Axial Cracks

The residual stress distribution for the most critical path for hoop stresses at the center of the weld was assumed. For the evaluation, a hypothetical 0.1515-inch depth crack with a constant 2:1 (l/a) aspect ratio was assumed, and the crack growth was calculated based on the deepest point stress intensity factor.

The analysis showed that there is no predicted crack growth for cracks with depths less than 0.3 inches, since the combination of residual, pressure, and thermal transient stresses does not produce a positive stress intensity factor at depths less than this value.

To investigate the behavior of larger postulated cracks, a crack with initial depth of 0.31 inches was evaluated. Figure 8-21 shows that an axial crack grows very slowly until a depth of about 0.42 inches. At this point, the effect of the compressive residual stresses is not sufficient to maintain a negative stress intensity factor, even for normal operation, as shown in Figure 8-22.

The evaluation clearly demonstrates that growth of axially-oriented cracks is highly unlikely.

- No crack growth is predicted for crack depths that are twice the initial 0.1515-inch crack (up to ~20 percent of wall crack)
- The crack growth is relatively stable up to 0.42 inches in depth.
- The model assumes that a constant aspect ratio crack exists. For an actual axial crack, the length direction cracking would be retarded by interaction with the low alloy steel or stainless steel at the near-surface position crack tips. Although not quantified, this would also reduce the crack tip stress intensity factor at the deepest point, and thus the rate of through wall crack growth.

However, for this surge nozzle, with its relatively high thermal stratification loads and cycling, a pre-overlay inspection is clearly required. The assumption of an axial flaw with a through-wall

depth of 50% of the original wall thickness would result in predicted crack depths greater than the PWOL design basis (100% of the original wall thickness) in less than ten years, and thus would not justify the ten year ASME Section XI inspection interval.

8.5 Fatigue Usage Evaluation

This section presents the fatigue analyses of the surge line weld overlay performed in accordance with the requirements of the ASME Code, Section III for Class 1 components. Specifically, the analysis was conducted at the discontinuity regions where the weld overlay intersects the piping and will result in axial stress discontinuity effects due to the thickness change and bimetallic effects due to the difference in temperature between the weld overlay (Alloy 690) and the adjacent piping (stainless steel). The intersection of the overlay with the nozzle was not evaluated since this end is protected by a thermal sleeve and is much thicker. The overlay region at the Alloy 82/182 weldment was also not included, since crack growth analyses were conducted to qualify this region for fatigue, as previously described in Section 8.3.

The analysis is conducted to the requirements of the ASME Code, Paragraph NB-3222 [33], and using material properties from Section II of the Code [34]. Since the simplified rules of NB-3650 do not apply to the weld overlaid section, the design-by-analysis rules of NB-3200 were used, as permitted in NB-3600. To perform these analyses, the following steps were taken:

- Based on the cyclic loads at the nozzle, stress components were developed directly from finite element analysis of the weld overlaid piping for all load states. The loads included the effects of pressure, attached piping loads (moments and forces), and thermal effects (stratification, bimetallic differential expansion and thermal transients). A list of transients and numbers of cycles considered is provided in Table 8-5.
- The stress components, for both primary-plus-secondary (P+Q) and primary-plus-secondary + peak (P+Q+F) categories were used to determine the range of stress intensity between all load set pairs.
- The fatigue analysis was then performed per the requirements of NB-3222.4 Analysis for Cyclic Operation. For some load states, more than one candidate stress condition was defined. The maximum stress ranges were determined between the candidates of each of the load states for all possible load set pairs.
- Analyses were also conducted to show that the other requirements identified in Figure NB-3221-1 (Limits of Stress Intensity) and NB-3227.5 (Thermal Ratchet) were met.
- The axial stresses for the P+Q+F stress classification were increased by a stress concentration factor (K) at outside surface locations to account for any discontinuities at the outer surface location transitions. Consistent with the piping analysis requirements in NB-3600, Table NB-3681(a)-1 [33], these stress concentration factors were taken as the K indices for as-welded girth butt welds. For conservatism, when used with FEM results, the concentrated axial stresses were taken as the greater of the peak stress predicted by the finite element analysis or $K \times (P+Q)$ stresses. Other components of stress determined directly from finite element analyses were assumed to be detailed enough that no additional stress concentration factor is required.

- When performing the fatigue analysis, the complete range of locations around the circumference was considered, since the moment loading vary around the circumference.

A summary of the maximum computed usage factors for each of the locations analyzed is shown in Table 8-7. The details of the fatigue usage calculation for the most limiting location are shown in Table 8-8.

The analysis showed that all limits of the Code were met, including thermal ratchet requirements. This shows that usage factors should not be an issue for the transition ends of a weld overlay.

Table 8-1
ASME Section XI Table for Allowable Flaws in Piping (Reference 37, Appendix C)

TABLE C-5310-2
 ALLOWABLE END-OF-EVALUATION-PERIOD FLAW DEPTH-TO-THICKNESS RATIO⁽¹⁾
 FOR CIRCUMFERENTIAL FLAWS — SERVICE LEVEL B CONDITIONS

Stress Ratio [Note (2)]	Ratio of Flaw Length to Pipe Circumference $l_f / \pi D$ [Note (3)]							
	0.0	0.1	0.2	0.3	0.4	0.5	0.6	0.75 or Greater
≥ 0.70	0.75	(4)	(4)	(4)	(4)	(4)	(4)	(4)
0.65	0.75	0.30	0.15	0.11	(4)	(4)	(4)	(4)
0.60	0.75	0.66	0.34	0.24	0.20	0.18	0.17	0.17
0.55	0.75	0.75	0.53	0.37	0.30	0.27	0.25	0.25
0.50	0.75	0.75	0.70	0.49	0.40	0.35	0.33	0.32
0.45	0.75	0.75	0.75	0.61	0.49	0.43	0.40	0.39
0.40	0.75	0.75	0.75	0.73	0.59	0.51	0.48	0.46
0.35	0.75	0.75	0.75	0.75	0.67	0.59	0.54	0.52
0.30	0.75	0.75	0.75	0.75	0.75	0.66	0.61	0.57
0.25	0.75	0.75	0.75	0.75	0.75	0.73	0.67	0.63
0.20	0.75	0.75	0.75	0.75	0.75	0.75	0.74	0.68
≤ 0.15	0.75	0.75	0.75	0.75	0.75	0.75	0.75	0.75

NOTES:

- (1) Flaw depth = a_{allow} for a surface flaw
 = $2a_{allow}$ for a subsurface flaw
 t = pipe wall thickness
 Linear interpolation is permissible.
- (2) Stress Ratio = $(\sigma_m + \sigma_b) / \sigma_f$ for limit load evaluation
 = $Z[\sigma_m + \sigma_b + \sigma_e / SF_b] / \sigma_f$ for EPFM evaluation
 σ_m = primary membrane stress. The tabular values are valid for $\sigma_m \leq 0.2\sigma_f$;
 otherwise use analytical solution method.
 σ_b = primary bending stress
 σ_e = secondary bending stress
 σ_f = flow stress
 Z = Z-factor load multipliers from C-6330
- (3) Circumference based on pipe outside diameter.
- (4) Acceptance standards for the applicable class shall be used.

Table 8-2
Nozzle Dimensions and Stresses (Including OBE Seismic Loads) for Example Nozzles

Nozzle	Dimensions (inches)			Stresses (ksi)					Stress Ratios	
				Pressure		OBE + DW	Pm	Pm + Pb	(Pm + Pb) / S_{flow}	(Pm + Pb) / S_{flow}
	OD	ID	Thickness	Hoop	Axial	Axial	Hoop	Axial	WOL ¹	SS Safe End ²
Pressurizer Spray	6	4.25	0.875	7.7	3.8	7.3	7.7	11.1	0.159	0.230
Pressurizer Surge	15	12.44	1.28	13.1	6.55	1.1	13.1	7.65	0.109	0.158
RPV Outlet	33	28.34	2.33	15.8	7.9	11	15.8	18.9	0.270	0.391

1. WOL: $S_{flow} = 69.9$ ksi
2. SS Safe End: $S_{flow} = 48.3$ ksi

**Table 8-3
Weld Overlay Structural Sizing Results**

Nozzle	WOL Thickness (in.)		Minimum Length (in.)
	Optimized Structural	Full Structural	
Pressurizer Spray	0.21	0.29	4.28
Pressurizer Surge	0.21	0.43	6.27
RCS Hot Leg	0.29	0.78	11.30

**Table 8-4
Final Weld Overlay Design Dimensions,
Reflecting Residual Stress and Inspectability Considerations**

Nozzle	WOL Thickness (in.)	WOL Length (in.)
Pressurizer Spray	0.30	7.19
Pressurizer Surge	0.44	9.81
RCS Hot Leg	0.50	11.60

**Table 8-5
Cycles Considered in Fatigue Analysis**

Number Transient	Name/Identifier	Number of Cycles
1	Heatup (HEATUP)	500
2	Cooldown (COOLDOWN)	500
3	Plant Loading (LOADINGA)	15000
4	Plant Loading (LOADINGB)	15000
5	Plant Unloading (UNLOADA)	15000
6	Plant Unloading (UNLOADB)	15000
7	Step Load Increase (STEPINCR)	2000
8	Step Load Decrease (STEPDECR)	2000
9	Reactor Trip (RTRIPA)	400
10	Reactor Trip (RTRIPB)	400
11	Loss of Flow/Load (LFLOSSA)	80
12	Loss of Flow/Load (LFLOSSB)	80
13	Loss of Sec. Pressure (SPLOSSA)	5
14	Loss of Sec. Pressure (SPLOSSB)	5
15	Hydrotest (HYDROTEST)	10
16	Leak Test (LEAKTEST)	320
17	Hydro/Leak Test 0 Pres. (ZERoload)	330
18	Normal Variation (NORMVAR)	1000000
19	OBE Seismic (NORM+OBE)	20
20	Seismic Self Cycle (OBE OBE)	980
21	HLST320	75
22	HLST250	375
23	HLST200	400
24	HLST150	500
25	HHST320	75
26	HHST250	375
27	HHST200	400
28	HHST150	500
29	HHST90	87710
30	CLST320	75
31	CLST250	375
32	CLST200	400
33	CLST150	500
34	CHST320	75

HLST = Heatup Low Pressure Stratification, HHST = Heatup High Pressure Stratification,
CLST = Cooldown Low Pressure Stratification, CHST = Cooldown High Pressure Stratification

Table 8-6
Summary of Primary-plus-Secondary Stress and Fatigue Analysis Results for Pressurizer Surge Nozzle

Location	CUF ¹	(P+Q) _{max} , Compared to 3S _m , ksi
Overlay Transition (On Weld Overlay, Inner Surface of Pipe)	0.0185	46.2 < 49.9
Overlay Transition (On Weld Overlay, Outer Surface of Overlay)	0.0019	50.6 < 69.9 (Alloy 690)
Overlay at Pipe End (At Weld Overlay End, Inner Surface of Pipe)	0.0133	54.1 > 49.9 ²
Overlay at Pipe End (At Weld Overlay End, Outer Surface of Pipe)	0.1127	60.5 > 49.9 ²

- Notes:
1. CUF = Cumulative Usage Factor
 2. K_e applied and thermal ratchet check performed when (P+Q) exceeded 3S_m

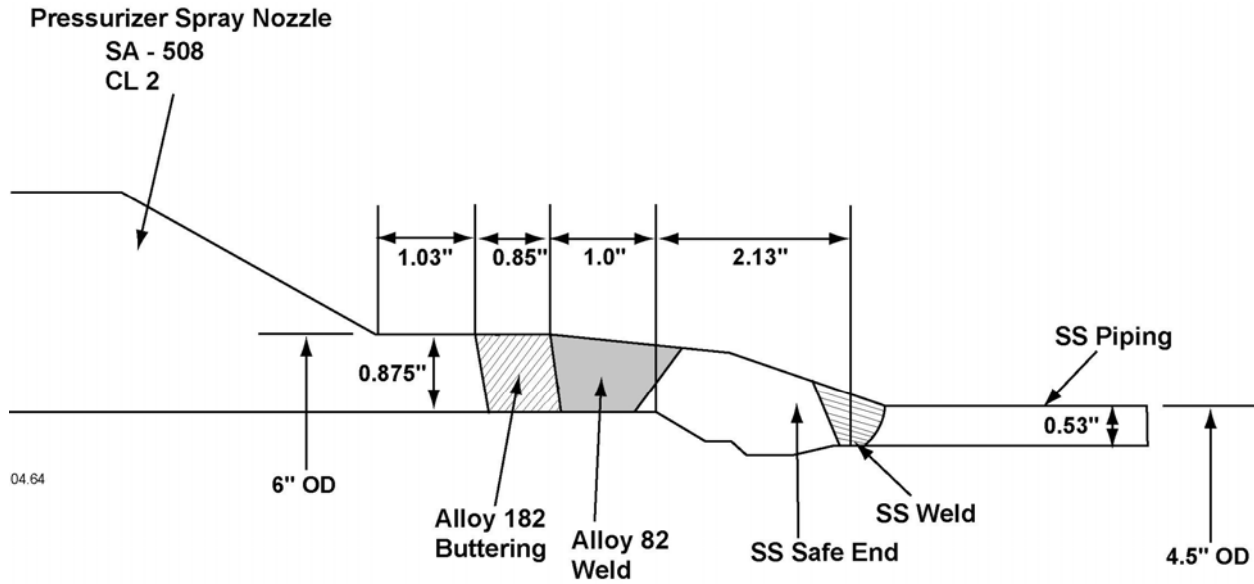


Figure 8-1
Pressurizer Spray Nozzle Geometry chosen for Analysis
 (chosen as representative of all pressurizer steam space nozzles)

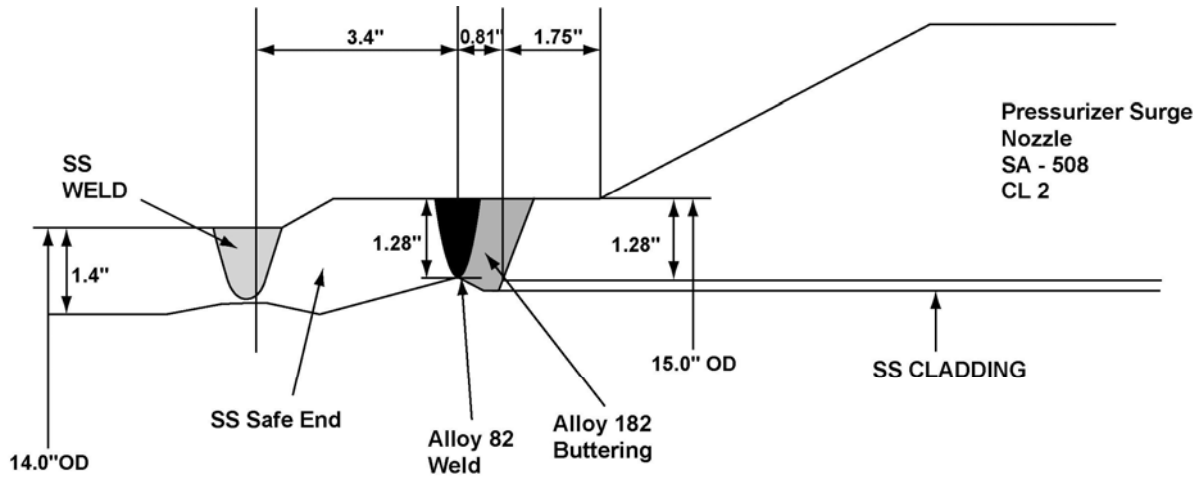


Figure 8-2
Pressurizer Surge Nozzle Geometry chosen for Analysis

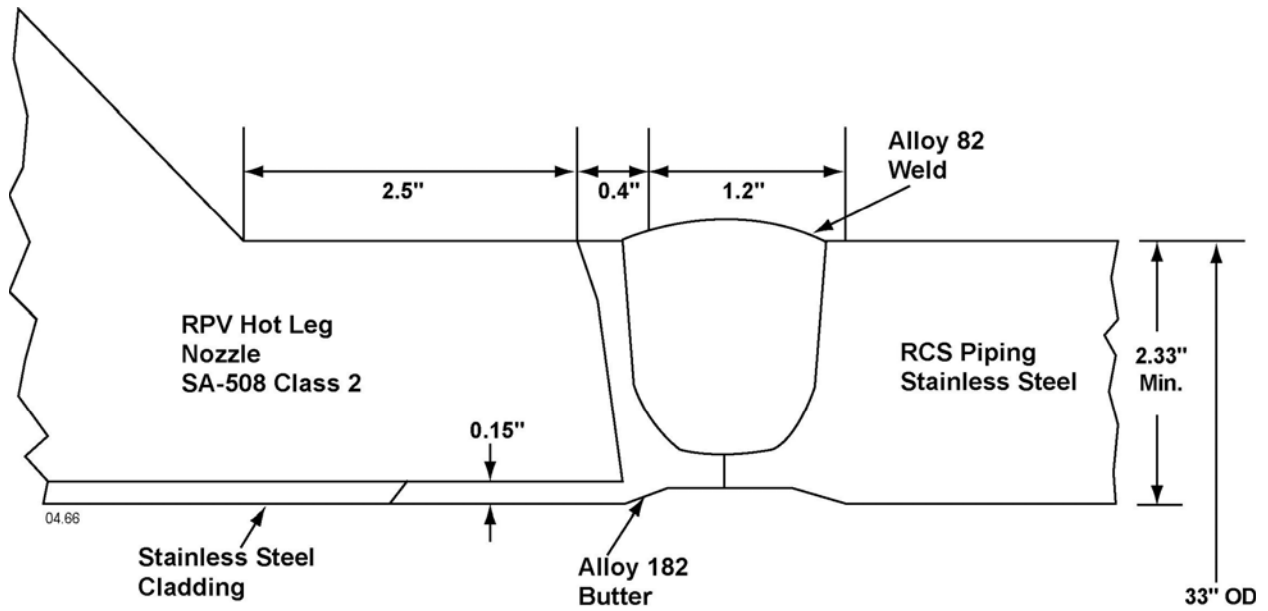


Figure 8-3
RPV Hot Leg Nozzle Geometry Chosen for Analysis

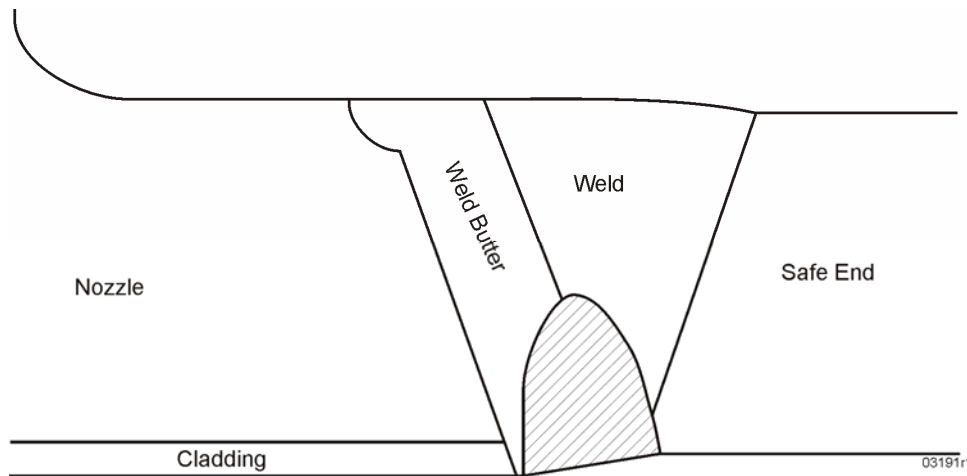


Figure 8-4
Illustration of Simulated In-process ID Weld Repair used as Starting Point for Residual Stress Analysis (Used for all three example nozzles.)

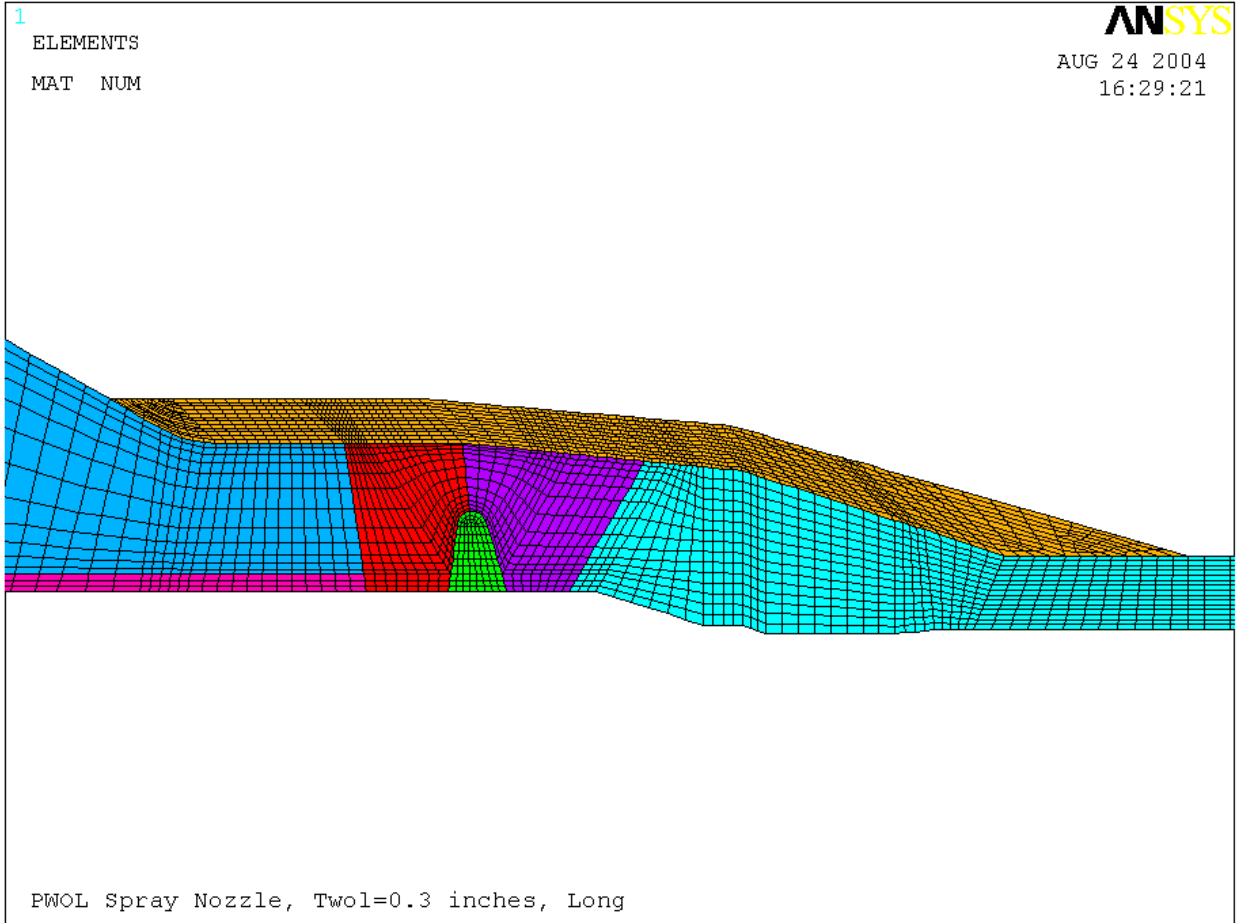


Figure 8-5
Finite Element Model for Pressurizer Spray Nozzle Weld Overlay
Weld Residual Stress Analysis

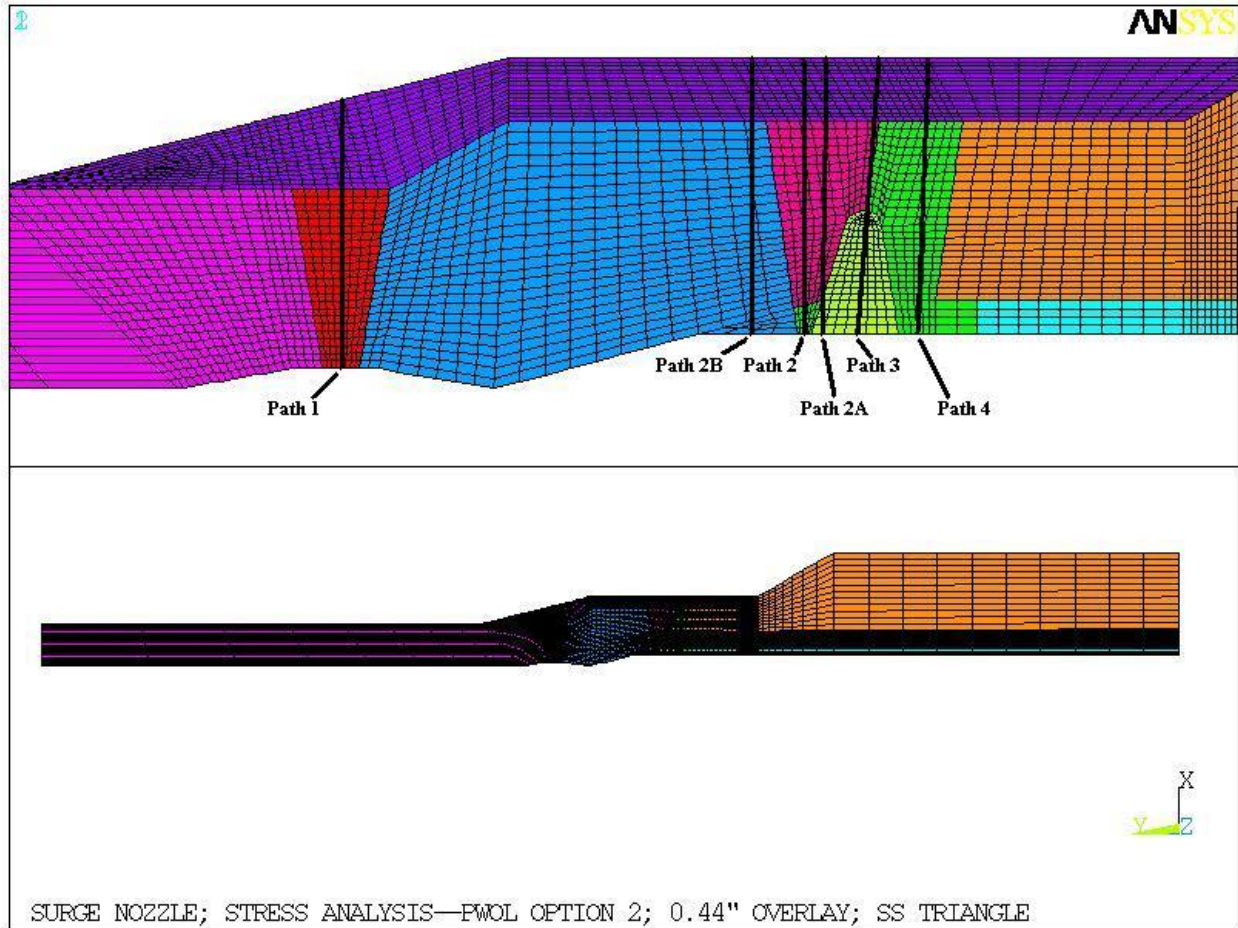


Figure 8-6
Finite Element Model for Pressurizer Surge Nozzle Weld Overlay
Weld Residual Stress Analysis

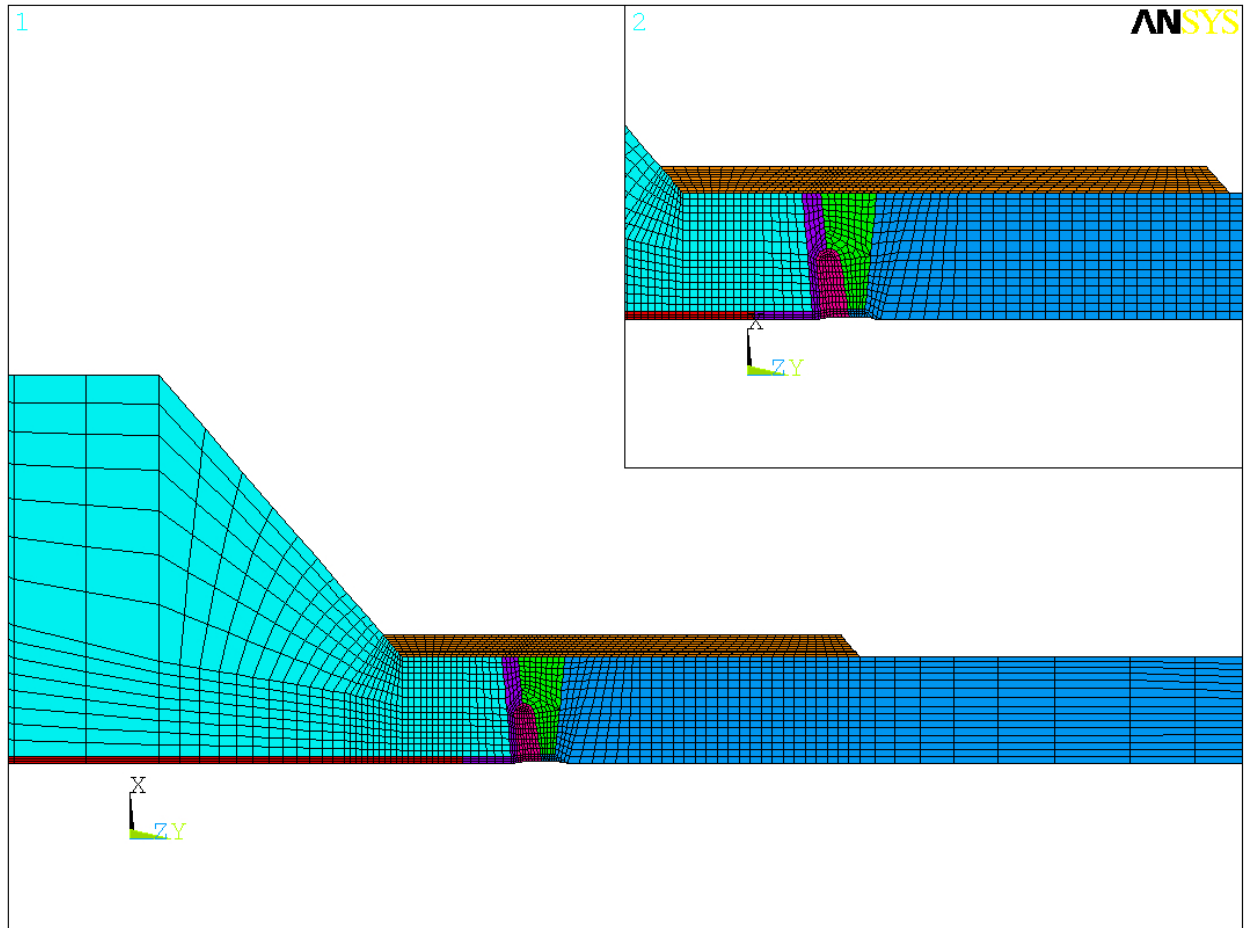


Figure 8-7
Finite Element Model for RPV Hot Leg Nozzle Weld Overlay
Weld Residual Stress Analysis

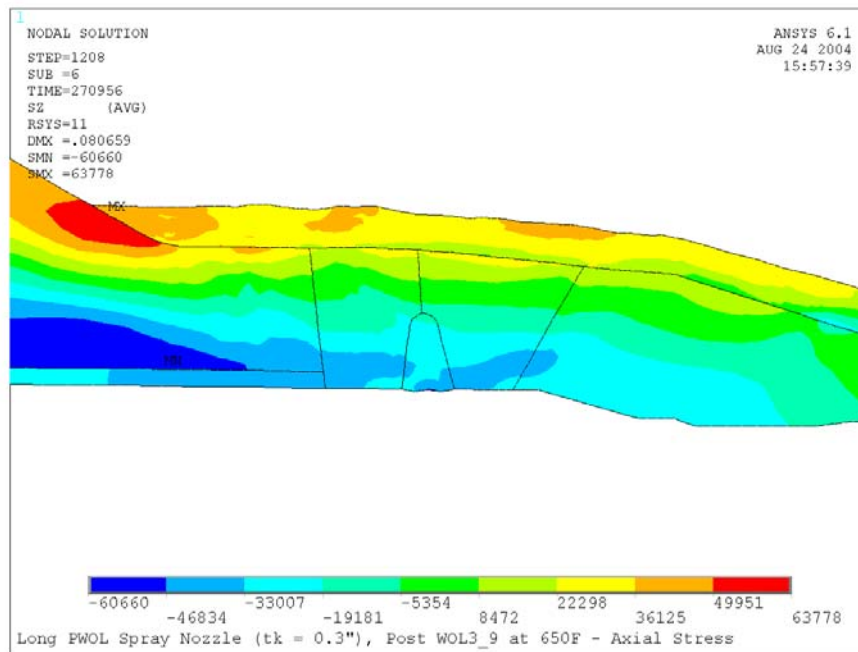
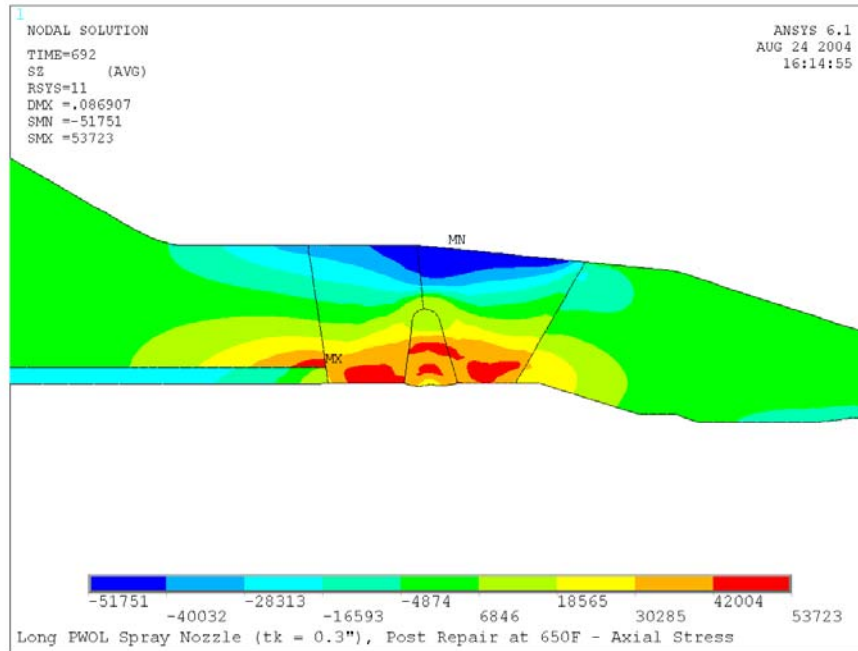


Figure 8-8
Pressurizer Spray Nozzle Pre- and Post-WOL Residual Stress Contour Plots (Axial Stress)

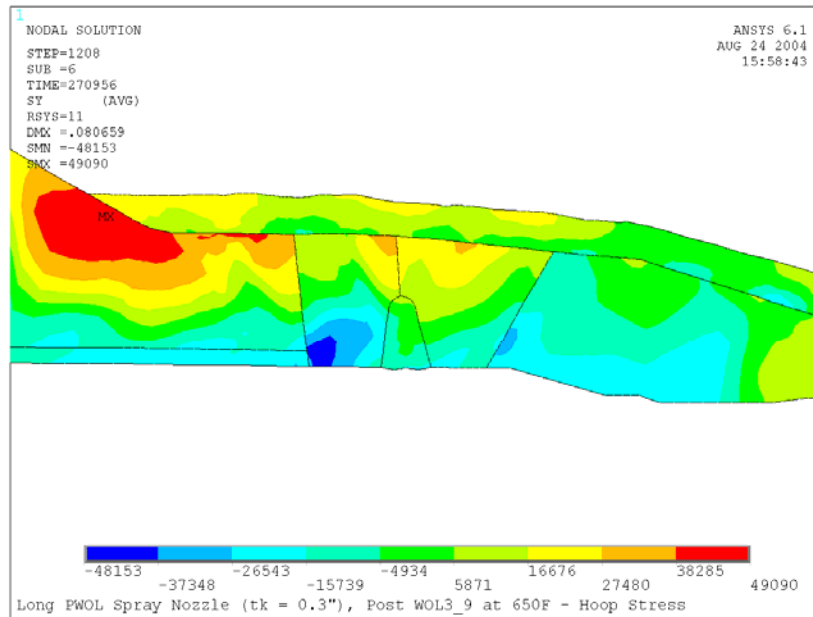
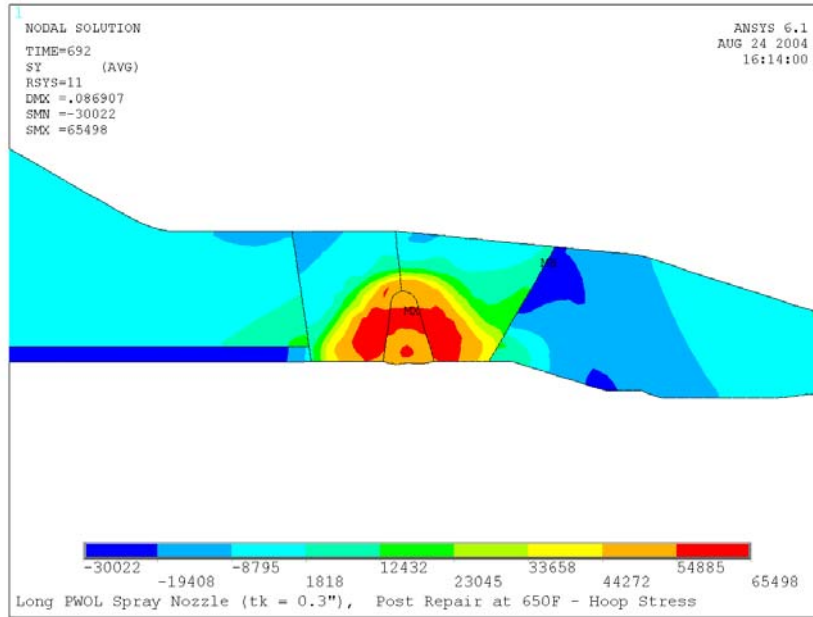


Figure 8-9
Pressurizer Spray Nozzle Pre- and Post-WOL Residual Stress Contour Plots (Hoop Stress).

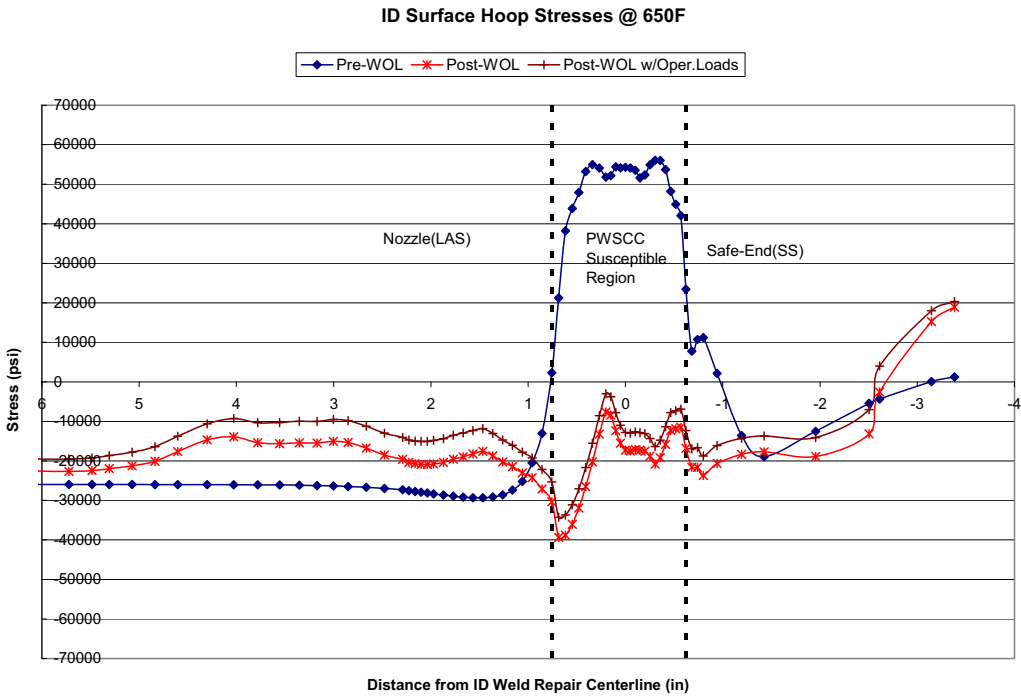
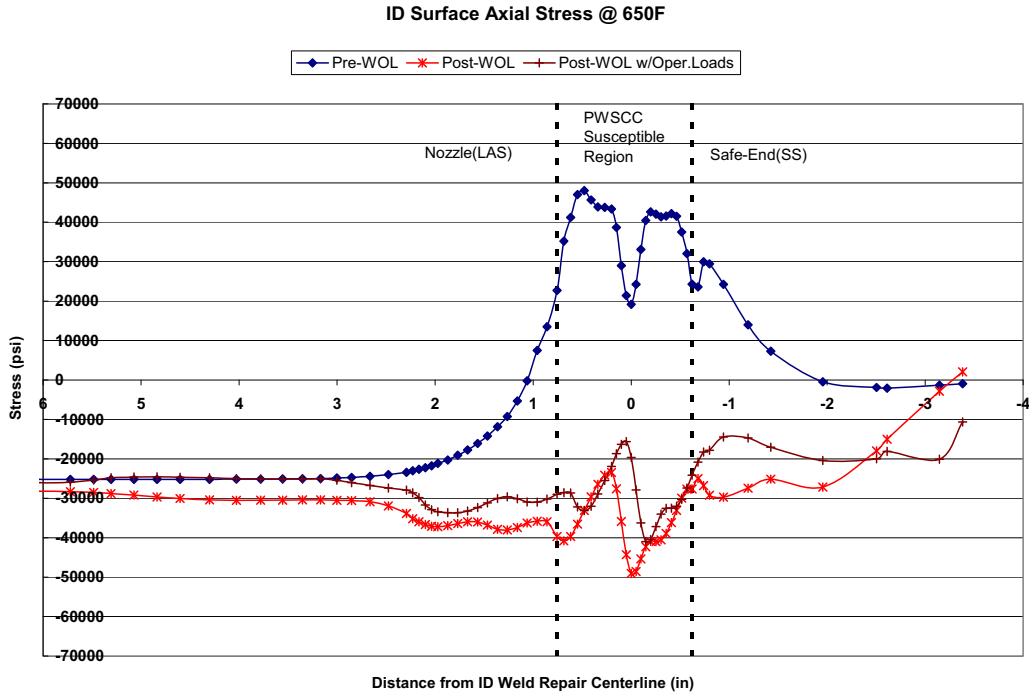


Figure 8-10
Pressurizer Spray Nozzle Inside Surface Stress Plots

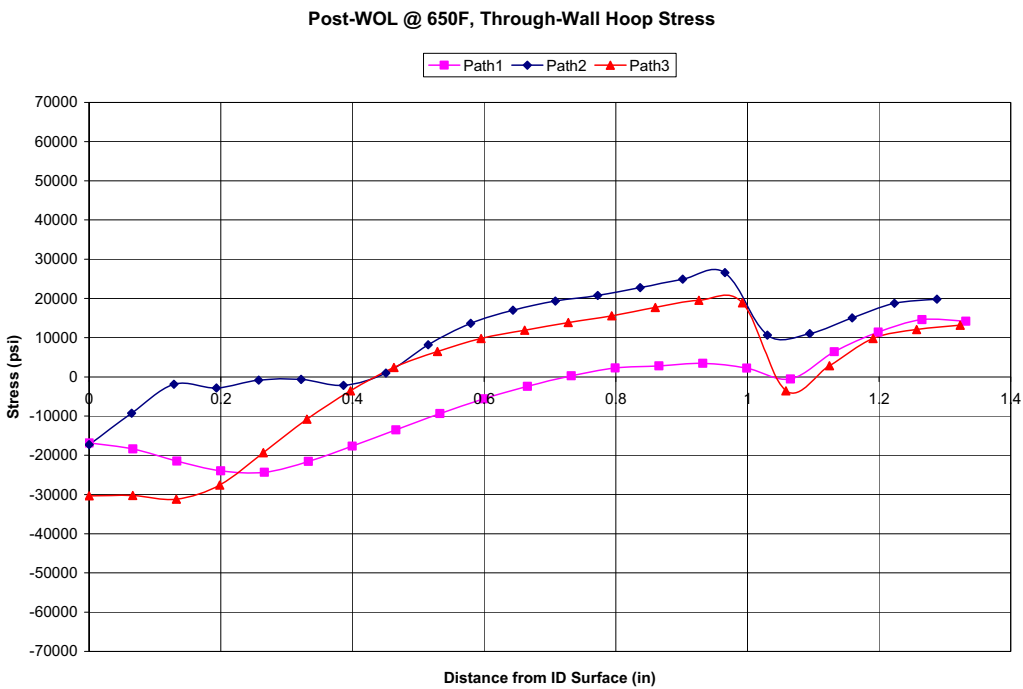
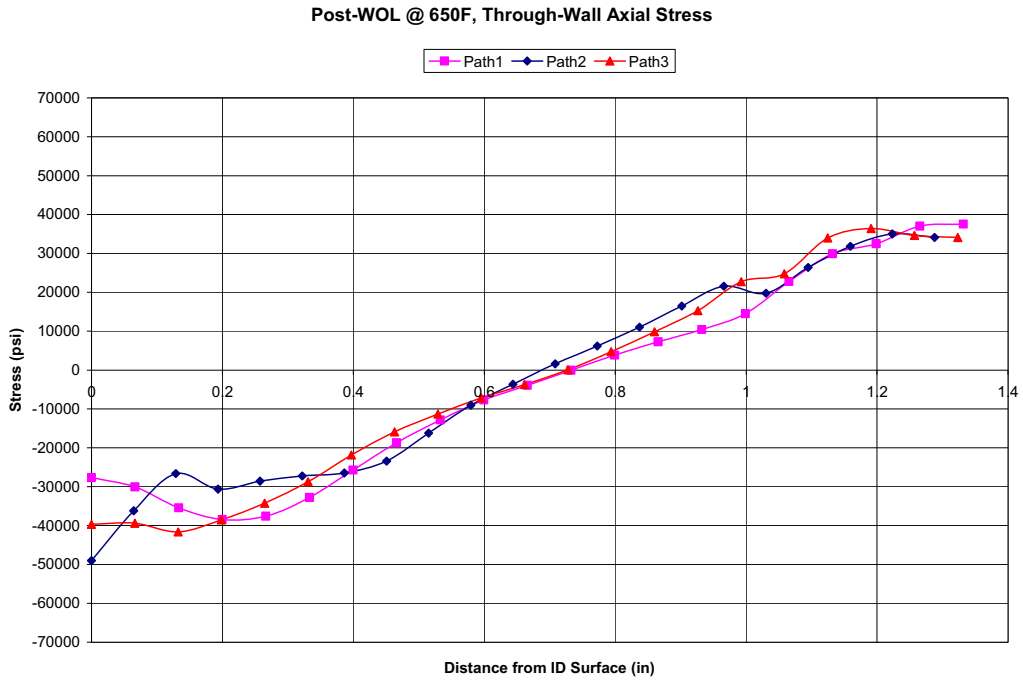


Figure 8-11
Pressurizer Spray Nozzle Post-WOL Through-Wall Stress Plots

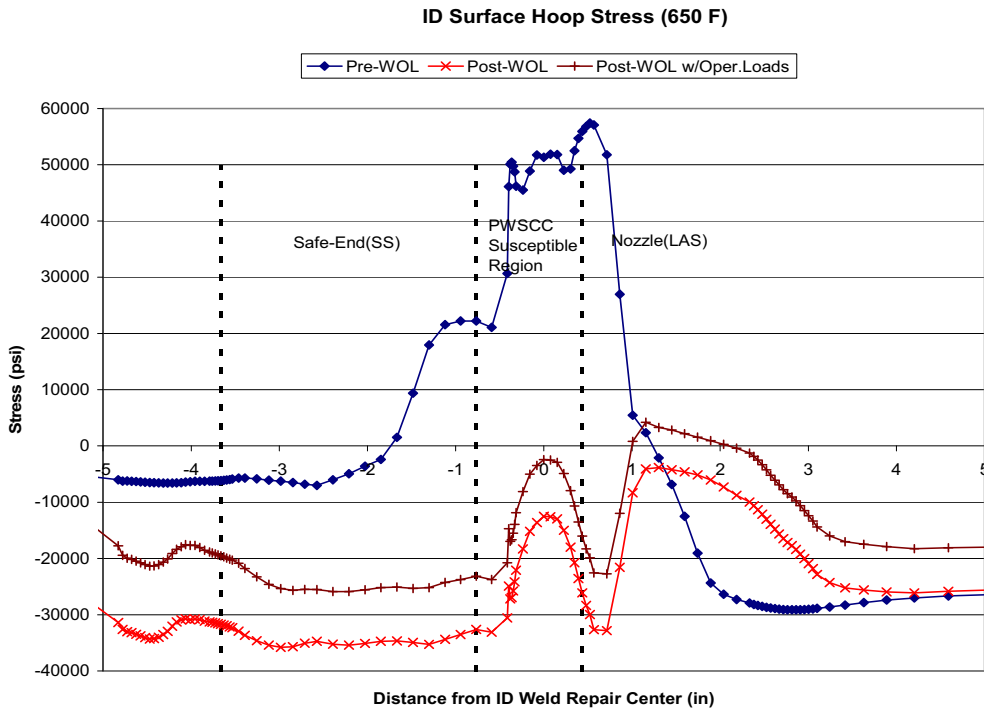
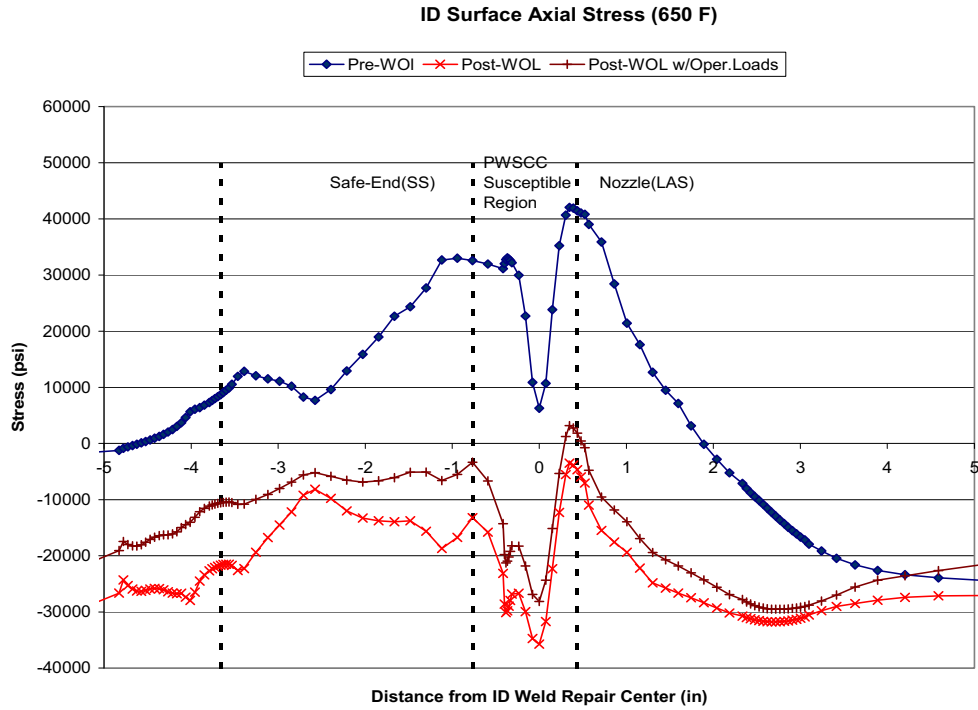


Figure 8-12
Pressurizer Surge Nozzle Inside Surface Stress Plots

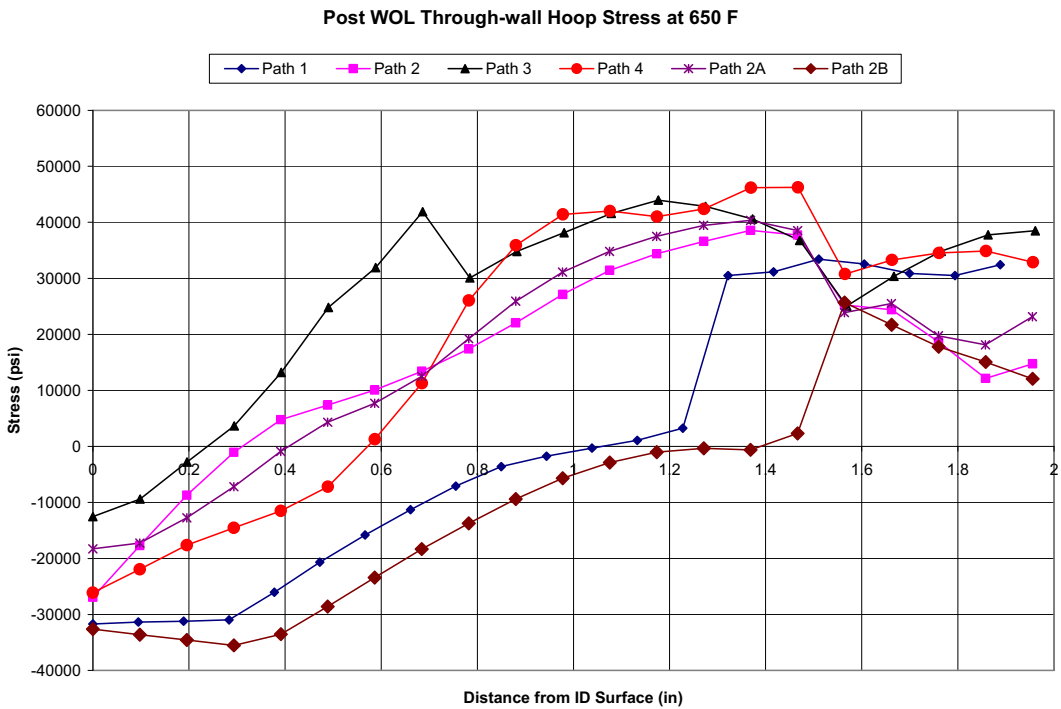
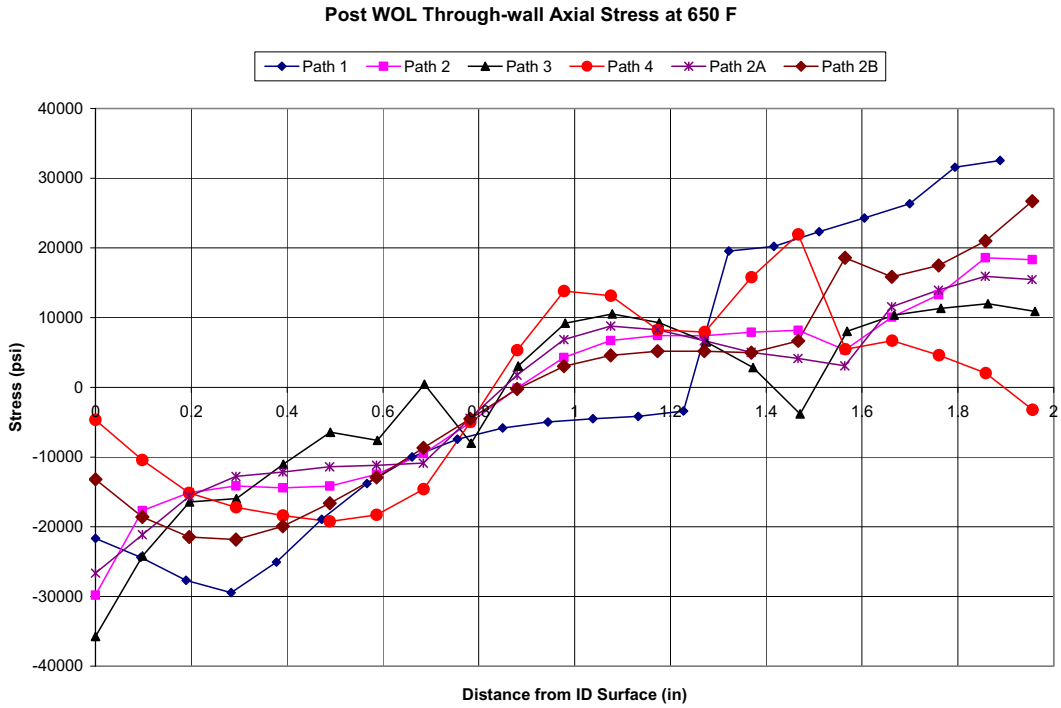


Figure 8-13
Pressurizer Surge Nozzle Post-WOL Through-Wall Stress Plots

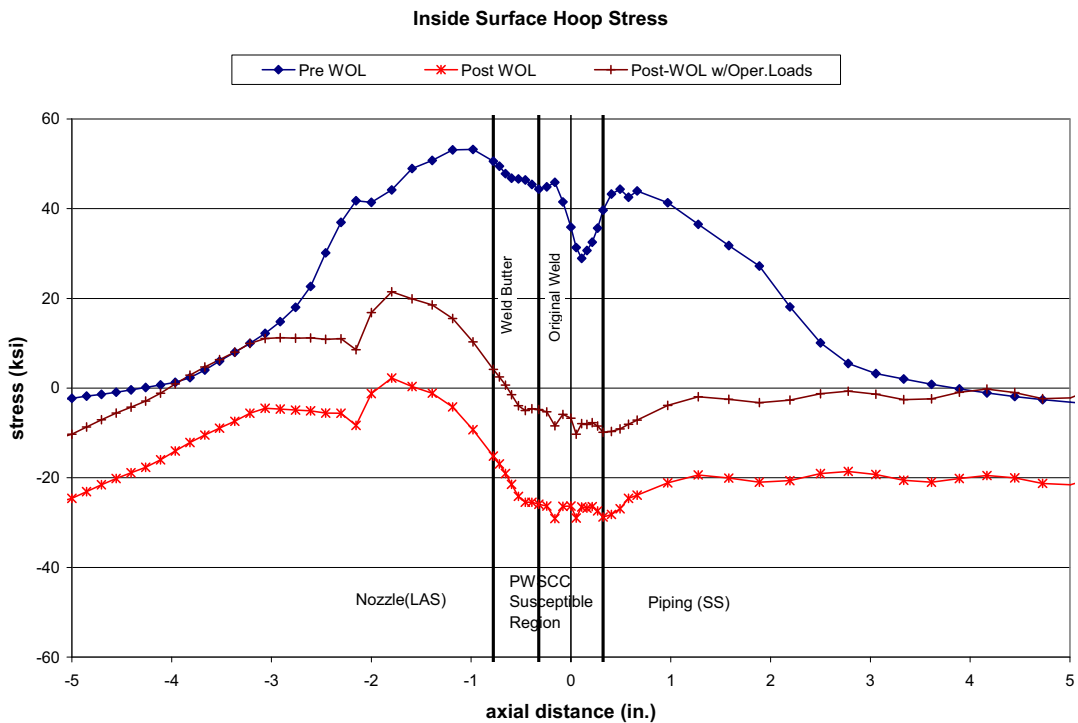
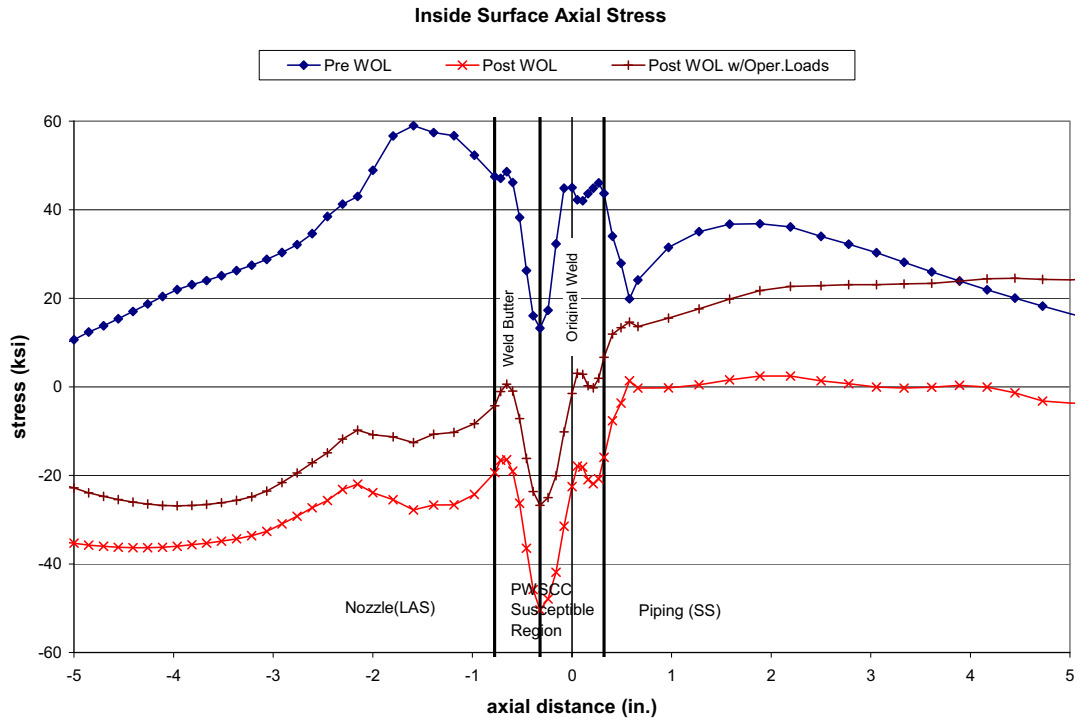


Figure 8-14
RPV Hot Leg Nozzle Inside Surface Stress Plots

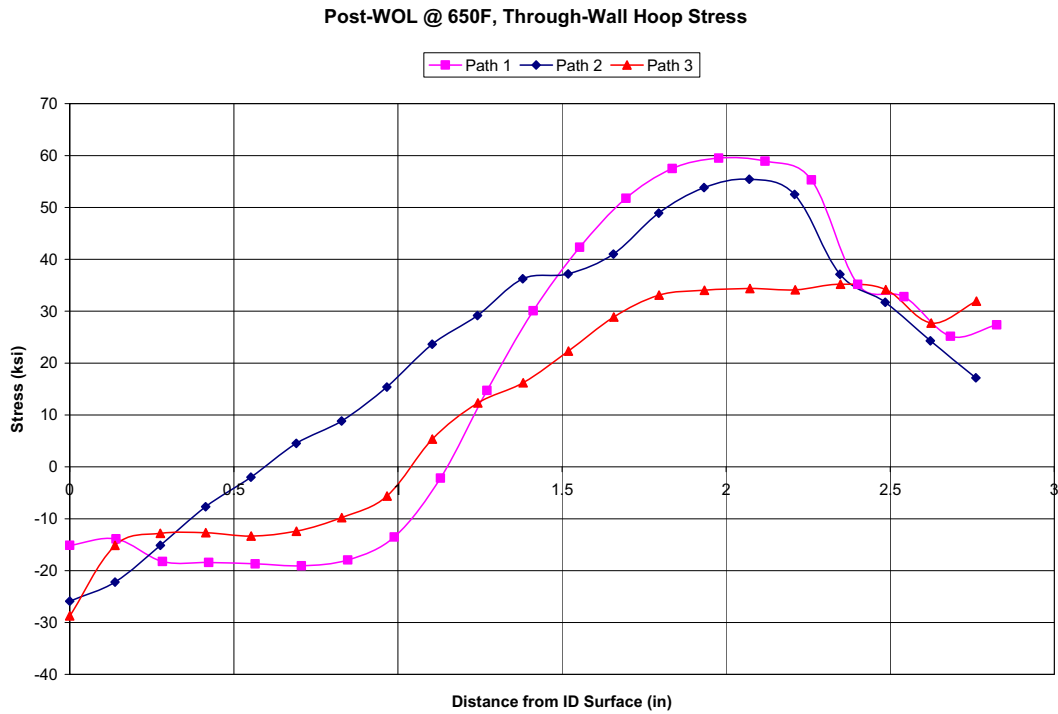
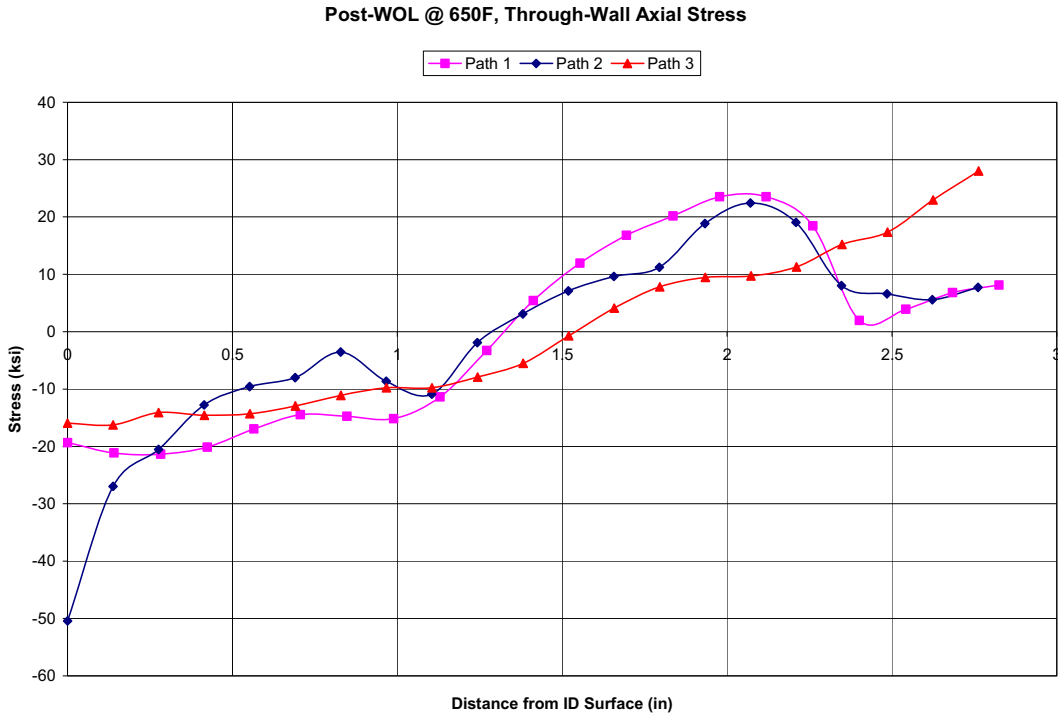


Figure 8-15
RPV Hot Leg Nozzle Post-WOL Through-Wall Stress Plots

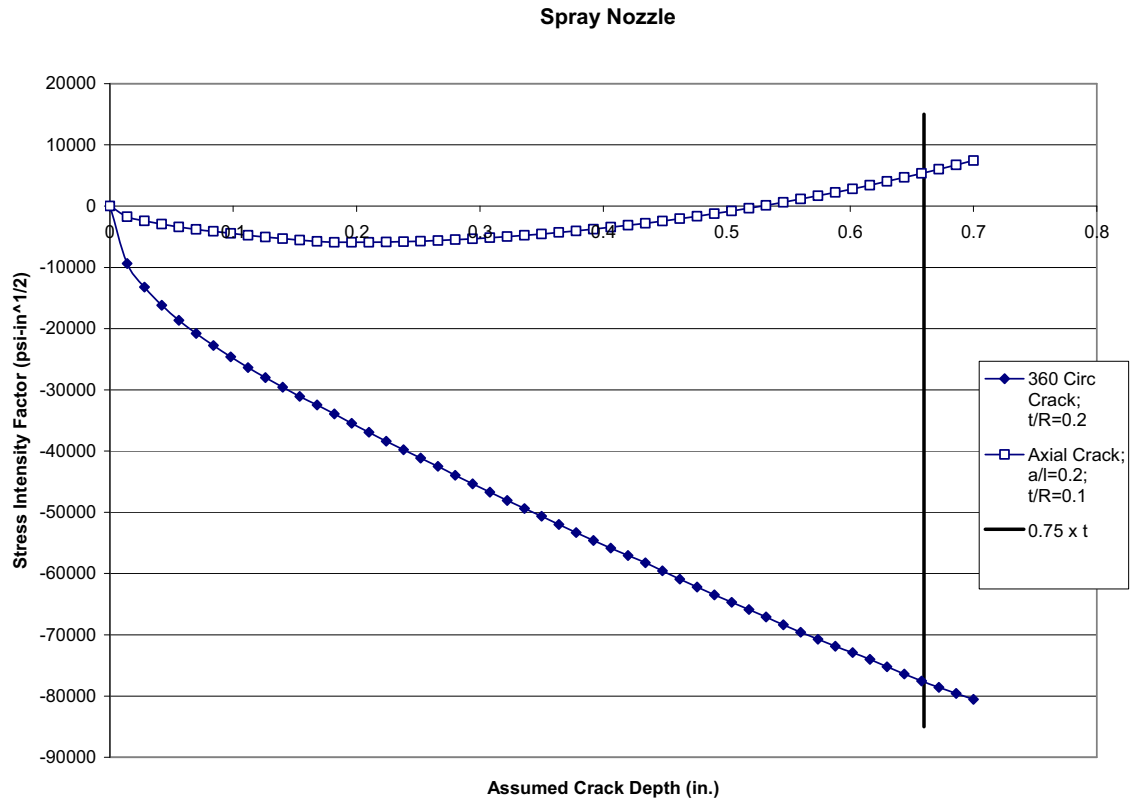


Figure 8-16
Spray Nozzle Post-WOL Stress Intensity Factor Plots – Normal Operating Sustained Loads plus Residual Stresses

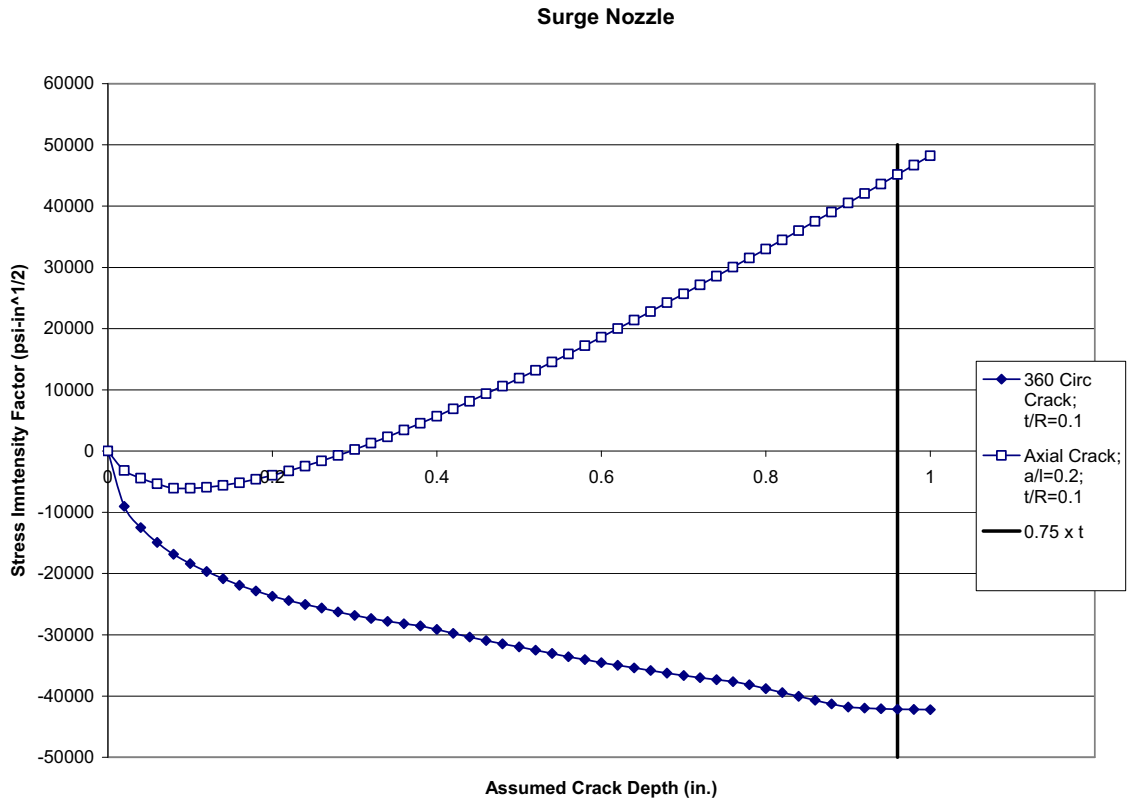


Figure 8-17
Surge Nozzle Post-WOL Stress Intensity Factor Plots – Normal Operating Sustained Loads plus Residual Stresses

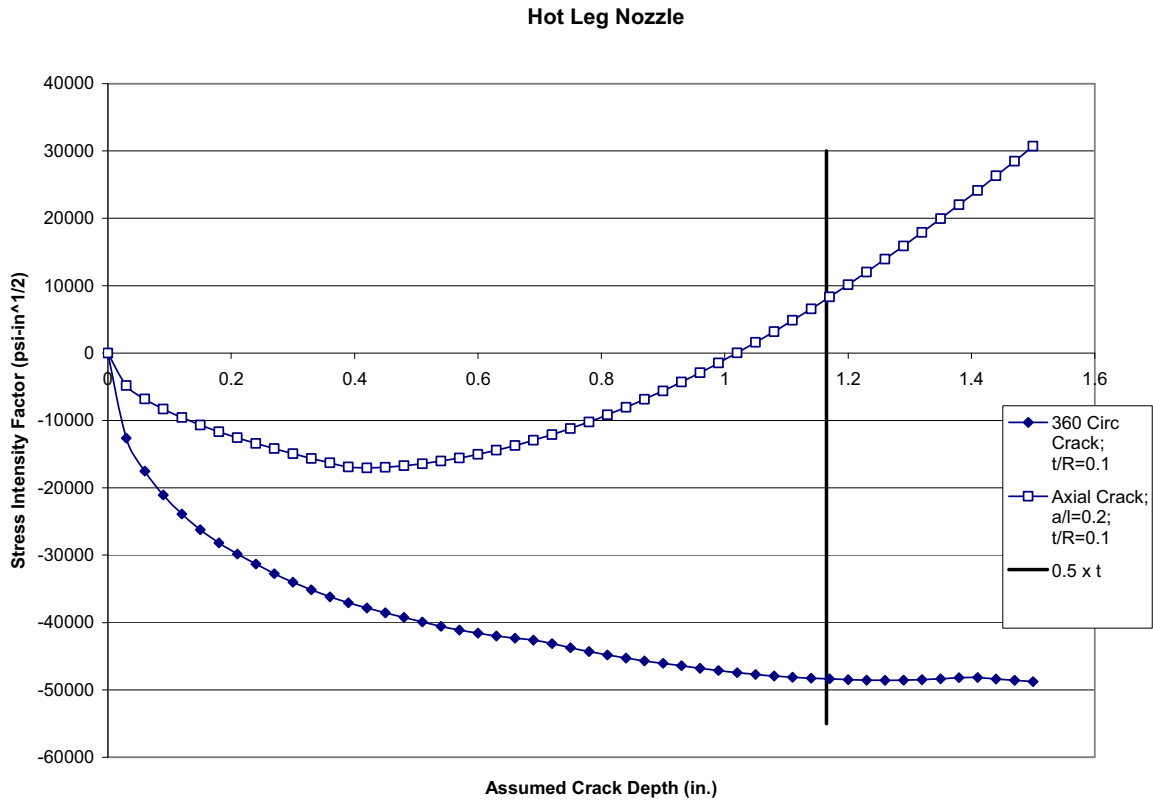


Figure 8-18
RPV Hot Leg Nozzle Post-WOL Stress Intensity Factor Plots – Normal Operating Sustained Loads plus Residual Stresses

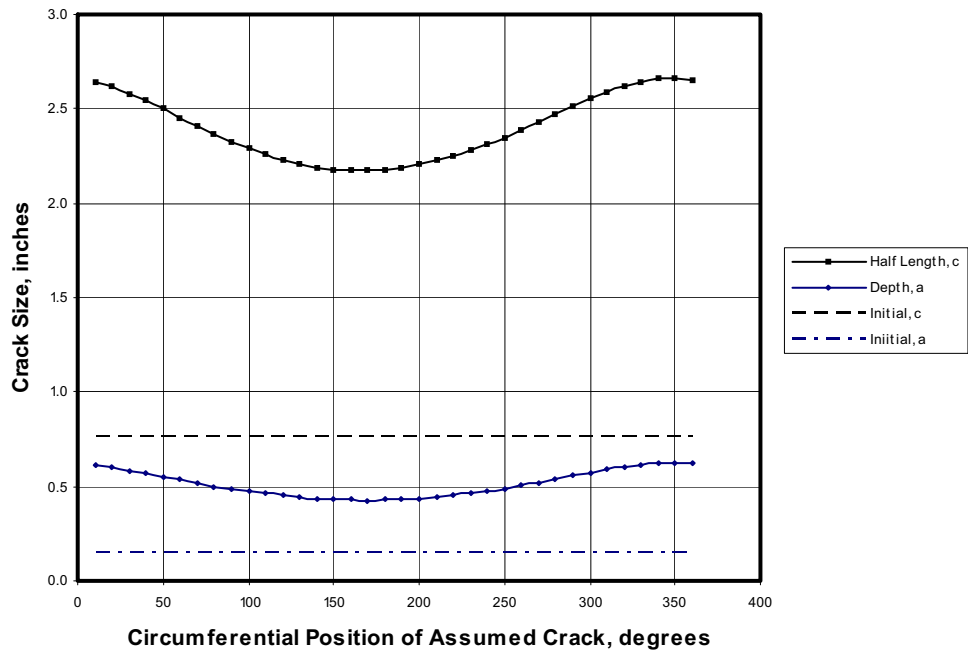


Figure 8-19
Growth of Postulated Circumferential Crack for 500 Design Heatup/Cooldown Cycles

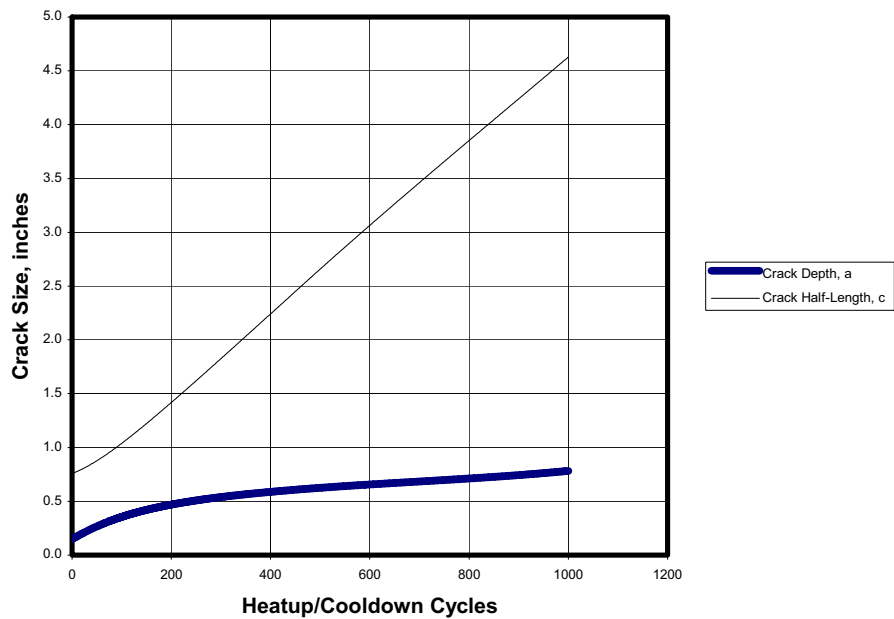


Figure 8-20
Growth of Circumferential Crack

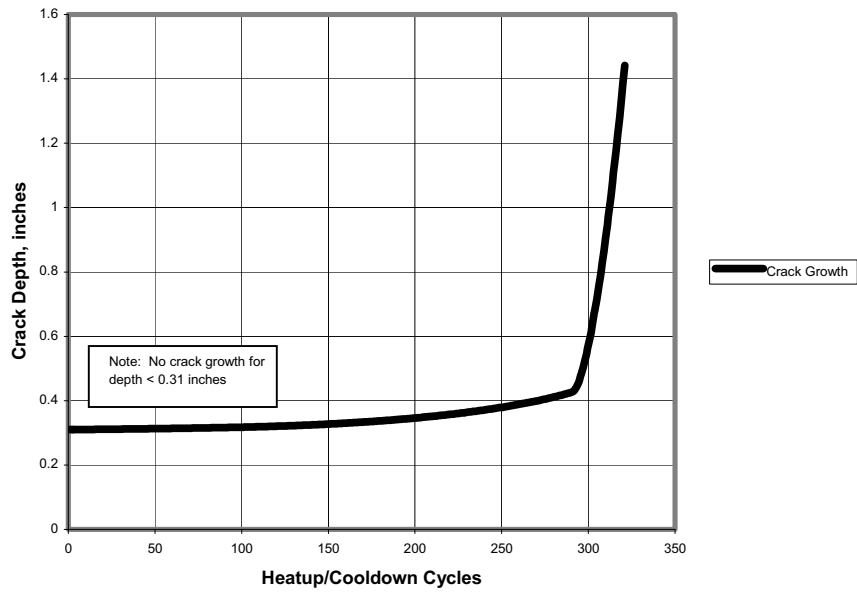


Figure 8-21
Growth of a Postulated 0.31-inch Depth Axial Crack

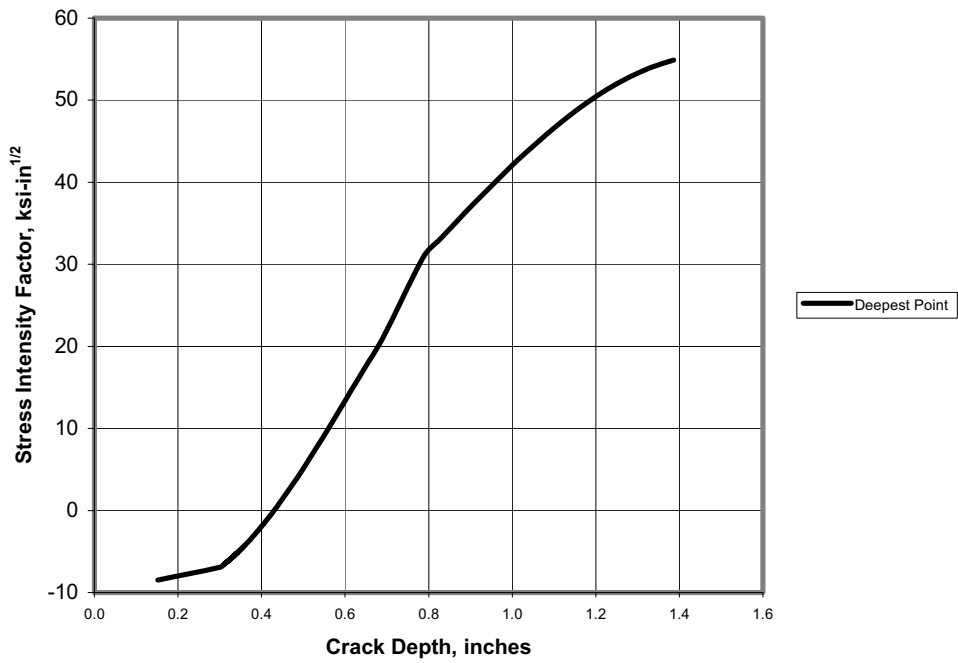


Figure 8-22
Stress Intensity Factor for Axially-Oriented 2:1 Aspect Ratio Crack

9.0 CONCLUSIONS

A comprehensive discussion of weld overlay (WOL) repair technology used in U.S. nuclear power plants is presented, and a set of criteria and benefits are presented for application of this technology preemptively, as a mitigation procedure for uncracked locations in Alloy-82/182 dissimilar metal butt welds (PWOLs). Two types of preemptive overlays are defined, full structural weld overlays (FSWOL) and optimized weld overlays (OWOL) and detailed design, analysis and inspection requirements are specified for each in Section 4. The design criteria include sufficient thickness of resistant material (Alloy 52, 52M or 52MS weld metal) to provide new structural reinforcement of the original pipe weld sufficient to sustain design basis loads within ASME Code margins, under a set of design basis flaw assumptions. The PWOL must also supply sufficient thickness and length to effectively reverse the highly tensile residual stresses from the original DMW, including the potential detrimental effects of an assumed, in-process repair weld during plant construction, and must be designed to permit UT coverage of the applicable examination volumes for each overlay type.

Data from prior experimental programs that support WOL residual stress and structural integrity benefits are presented, and a review of over fifteen years of operating experience with WOLs in BWRs is cited to support the theoretical work in this report. A recent EPRI/MRP PWOL program, which included fabrication of a PWOL mockup for residual stress confirmation, is also discussed. The results of that program confirmed the beneficial residual stress effects of the overlay, and demonstrated conservatism in the residual stress analytical procedures used for overlay design. In addition, a review of materials and welding considerations essential to producing PWSCC resistant weld overlays is presented, and detailed discussion of post-PWOL pre- and inservice inspection requirements is presented.

Finally, structural and residual stress calculations are presented for three example cases representative of typical nozzle geometries in a PWR, ranging from small to large diameter (a pressurizer top head nozzle, a pressurizer surge nozzle, and a reactor vessel hot leg nozzle). The example calculations demonstrate application of the criteria defined in the report and the resulting weld overlay designs for these nozzles. Analyses are also presented to demonstrate acceptable fatigue life in the fatigue sensitive surge nozzle.

Based on these studies and results, NRC approval of the following position is requested. Namely, if a PWOL is applied that meets the design requirements of Section 4 of this report, plus the metallurgical and welding conditions described in Section 6, then the inspection requirements described in Section 7 shall apply, and credit may continue to be taken for Leak Before Break of the PWOL-treated weld in the licensing basis for the plant.

10.0 REFERENCES

1. Material Reliability Program, Primary System Piping Butt Welds Inspection and Evaluation Guideline (MRP-139), July, 2005
2. BWR Vessel and Internals Project: Technical Basis for Revisions to Generic Letter 88-01 Inspection Schedules (BWRVIP-75), EPRI, Palo Alto, CA, and BWRVIP: 1999, TR-113932.
3. ASME Code Case N-504-2, "Alternative Rules for Repair of Classes 1, 2, and 3 Austenitic Stainless Steel Piping," Section XI, Division 1.
4. ASME Code Case N-740-2, "Dissimilar Metal Weld Overlay for Repair or Mitigation of Class 1, 2, and 3 Items, Section XI, Division 1
5. TMI Weld Overlay, NRC Approval of Relief Request dated July 21, 2004
6. NUREG/CR-6721, "Effects of Alloy Chemistry, Cold Work, and Water Chemistry on Corrosion Fatigue and Stress Corrosion Cracking of Nickel Alloys and Welds," U.S. Nuclear Regulatory Commission (Argonne National Laboratory), April 2001.
7. NUREG/CR-6443, *Deterministic and Probabilistic Evaluations for Uncertainty in Pipe Fracture Parameters in Leak-Before-Break and In-Service Flaw Evaluations*, U. S. Nuclear Reg. Commission, 1996.
8. EPRI NP-7103-D, "Justification for Extended Weld-Overlay Design Life", Topical Report, January 1991
9. EPRI NP-5881-LD, "Assessment of Remedies for Degraded Piping," June 1988.
10. S. Timoshenko, *Strength of Materials, Part II, "Advanced Theory and Problems"*, D. Van Nostrand, March 1956.
11. "Assessment of Design Basis for Load Carrying Capacity of Weld Overlay Repair" Topical Report, NUREG/CR-4877, Paul Scott, Battelle Columbus Division, February, 1987.
12. Structural Integrity Final Report SIR-91-010, "Overview: Evaluation of Weld Overlay Repairs Without Water Backing," May 1991.
13. "Technical Justification for Extension of the Interval Between Inspections of Weld Overlay Repairs," EPRI TR-110172, Charlotte, NC, February 1999.
14. EPRI-NP-7085-D, "Inconel Weld Overlay Repair for Low Alloy Steel Nozzle to Safe-End Joint", Final Report, January 1991

15. Sarver, J. M., Crum, J. R., and Mankins, W. L. "Effect of Carbide Precipitation on the Corrosion Behavior of Inconel Alloy 690," *Proceedings of Corrosion 87*, NACE, 1987.
16. Scott, P. M., Combrade, P. "On the Mechanism of Stress Corrosion Crack Initiation and Growth in Alloy 600 Exposed to PWR Primary Water," *Proceedings of the 11th International Symposium on Environmental Degradation of Materials in Nuclear Systems – Water Reactors*, ANS, 2003, pp. 29-38.
17. Was, G. S. and Lian, K., "Role of Carbides in Stress Corrosion Cracking Resistance of Alloy 600 and Controlled-Purity Ni-16% Cr-9% Fe in Primary Water at 360°C," *Corrosion*, Vol. 54, No. 9, NACE, 1998, pp 675-688.
18. Vaillant, Francois et al. "Influence of Chromium Content and Microstructure on Creep and PWSCC Resistance of Nickel Base Alloys," *Proceedings of the 9th International Symposium on Environmental Degradation of Materials in Nuclear Systems – Water Reactors*, ANS, 1999, pp. 251-258.
19. Crum, J. R., Heck, K. A., Angeliu, T. M. "Comparison of Different Thermal Treatments for Alloy 690," *Proceedings of Corrosion 90*, NACE, 1990.
20. Was, G., Sung, J. K. "Intergranular Cracking of Ni16Cr-9Fe Alloys in High Temperature High Purity Water," *Proceedings of Corrosion 90*, NACE, 1990.
21. INCO Alloys International Welding Products, No. IAI-27-3, 1993.
22. J. Panter, et al., "Surface Layers on Alloys 600 and 690 in PWR Primary Water: Possible Influence on Stress Corrosion Crack Initiation," paper 02519 presented at Corrosion 2002, Houston, TX, April 7-11, 2002, NACE< Houston, TX.
23. P. M. Scott, "An Overview of Internal Oxidation as a Possible Explanation of Intergranular Stress Corrosion Cracking of Alloy 600 in PWRs," paper presented at the 9th International Symposium on Environmental Degradation of Materials in Nuclear Power Systems – Water Reactors, Newport Beach, CA, August 1-5, 1999, published in proceedings of same, TMS, Warrendale, PA, p. 387.
24. S. A. Attanasio, et al., "Measurement of the Fundamental Parameters for the Fil-Rupture/Oxidation Mechanism – The Effect of Chromium," paper presented at the 9th International Symposium on Environmental Degradation of Materials in Nuclear Power Systems – Water Reactors, Newport Beach, CA, August 1-5, 1999, published in proceedings of same, TMS, Warrendale, PA, p. 49.
25. S. S. Hwang and J. S. Kim, "Electrochemical Interaction of Lead with Alloy 600 and Alloy 690 in High Temperature Water," *Corrosion*, Vol. 58, No. 5, May 2002, p. 392.
26. S. McCracken, "Review of Thermo-Mechanical Testing and Micro-Characterization Studies of Nickel Based Alloy 52 Weld Filler Metal for Susceptibility to Ductility Dip Cracking," paper presented at the 6th International EPRI Conference on Welding and Repair Technology for Power Plants, Sandestin, FL, June 2004.

27. ASME Boiler and Pressure Vessel Code, Section XI, 2004 Edition, Appendix VIII.
28. **pc-CRACK** for Windows Computer Software, Version 3.1 , Structural Integrity Associates.
29. Welding Procedure Specification #WPS-01-08-T-801, Welding Services, Inc., November 13, 2003
30. ANSYS/MECHANICAL, Release 6.1, ANSYS, Inc., November 2002
31. CEN 387-NP, "Pressurizer Surge Line Flow Stratification Evaluation," ABB Combustion Engineering, Rev. 1-NP, December 1991
32. S. Chapuliot, M.H. Lacire and P. Le Delliou, "Stress Intensity Factors for Internal Circumferential Cracks in Tubes Over a Wide Range of Radius Over Thickness Ratios", *PVP-Vol.365, Fatigue, Fracture, and High Temperature Design Methods in Pressure Vessels and Piping*, ASME 1998
33. EPRI Report NP-6301-D, "Ductile Fracture Handbook," June 1989
34. ASME Boiler and Pressure Vessel Code, Section III, 1992 Edition
35. ASME Boiler and Pressure Vessel Code, Section II, 1992 Edition
36. ASME Section XI Task Group for Piping Flaw Evaluation, ASME Code, "Evaluation of Flaws in Austenitic Steel Piping," *Journal of Pressure Vessel Technology*, Vol. 108, August 1986, pp. 352-366.
37. ASME Boiler and Pressure Vessel Code, Section XI, 2004 Edition.
38. U.S. Nuclear Regulatory Commission, NUREG-0800, "Standard Review Plan", 3.6.3 Leak Before Break Evaluation Procedures, Draft March 1987
39. EPRI Report NP-3596-SR, "PICEP: Pipe Crack Evaluation Computer Program," Rev. 1, July 1987.
40. EPRI Report NP-3395, "Calculation of Leak Rates Through Crack in Pipes and Tubes," December 1983.
41. U.S. Nuclear Regulatory Commission, 10CFR50.55a.
42. Performance Demonstration Initiative (PDI) Program Description, Rev. 2, Oct. 1, 2000.
43. Rahman, S., Ghadiali, N., Paul, D., and Wilkowski, G, "Probabilistic Pipe Fracture Evaluations for Leak-Rate Detection Applications," NUREG/CR-6004, April 1995.
44. D. Rudland, R. Wolterman, G. Wilkowski, R. Tregoning, "Impact of PWSCC and Current Leak Detection on Leak-Before-Break," Proceedings of Conference on Vessel

Head Penetration, Inspection, Cracking, and Repairs, Sponsored by USNRC, Marriot Washingtonian Center, Gaithersburg, MD, September 29 to October 2, 2003.

45. Materials Reliability Program, Crack Growth Rates for Evaluating Primary Water Stress Corrosion Cracking ((PWSCC) of Alloy 82, 182 and 132 Welds (MRP-115), EPRI, Palo Alto, CA; 1006696, 2004.
46. Materials Reliability Program, Resistance to Primary Water Stress Corrosion Cracking of Alloys 690, 52 and 152 in Pressurized Water Reactors (MRP-111), EPRI, Palo Alto, CA; 1009801, 2004.
47. NUREG/CR-6907, "Crack Growth Rates of Nickel Alloy Welds in a PWR Environment," U.S. Nuclear Regulatory Commission (Argonne National Laboratory), May 2006.
48. Materials Reliability Program, Development of Preemptive Weld Overlay (PWOL) for Alloy 600 PWSCC Mitigation (MRP-208), EPRI, Palo Alto, CA, Draft, June 2006.
49. G. Wilkowski, H. Xu, D.-J. Shim, and D. Rudland, "Determination of the Elastic-Plastic Fracture Mechanics Z-factor for Alloy 82/182 Weld Metal Flaws for Use in the ASME Section XI Appendix C Flaw Evaluation Procedures," PVP2007-26733, Proceedings of ASME-PVP 2007: 2007 ASME Pressure Vessels and Piping Division Conference, San Antonio, TX, 2007.
50. NUREG/CR-4082, Volume 8, "Summary of Technical Results and Their Significance to Leak-Before-Break and In-Service Flaw Acceptance Criteria, March 1984- January 1989
51. A.F. Deardorff et al, "Net Section Plastic Collapse Analysis of Two-Layered Materials and Application To Weld Overlay Design", ASME PVP 2006 Pressure Vessels and Piping Division Conference, Vancouver, Canada, July 2006, PVP2006-ICPVT11-93454
52. W. Hübner, B. Johansson, and M. de Pourbaix, Studies of the Tendency to Intergranular Stress Corrosion Cracking of Austenitic Fe-Cr-Ni Alloys in High Purity Water at 300°C, Studsvik report AE-437, Nykoping, Sweden, 1971.
53. W. Debray and L. Stieding, Materials in the Primary Circuit of Water-Cooled Power Reactors, International Nickel Power Conference, Lausanne, Switzerland, May 1972, Paper No. 3.
54. C. Amzallag, et al., "Stress Corrosion Life Assessment of 182 and 82 Welds used in PWR Components," Proceedings of the 10th International Symposium on Environmental Degradation of Materials in Nuclear Power Systems - Water Reactors, NACE, 2001.